Expression of SLC transporters in Chronic Lymphocytic Leukaemia cells and their interaction with cytostatics

Dissertation

zur Erlangung des mathematisch-naturwissenschaftlichen Doktorgrades

"Doctor rerum naturalium"

der GeorgAugustUniversität Göttingen

vorgelegt von

Shivangi Gupta

aus New Delhi, India

Göttingen 2009

Mitglieder des Betreuungsausschusses

Referentin/Referent: Prof. Dr. T. Pieler

Koreferentin/Koreferent: Prof. Dr. U. Groβ

Koreferentin/Koreferent: PD Dr. Y. Hagos

Tag der mündlichen Prüfung: 12.10.2009

Table of Contents

I Abbreviations

APS	Ammonium persulphate
ATP	Adenosine triphosphate
BSA	Bovine Serum Albumin
cDNA	complementary DNA
CHO	Chinese Hamster Ovary
°C	degree Celsius
dd	double distilled
DMEM	Dulbecco's modified Eagle's medium
DNA	deoxyribonucleic acid
dNTP	deoxy nucleotide triphosphate
dsDNA	double stranded DNA
DTT	dithiothreitol
ECL	Enhanced Chemiluminescence
FCS	Fetal Calf Serum
Fig	Figure
g	gram(s)
h	hour(s)
HEK	Human Embryonic Kidney
kDa	kilo Daltons
K_m	Michaelis- Menten constant
LB	Luria Bertani broth
M	Molar
mM	milli Molar
µM	micro Molar
MPP	4-methyl-pyridinium iodide
PBS	Phosphate Buffer Saline
PCR	Polymerase Chain Reaction
RNA	Ribonucleic acid
rpm	revolutions per minute
RT-PCR	Reverse Transcriptase PCR
SEM	Standard error of mean
SDS	Sodium dodecyl sulphate

SDS-PAGE	SDS-Polyacrylamide gel electrophoresis
TBS	Tris buffered saline
TEMED	tetramethylenediamine
Tris	tris (hydroxymethyl) aminomethane
UV	Ultraviolet
V	Volts
WB	Western Blot

II Summary

Chronic Lymphocytic Leukaemia, CLL, is one of the most common forms of leukaemia in the elderly. The treatment regimen determines the outcome of patients with CLL and the efficiency of this treatment is modulated by the concentration of cancer treating drugs in cancer cells. Uptake transporters of the SLC (solute carrier) family can help overcome chemoresistance by the application of transporter-specific cytostatics. In the present study, we investigated the expression of SLC transporters in six lymphoma cell lines and in CLL patient samples. Five of the six cell lines tested, as well as samples from CLL patients demonstrated a higher expression of SLC22A1 (OCT1) than in healthy lymphocytes. The uptake of the organic cation [^{3}H]MPP into OCT1 stably transfected CHO cells was significantly inhibited by irinotecan, mitoxantrone and paclitaxel. The K_i values as determined using Dixon plot analyses were 1.71 µM, 85.2 µM and 50.1 µM, respectively. [^{3}H]MPP uptake by OCT2 stably transfected CHO cells was inhibited by irinotecan and the K_i value was calculated to be 86.3 µM. Transporter mediated cytototoxicity of these drugs was analyzed using MTT assays on CHO-OCT1, CHO-OCT2, L-428 (B-lymphoma cell line expressing OCT1) and SUDHL-4 (B-lymphoma cell line with no expression of OCT1). The growth of CHO-OCT1 and CHO-OCT2 on irinotecan treatment was inhibited by 30% and 23%, respectively, compared to non-transfected CHO cells. Mitoxantrone resulted in a 45% decrease of CHO-OCT1 cells compared to CHO cells, while paclitaxel treatment resulted in a 30% decrease in cell viability of CHO-OCT1 cells. In L-428 and SUDHL-4, results were similar with lowered cell viability seen in OCT1 expressing L-428 on irinotecan and paclitaxel treatment, by 15% and 45%, respectively; with no change in SUDHL-4. The data shown here support the hypothesis that sensitivity of cancer cells to cytostatics is mediated by the specific uptake transporter proteins. The expression analysis of transporters and the application of transporter-specific cytostatics could help tailor cancer therapy to suit individual needs.

Zusammenfassung

Chronische lymphatische Leukämie (CLL) ist bei älteren Menschen eine der häufigsten Formen der Leukämie. Das Behandlungskonzept bestimmt den Krankheitsverlauf der CLL, da die Effektivität der Behandlung durch die Konzentration an Krebsmedikamenten in den Krebszellen bestimmt wird. Durch die Anwendung transporterspezifischer Zytostatika können Aufnahmetransporter der „solute carrier“ (SLC) Familie dazu beitragen, die Chemoresistenz von Zellen zu überwinden. In der vorliegenden Arbeit wurde die Expression von SLC Transportern in sechs Lymphomzelllinien und in CLL-Patientenmaterial untersucht. Fünf der sechs getesteten Zelllinien, sowie die Proben von CLL-Patienten zeigten eine höhere Expression des SLC22A1 (OCT1) als gesunde Lymphozyten. Die Aufnahme des organischen Kations [^{3}H]MPP in mit OCT1 stabil transfizierte CHO Zellen wurde durch Irinotekan, Mitoxantron und Paclitaxel signifikant gehemmt. Mit Hilfe von Dixon Plot Analysen konnten K_i-Werte von 1,71 µM, 85,2 µM bzw. 50,1 µM ermittelt werden. Die [^{3}H]MPP-Aufnahme in mit OCT2 stabil transfizierte CHO Zellen wurde durch Irinotekan gehemmt und eine K_i von 86,3 µM konnte ermittelt werden. Die transportervermittelte Zytotoxizität dieser Medikamente wurde unter Verwendung des MTT-Tests an CHO-OCT1, CHO-OCT2; L-428 (OCT-1 exprimierende B-Lymphomzelllinie) und SUDHL-4 (nicht OCT-1 exprimierende B-Lymphomzelllinie) getestet. Das Wachstum von CHO-OCT1 und CHO-OCT2 wurde durch Irinotekan, verglichen mit nichttransfizierten Zellen, um 30% bzw. 23% reduziert. Mitoxantron führte zu einer Abnahme der überlebenden CHO-OCT1 Zellen um 45% verglichen mit CHO Zellen, während die Behandlung mit Paclitaxel das Überleben der CHO-OCT1 Zellen um 30% reduzierte. Versuche mit L-428 und SUDHL-4 führten zu vergleichbaren Ergebnissen: Die Behandlung mit Irinotekan und Paclitaxel führte zu einer um 15% bzw. 45% verminderten Überlebensrate der OCT1 exprimierenden L-428 Zellen, auf das Überleben von SUDHL-4 Zellen hatten diese Medikamente keinen Einfluss. Die hier gezeigten Daten unterstützen die Hypothese, die Empfindlichkeit von Krebszellen gegenüber Zytostatika sei durch spezifische Transportproteine vermittelt. Die Expressionsanalyse von Transportern und die Anwendung transporterspezifischer Zytostatika könnten helfen, die Krebstherapie auf individuelle Anforderungen maßzuschneidern.

1. INTRODUCTION

1.1 Chronic Lymphocytic Leukaemia

Leukaemia is a collective term used to describe a group of cancers characterized by an abnormal proliferation of leukocytes. Acute leukaemia is due to a rapid increase of immature blood cells and immediate treatment is required because of rapid disease progression. Chronic leukaemia is characterized by a slow buildup of mature, albeit abnormal, blood cells. It can take months or years to progress and unlike acute leukaemia, treatment of chronic leukaemia involves monitoring the disease to ensure maximum efficacy. Depending on the blood cell affected, leukaemia may further be divided into myeloid or lymphocytic. In myeloid leukaemia, mutations develop in the marrow cell which goes on to form red blood cells and platelets. Lymphocytic leukaemia starts with a cancerous change in the marrow cell that develops into lymphocytes (128).

Acute myeloid leukaemia (AML) is morphologically defined by abnormal promyelocytes (76). The disease is characterized by frequent coagulopathy associated with bleeding. The disease incidence increases with age and it accounts for 90% of all acute leukaemias in adults.

Chronic myeloid leukaemia, CML, is characterized by the presence of the Philadelphia (Ph) chromosome, formed due to translocation between two chromosomes. Translocation between the long arms of chromosomes 9 and 22 results in the formation of two new genes: BCR-ABL and ABL-BCR. The BCR-AML gene encodes a protein with deregulated tyrosine kinase activity, crucial for malignant transformation in CML (39).

Acute lymphoblastic leukaemia, ALL, results in the accumulation of early B- and T-lymphocyte progenitors in the bone marrow. ALL affects children and adults, with highest incidence in children between the ages of 2-5 (30).

B-cell chronic lymphocytic leukaemia (B-CLL) is characterized by the accumulation of abnormal lymphocytes in the blood and the bone marrow. One of the most common forms of leukaemia in North America and Europe, it mainly affects the elderly (29).

CLL is a lymphoproliferative disease and the B-CLL cells are $CD5^+$, $CD19^+$, $CD20^+$ and $CD23^+$, mature, non-functional B-cells (19). B-CLL cells can account for up to 99% of circulating peripheral blood mononuclear cells and compared to normal B-cells, B-CLL cells can survive for a few months in the blood circulation. This increase in abnormal B-CLL cells, combined with a decrease in normal immune cells, results in immune deficiency in CLL (47).

Two classification systems are commonly used to divide patient populations into three prognostic groups: Rai system (Table 1.1), which is commonly used in USA; and the Binet classification system (Table 1.2), more popular in Europe (9). These systems provide the basis of treatment and medical follow-up.

Table 1.1 Rai classification system

Risk level	Stage	Clinical features at diagnosis	Median survival time (years)
Low	0	Blood and marrow lymphocytosis	≥10
Intermediate	I	Lymphocytosis and lymphadenopathy	9
	II	Lymphocytosis and splenomegaly	5
High	III	Lymphocytosis and anaemia	5
	IV	Lymphocytosis and thrombocytopenia	5

Table 1.2 Binet classification system

Stage	Clinical features at diagnosis	Median survival time (years)
A	Blood and marrow lymphocytosis and less than three areas of palpable lymphoid involvement	> 7-10
B	Same with three or more areas of palpable lymphoid involvement	5-7
C	Same plus anaemia or thrombocytopenia	< 2-5

Characterized by a loss of proper apoptotic controls, B-CLL may be influenced by either activation of anti-apoptosis pathways or blockage of pro-apoptosis pathways

(22). Many gene and chromosomal abnormalities as well as advancing age correlate with CLL disease development. Several chromosomal abnormalities occur in CLL (31). The most common includes the loss of a region of chromosome 13 encoding microRNAs, which may play a role in silencing certain target genes (5). Deletion of *miR-15a* and *miR-16-1* are seen in more than 50% CLL cases (80) and is also associated with an increase in Bcl2, an inhibitor of apoptosis (9). The deletion of *miR-15a* and *miR-16-1* is associated with good prognosis. Trisomy 12 occurs in 15% cases but has no significant prognostic influence (9). The tumour suppressor and pro-apoptotic gene, *p53*, is also often deleted as a consequence of deletion on chromosome 17 and this is associated with a bad median survival time (109;127). The loss of *p53* is associated with chemotherapeutic resistance to alkylating agents like chlorambucil and purine analogues like fludarabine (9).

Protein abnormalities are common, as represented by ZAP-70. Expressed in T-lymphocytes, natural killer cells and activated splenic B-cells, ZAP-70 is a receptor-associated protein tyrosine kinase (3). ZAP-70 can promote the survival of B-CLL cells by enhanced B-cell receptor signaling and ZAP-70 expression in B-cells is frequently used as a prognostic marker for CLL (2). Another prognostic marker for CLL patients is the mutational status of the immunoglobulin heavy chain (IgV_H). Patients with somatic unmutated IgV_H develop progressive CLL with poorer prognosis than those with mutated IgV_H. B cells from patients with favourable prognostic markers of CLL- mutated IgV_H, $CD38^-$, $ZAP\text{-}70^-$, are less capable of triggering apoptosis, survival or proliferation. This lack of receptor stimulation could be due to the inability to bind antigen by B- cell receptors, and favours a less aggressive form of CLL (25). Figure 1.1 below depicts the development and evolution of CLL cells resulting in mutated or unmutated CLL.

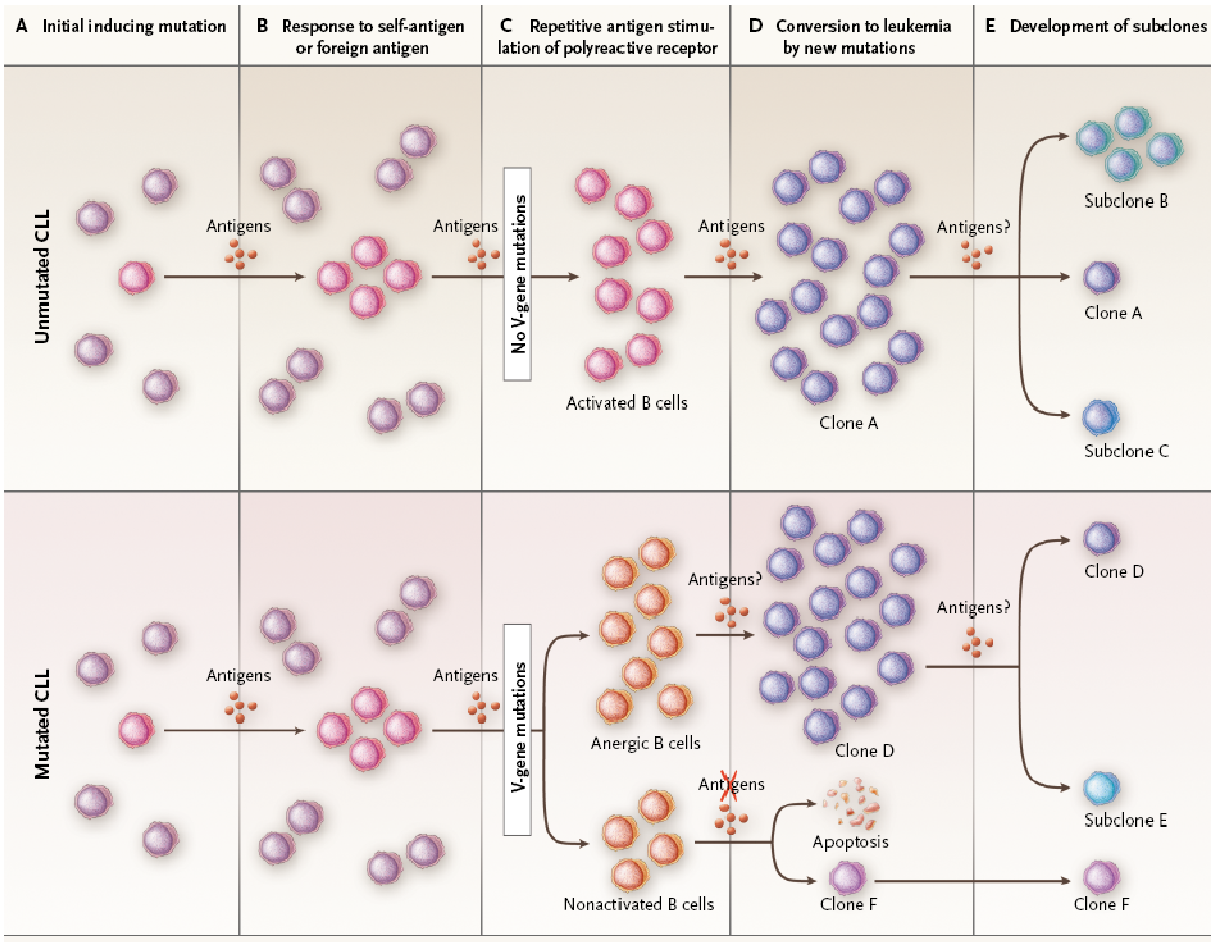

Fig 1.1 Model depicting the development and evolution of CLL cells. An initial inducing lesion occurs in a single B lymphocyte (pink cell in upper and lower portions of Panel A). Interactions between antigens and B-cell receptors of adequate affinity induce clonal amplification (Panel B). The initial inducing lesion provides the marked cell with a growth advantage over other clones stimulated by the same or other antigens. In clones destined to become unmutated CLL cells, repetitive interactions between antigens and polyreactive B-cell receptors of the initially selected clone promote clonal growth, which persists because V-gene mutations do not occur (Panel C, top). In others, destined to become mutated CLL cells (Panel C, bottom), V-gene mutations develop that can abrogate the polyreactivity of the B-cell receptors and thereby alter their ability to bind the original antigen or autoantigen ("clonal ignorance"). Alternatively, these mutated cells become anergic owing to excessive B-cell–receptor stimulation because of the acquisition of more avid receptors. In both instances, the promoting effect of antigenic stimulation is neutralized. Additional DNA mutations cause the cells to become leukaemic (Panel D). Continued cycling leads to other genetic changes (e.g., deletions at 13q, 11q, and 17p or duplication of chromosome 12) that determine the course of the disease (Panel E) (Figure reproduced without permission from Chiorazzi et al, 2005).

Chronic lymphocytic leukaemia may be stable or progressive. Patients suffering from stable CLL can survive long periods without treatment while progressive CLL is characterized by the rapid doubling-time of B-CLL cells, and can thus be fatal in a short time (22). Chemotherapy for CLL involves administration of drugs like fludarabine (70) or cyclophosphamide. Fludarabine is a purine analog and can induce

p53- dependent apoptosis. Monoclonal antibodies for CLL treatment have also been developed and include anti-CD52 (Alemtuzumab) and anti-CD20 (Rituximab) (2). Bendamustine, which has properties of an alkylating agent as well as antimetabolites, is also gaining use in the treatment of this disease (7;94).

The outcome of patients with leukaemia is affected by the treatment regimen. The efficacy of cytostatic drugs in cancer therapy is modulated by the concentration of these drugs in cancer cells (54). Uptake transporters belonging to the superfamily of solute carriers (SLC) and efflux pumps belonging to the ATP-binding cassette transporter (ABC transporter) superfamily are the key agents controlling drug concentrations in cells. The efflux ABC transporters are one of the key factors responsible for the chemoresistance of tumours, due to their high expression in these cells (11;12). Solute carrier transporters, SLCs, are represented by 47 families. Broadly expressed in the human body, SLCs may obtain energy for substance (drug) translocation from the electrochemical gradient of Na^+, H^+ and organic ions such as dicarboxylates (100).

1.2 Transport systems

Membrane transporters mediate the absorption, distribution and excretion of most nutrients, xenobiotics, drugs, environmental toxins and their metabolites. By controlling the cellular milieu through the influx and efflux of nutrients, metabolites and drugs, transporter proteins play essential roles in cell function, proliferation and death (54).

1.2.1 Efflux transporters

ATP-binding cassette (ABC) transporters are primary-active transporters that utilize ATP hydrolysis as the energy source to drive active transport. 50 different ABC transporter genes have been identified and these are grouped into seven families based on sequence homology (54;96). These ATP-dependent transporters mediate the translocation of various substrates across membranes. ABC transporters consist of at least four domains: two transmembrane units consisting of six transmembrane domains each, embedded in the membrane bilayer; and two ABCs binding domains, located in the cytoplasm (96).

ABC transporters may function as either importers or exporters, transporting substrate molecules in or out of cells. ABC transporters that function as importers are only reported in prokaryotes. In eukaryotes, ABC transporters are important in the cellular exit of lipids, fatty acids and cholesterol (96).

A variety of ABC transporters have been implicated in chemoresistance of cancer cells by mediating the efflux of chemotherapeutic drugs (115). Various factors may result in the increased expression of ABC efflux transporters in drug-resistant cancer cells. These include altered activity of transcriptional factors, gene polymorphisms as well as changes in the methylation status of promoters (60). These factors modulating the functional characteristics of transporters are directly responsible for drug pharmacokinetics.

The overexpression of MDR1 (ABCB1; P-glycoprotein) in cancer cells confers chemoresistance to various classes of compounds with unrelated chemical structures. Known substrates of MDR1 include etoposide and vinblastine (95). Polymorphisms in the gene encoding MDR1 can significantly affect response to pharmacotherapy for many diseases (54). Recently, MDR1 gene polymorphisms have been associated with MDR1 activity in B-CLL (57). According to Jamroziak and colleagues, a single nucleotide polymorphism in MDR1, C3435T, increases the risk of developing B-CLL, possibly due to decreased protection against MDR1 substrate carcinogens.

MRP1, Multidrug Resistance Protein 1 (ABCC1), has been shown to transport glutathione and other drug conjugates. Coupling to glutathione also appears to play a role in the transport of MRP1 substrates. Since glutathione is a physiological substrate of MRP1, this transporter has been suggested to play a role in the cellular antioxidative defense system (71-73).

Overexpression of MRP2, Multidrug Resistance Protein 2 (ABCC2), can induce resistance against various drugs like cisplatin, doxorubicin and methotrexate. Genetic variations in MRP2 can lead to nephrotoxicity due to reduced drug clearance (55).

The ABC transporters are relatively well characterized, with many studies on their substrate specificity and mechanism of substrate efflux. In the current study, we were interested in the influx of cytostatics into tumour cells; and therefore we concentrated on the expression and functional characterization of SLC transporters.

1.2.2 Influx transporters

The solute carrier (SLC) superfamily is a major group of membrane transporters responsible for the uptake of nutrients, metabolites, drugs and toxins. At present there are 47 known SLC families and these are organized on the basis of alignment similarities and substrate specificities (49). SLC transporters undergo sequential conformational changes during the transport cycle and these proteins are capable of transporting more than one substrate simultaneously (6). The specific SLC transporter families studied in the course of this work are briefly described.

1.2.2.1 SLC7

SLC7 family of transporters includes two system L transporters which function independently of Na^+ and other ions to transport large, neutral amino acids across plasma membranes (Table 1.3). They function as obligatory exchangers with a 1:1 stoichiometry and the activity of LAT1 and LAT2 depends on the amount of intracellular substrate amino acids (59). The single membrane spanning glycoprotein 4F2 heavy chain (hc) is essential for amino acid transport by LATs (59). These transporters consist of membrane spanning light chain and heavy chain. An important cytostatic, melphalan, is a known substrate of LAT1 (66).

Table 1.3 Tissue distribution and substrates of selected members of SLC7 family

Gene	Protein	Tissue distribution	Substrates/ cytostatics
SLC7A5	LAT1	Brain, placenta, testis, tumour cells, bone marrow	L-type amino acids, L-Dopa, Melphalan
SLC7A8	LAT2	Brain, placenta, testis, kidney, small intestine	Gly, L-type amino acids

1.2.2.2 SLC10

The sodium bile salt co-transporter family includes the NTCP and ASBT transporters. Both systems mediate sodium-dependent uptake of conjugated and unconjugated bile salts (Table 1.4). The driving force for the uptake is provided by the inwardly directed Na^+ gradient maintained by the basolateral Na^+, K^+-ATPase as well as the negative intracellular potential (37). The two C-terminal putative transmembrane domains are hypothesized to constitute an important part of the binding pocket for bile salts in these transporters. SLC10 transporters can serve as possible targets of drugs conjugated to bile salts. The uptake of modified chlorambucil which keeps its potency even after conjugation to bile salts has been shown for NTCP (67).

Table 1.4 Tissue distribution and substrates of selected members of SLC10 family

Gene	Protein	Tissue distribution	Substrates/ cytostatics
SLC10A1	NTCP	Liver, pancreas	Bile salts, chlorambuciltaurocholate
SLC10A2	ASBT	Biliary tract, ileum, kidney	Bile salts

1.2.2.3 SLC13

The SLC13 gene family consists of sodium-coupled transporters mediating the transport of anions (like sulphate) and dicarboxylates. The five members of this family are electrogenic transporters, producing an inward current in the presence of sodium and substrates. Consisting of 11 transmembrane domains, the carboxy terminal half of these proteins is most important for determining function while the TMDs 9 and 10 form part of the substrate permeation pathway. All members contain one or two N-glycosylation sites at the C-terminus. NaDC3 is encoded by SLC13A3 gene and is a high affinity Na^+/ dicarboxylate transporter (Table 1.5). Transport by NaDC3 involves three Na^+ ions with each substrate and is inhibited by millimolar concentrations of lithium (88).

Table 1.5 Tissue distribution and substrates of NaDC3 from SLC13 family

Gene	Protein	Tissue distribution	Substrates/ cytostatics
SLC13A3	NaDC3 (SDCT2, NaC3)	Kidney (basolateral membrane), placenta, liver, brain	Dicarboxylates, N-acetylaspartate

1.2.2.4 SLC16

The monocarboxylate co-transporter (MCT) family comprises 14 members. MCT1-4 are known to catalyze the proton-linked transport of metabolically important monocarboxylates like lactate, pyruvate and ketone bodies (Table 1.6). Lactic acid transport by the MCTs across the plasma membrane is essential for the metabolism and the pH regulation of cells. The different MCT isoforms remove the lactic acid produced by glycolysis and allow uptake of lactate by cells utilizing it for gluconeogenesis (liver and kidney cells) or as a respiratory fuel (heart and red muscle cells). 10-12 α-helical transmembrane domains are predicted for MCTs, with the N- and C-termini located within the cytoplasm. C-terminus and the large intracellular loop between TMD 6 and 7 offers sites for large sequence variations between different isoforms (45).

Table 1.6 Tissue distribution and substrates of selected members of SLC16 family

Gene	Protein	Tissue distribution	Substrates/ cytostatics
SLC16A1	MCT1	Ubiquitous	Lactate, pyruvate, ketone bodies
SLC16A3	MCT4	Chondrocytes, heart, lung, placenta, skeletal muscle, testis	Lactate, pyruvate, ketone bodies
SLC16A7	MCT2	Brain, kidney	Pyruvate, lactate, ketone bodies

1.2.2.5 SLC19

The SLC19 gene family plays an important role in the transport and homeostasis of folate and thiamine in the body. The three members are expressed ubiquitously.

SLC19A1 (RFT) mediates transport of folate and its derivatives existing as anions at physiological pH, while SLC19A2 (ThTr1) and SLC19A3 (ThTr2) transport thiamine, which exists as a cation at physiological pH (Table 1.7). Folate influx via RFT is stimulated by an inwardly directed H^+ gradient ($pH_{out}<pH_{in}$), suggesting folate/H^+ symport or folate/OH^- antiport. Thiamine influx via ThTr1 and ThTr2 is enhanced by an outwardly directed H^+ gradient ($pH_{out}>pH_{in}$), suggesting thiamine/H^+ antiport. All three proteins are composed of 12 transmembrane domains with N-glycosylation sites (35).

Table 1.7 Tissue distribution and substrates of selected members of SLC19 family

Gene	Protein	Tissue distribution	Substrates/ cytostatics
SLC19A1	RFT	Ubiquitous	Folate, Methotrexate
SLC19A2	ThTr1	Ubiquitous	Thiamine
SLC19A3	ThTr2	Ubiquitous	Thiamine

1.2.2.6 SLCO (SLC21)

SLCO family members are organic anion transporting polypeptides (OATPs). They share a predicted membrane topology of 12 transmembrane domains with a large 5th extracellular loop. The OATPs contain N-glycosylation sites in the extracellular loops 2, 3 and 5, and in the transmembrane domain 6 (44). OATPs have a wide tissue distribution and mediate the cellular uptake of a broad range of compounds, including hormones, bile salts, steroids, antivirals and cytostatics (Table 1.8).

Table 1.8 Tissue distribution and substrates of selected members of SLC21 family

Gene	Protein	Tissue distribution	Substrates/ cytostatics
OATP1A2	OATP-A	Brain, testis	Prostaglandin E_2, Ouabain, Chlorambuciltaurocholate
OATP1B1	OATP-C	Hepatocytes	Bilirubin, Leukotrienes, Thyroxine, Methotrexate, Taurocholate
OATP2B1	OATP-B	Ubiquitous	Prostaglandin E_2, Benzylpenicillin

OATP3A1	OATP-D	Non-pigmented human ciliary body epithelium	Prostaglandin E_2, Benzylpenicillin
OATP4A1	OATP-E	Ubiquitous	Prostaglandin E_2, Taurocholate, Thyroxine

1.2.2.7 SLC22

Most transporters of the SLC22 gene family are polyspecific, being able to transport different substrates. The transporters have a predicted membrane topology of 12 α-helical transmembrane domains, a large glycosylated loop between TMDs 1 and 2, and a large intracellular loop between TMDs 6 and 7 with sites for phosphorylation. The SLC22 family includes organic cation transporters as well as organic anion transporters. Organic Cation Transporters, the OCTs, mediate the uptake of organic cations, but some weak bases, non-charged, as well as some anionic compounds are also transported (8;62;63). Organic anion transporters, the OATs, operate as anion exchangers. With a broad specificity, the OATs are known to interact with many commonly used anionic drugs like antibiotics and antivirals (100). Since the SLC22 family transporters are typically found at boundary epithelia, these play an important role in distribution of drugs (Table 1.9).

Table1.9 Tissue distribution and substrates of selected members of SLC22 family

Gene	Protein	Tissue distribution	Substrates/ cytostatics
SLC22A1	OCT1	Liver	TEA, MPP, serotonin, prostaglandin E_2
SLC22A2	OCT2	Kidney, brain, neurons	TEA, MPP, choline, dopamine, histamine, norepinephrine, cisplatin
SLC22A3	OCT3	Liver, skeletal muscle, placenta, kidney, heart, lung, brain	TEA, MPP, guanidine, dopamine, norepinephrine, histamine
SLC22A6	OAT1	Kidney, brain	PAH, prostaglandins, methotrexate, cisplatin
SLC22A7	OAT2	Liver, kidney	PAH, dicarboxylates, PGE_2, salicylate, methotrexate, 5-fluorouracil

SLC22A8	OAT3	Kidney, brain, skeletal muscle developing bone	PAH, estrone sulphate, methotrexate
SLC22A11	OAT4	Kidney, placenta	Estrone sulphate, ochratoxin A, prostaglandin E_2, prostaglandin $F_{2\alpha}$, methotrexate
SLC22A16	OCT6	Testis, bone marrow, leukocytes, kidney	TEA, L-carnitine, doxorubicine

1.2.2.8 SLC28

The SLC28 family, at present, includes three concentrative nucleoside transporters: CNT1 (SLC28A1), CNT2 (SLC28A2) and CNT3 (SLC28A3). These proteins are membrane bound transporters and mediate a high affinity transport of nucleosides and nucleoside analogs actively into cells by coupling transport to the inwardly directed sodium gradient (41). The SLC28 family transporters consist of 13 transmembrane domains with the cation and substrate recognition sites in the carboxy half of the protein. These transporters are located in the plasma membrane of many cell types and are involved in the tissue-specific uptake of antiviral and anticancer nucleoside analogs. The following table (Table 1.10) gives the tissue distribution and known substrates of SLC28 transporters.

Table 1.10 Tissue distribution and substrates of selected members of SLC28 family

Gene	Protein	Tissue distribution	Substrates/ cytostatics
SLC28A1	CNT1	Kidney, liver, small intestine	Pyrimidine nucleosides, adenosine, gemcitabine
SLC28A2	CNT2	Brain, colon, heart, kidney, liver, pancreas, placenta, rectum, skeletal muscle, small intestine	Purine nucleosides, uridine
SLC28A3	CNT3	Bone marrow, intestine, liver, lung, mammary glands, pancreas, placenta, prostrate, testis, trachea	Purine and pyrimidine nucleosides, cladrabine, gemcitabine, fludarabine,

1.2.2.9 SLC29

Equilibrative nucleoside transporters, ENTs, belong to the human SLC29 family of proteins. The four members of this family have a predicted topology of 11 transmembrane domains with a cytoplasmic N-terminus and an extracellular C-terminus. The four isoforms are widely distributed in mammalian tissues and play a role in transepithelial nucleoside transport (4). The ENTs are also responsible for the cellular uptake of nucleoside analogs used in cancer therapy (1) (Table 1.11).

Table 1.11 Tissue distribution and substrates of selected members of SLC29 family

Gene	Protein	Tissue distribution	Substrates/ cytostatics
SLC29A1	ENT1	Ubiquitous	Purine and pyrimidine nucleosides, gemcitabine, cladrabine, fludarabine,
SLC29A2	ENT2	Ubiquitous	Purine and pyrimidine nucleosides and nucleobases, gemcitabine, cladrabine, fludarabine,
SLC29A3	ENT3	Ubiquitous	Purine and pyrimidine nucleosides

1.3 Antitumour drugs

Cytostatic drugs have the ability to prevent growth and proliferation of cells. They are often used to prevent growth and development of malignant cells and neoplasms; and they are therefore referred to as anti-neoplastic drugs. Anti-cancer drugs can be broadly classified into three: (i) those acting on DNA, (ii) drugs acting on mitotic spindle; and (iii) drugs acting on steroid hormone receptors.

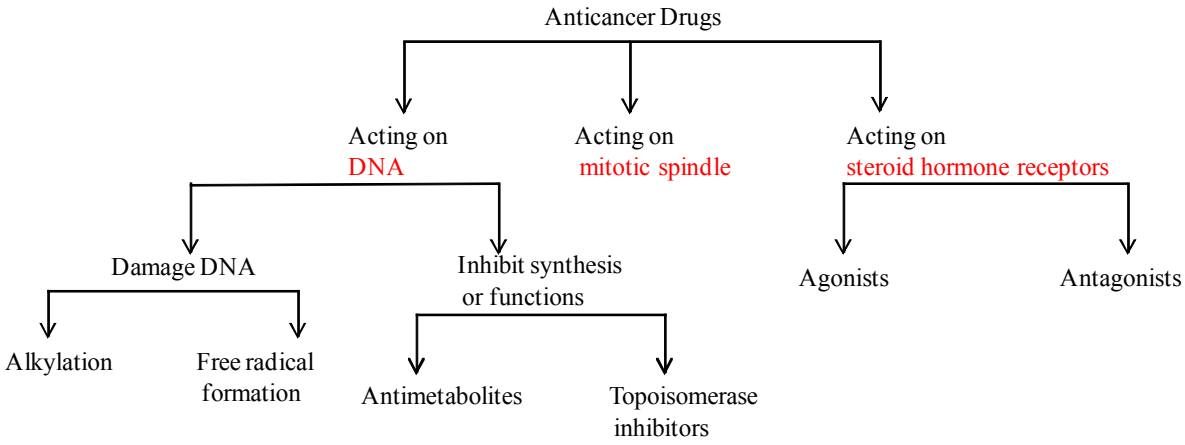

Fig 1.2 Classification of anticancer drugs on the basis of target of drug action

1.3.1 Cytostatics acting on DNA

1.3.1.1 Alkylating drugs

Drugs acting on DNA include covalent DNA binding drugs, the alkylating agents. Alkylating cytostatics function by forming covalent bonds with DNA, RNA or proteins resulting in adducts with an added methyl or ethyl group. Highly reactive, alkylating drugs substitute an alkyl group for the hydrogen atoms in cellular molecules, causing single or double strand breaks in DNA, thus preventing replication of the DNA. They are cell cycle non-specific and form the largest class of anticancer drugs. Examples include chlorambucil and cyclophosphamide.

Table 1.12 Alkylating drugs used in this work, their use in therapy and transporters involved in their uptake into cells

Name	Disease treated	Transporter involved in uptake
Chlorambucil	Chronic lymphocytic leukaemia (25)	NTCP
Bendamustine	Chronic lymphocytic leukaemia, non-Hodgkin's lymphoma (23)	Not identified
Melphalan	Multiple myeloma, ovarian cancer (116)	LAT1, OCT3 (107)

Cyclophosphamide	Breast cancer, leukaemia, ovarian cancer (21;116)	Not identified
Ifosfamide	Testicular cancer, acute lymphocytic leukaemia, breast cancer, bone cancer (34)	MCT1 (20)
Busulfan	Chronic myeloid leukaemia (27;51)	Not identified

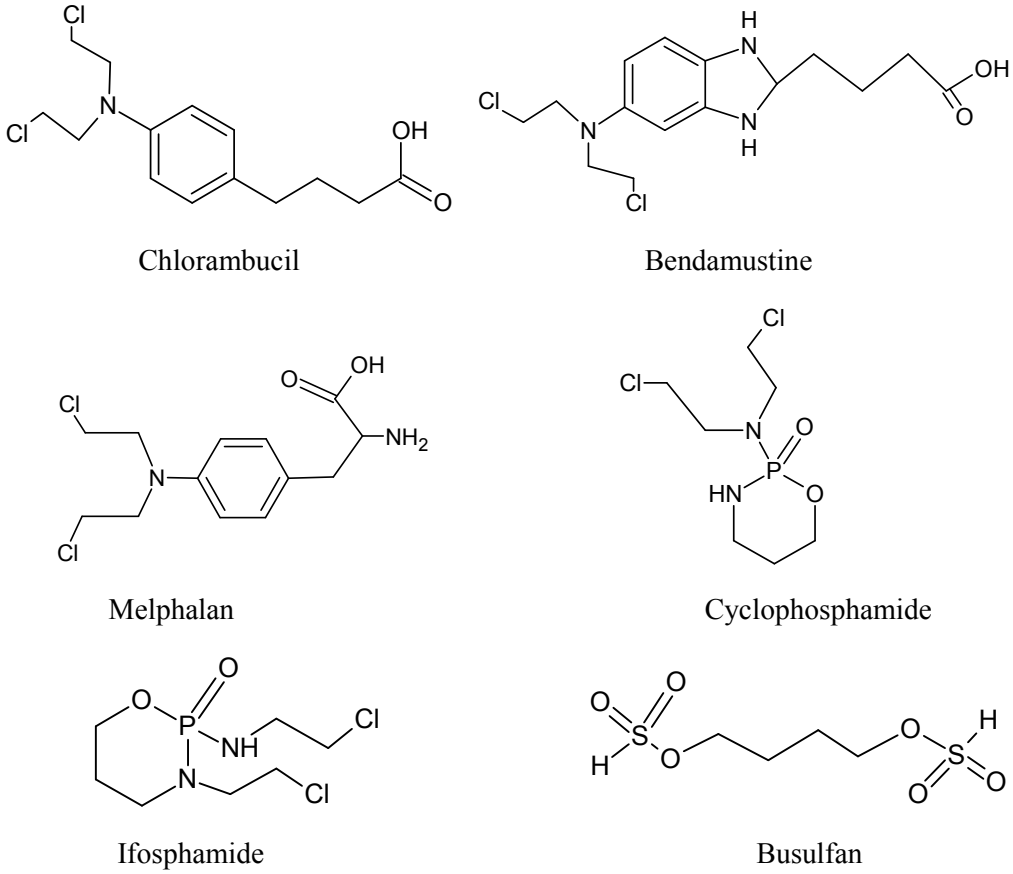

Fig 1.3 Structures of alkylating drugs used in this study

1.3.1.2 Free radical forming drugs

Non covalent binding drugs include intercalating drugs. These have planar regions that stack between paired bases in DNA forming drug-DNA interaction. Free radical damage causes DNA strand breaks. Examples include anthracyclines like doxorubicin and daunorubicin.

1.3.1.3 Antimetabolites

Antimetabolites generally alter the synthesis of RNA or DNA. Structural analogues of nucleotides are incorporated into cell components as if they were essential pyrimidine or purine and disrupt the synthesis of nucleic acids. 5-Fluorouracil is a pyrimidine analog while 6-Mercaptopurine is a purine analog. Other antimetabolites disrupt essential enzymatic processes of metabolism, like methotrexate. Sugar analogs like cytosine arabinoside are also used.

Table 1.13 Antimetabolites used in this work, their use in therapy and transporters involved in their uptake into cells

Name	Disease treated	Transporter involved in uptake
Fludarabine	Blood cancer (47)	ENT1, ENT2, CNT2, CNT3 (77;82;83;91)
Gemcitabine	Lung, pancreatic, bladder cancer (38)	ENT1, ENT2 (38)
Methotrexate	Acute lymphoblastic leukaemia, Crohn's disease, psoriasis (92)	OAT1, OAT2, OAT3, OAT4 (100)
Cytosine arabinoside	Acute myeloid leukaemia, non-Hodgkin lymphoma (126)	Not identified
Cladribine	Blood cancer (101)	ENT1, ENT2, CNT2, CNT3 (91)

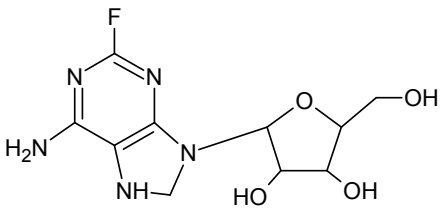

Fludarabine

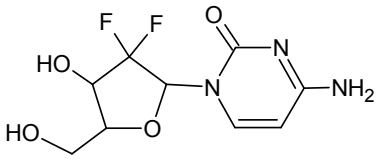

Gemcitabine

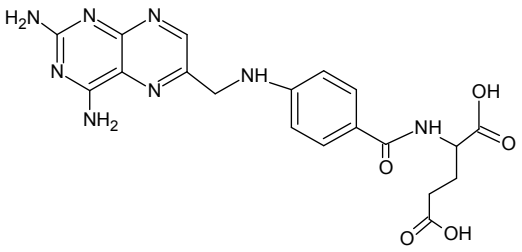

Methotrexate

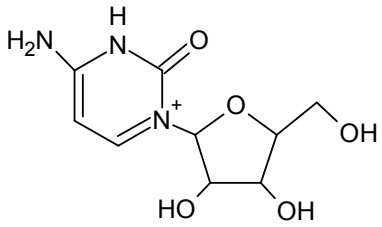

Cytosine arabinoside

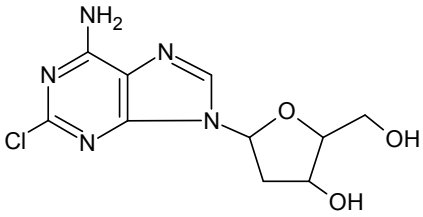

Cladribine

Fig 1.4 Structures of antimetabolites used in this study

1.3.1.4 Topoisomerase inhibitors

DNA topoisomerase inhibitors block DNA synthesis by inhibiting the re-ligation of DNA double strands. Examples are etoposide and mitoxantrone which stabilize the topoisomerase II- DNA complex, preventing it from making a topological change, resulting in irreversible double strand break.

Irinotecan is an example of topoisomerase I inhibitor which is activated to its metabolite SN-38 by hydrolysis. The inhibition of topoisomerase I by the active metabolite SN-38 eventually leads to inhibition of both DNA replication and transcription.

Table 1.14 Topoisomerase inhibitors used in this work, their use in therapy and transporters involved in their uptake into cells

Name	Disease treated	Transporter involved in uptake
Mitoxantrone	Breast cancer, acute myeloid leukaemia, non-Hodgkin's lymphoma (114)	Not identified
Etoposide	Lung, testicular cancer, lymphoma, non-lymphocytic	Not identified

	leukaemia (69)	
Irinotecan	Colon cancer (48)	OCT3 (107)

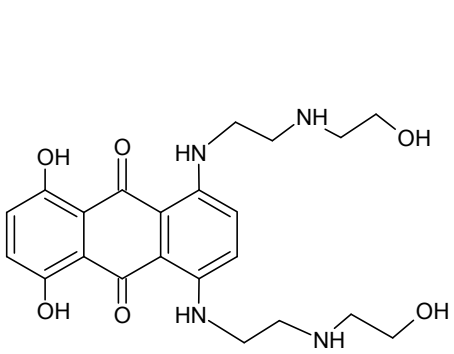

Mitoxantrone

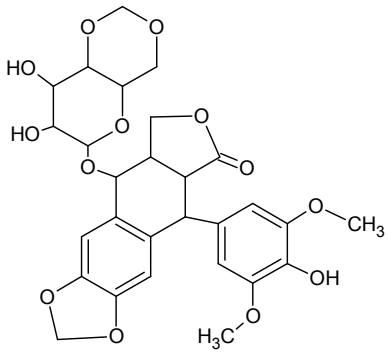

Etoposide

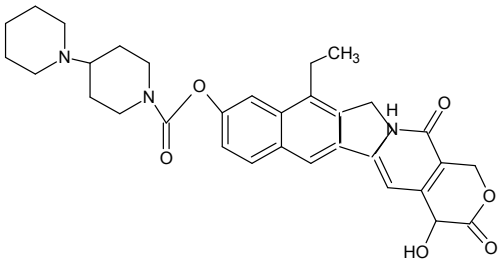

Irinotecan

Fig 1.5 Structures of topoisomerase inhibitors used in this study

1.3.2 Cytostatics acting on mitotic spindle

Inhibitors of chromatin function include microtubule inhibitors like vincristine, vinblastine and paclitaxel. These bind to tubulin, inhibiting microtubule and mitotic spindle formation. Cells are arrested in metaphase and cell division stopped.

Table 1.15 Drugs acting on the mitotic spindle used in this work, their use in therapy and transporters involved in their uptake into cells

Name	Disease treated	Transporter involved in uptake
Vincristine	Non-Hodgkin's lymphoma, Hodgkin's lymphoma, acute lymphoblastic leukaemia (110)	OCT3 (107)

Vinblastine	Hodgkin's lymphoma, non-small cell lung cancer, breast cancer, testicular cancer, urothelial cancer (110)	Not identified
Paclitaxel	Lung, ovarian, breast cancer (52)	Not identified

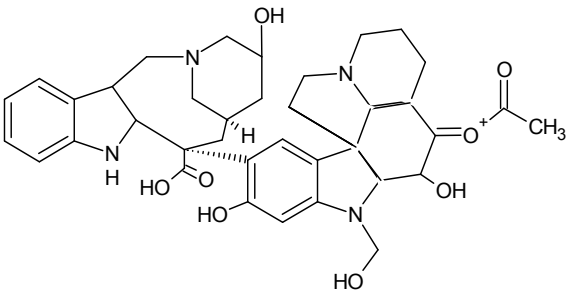

Vincristine

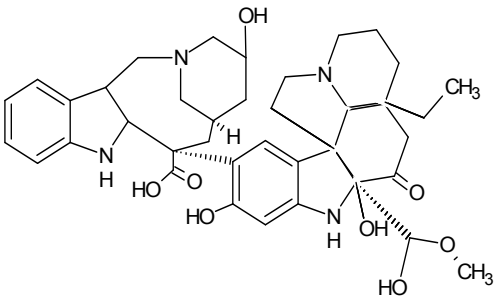

Vinblastine

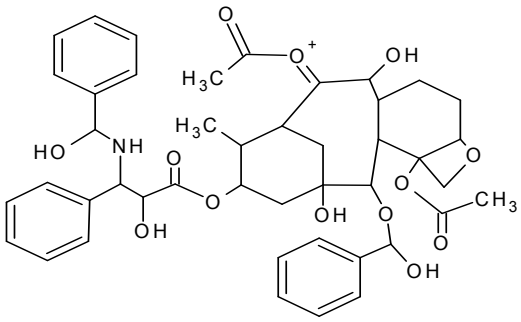

Paclitaxel

Fig 1.6 Structures of drugs acting on the mitotic spindle used in this study

1.3.3 Cytostatics acting on steroid hormone receptors

Drugs affecting endocrine function include glucocorticoids like prednisone. The application of these drugs manipulates the hormone environment of hormone-responsive tumours. An example is tamoxifen which is used as a synthetic anti-estrogen in breast cancer treatment. It competes with estrogen at the receptors. Tamoxifen binding results in the inhibition of estrogen response and death of malignant cells dependent on estrogen for survival.

Table 1.16 Drugs acting on steroid hormone receptors used in this work, their use in therapy and transporters involved in their uptake into cells

Name	Disease treated	Transporter involved in uptake
Prednisone	acute lymphoblastic leukemia, Non-Hodgkin's lymphomas, Hodgkin's Lymphoma, multiple myeloma (89)	Not identified
Clodronic acid	Paget's disease, malignant tumoral hypercalcemia, osteolytic metastases (43;97)	Not identified

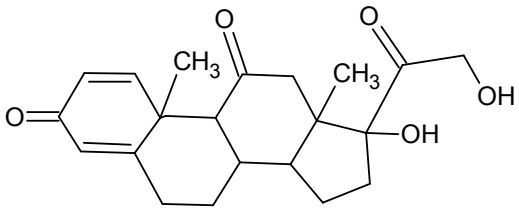

Prednisone

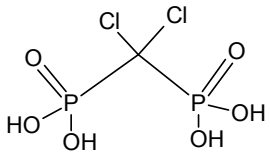

Clodronic acid

Fig 1.7 Structures of drugs acting on steroid hormone receptors used in this study

1.4 Aims

The effective treatment of CLL using various cytostatics can be modulated by active transport of these drugs in cancer cells. Uptake transporters interact with specific drugs and are capable of transporting these substrates into cells. The use of cytostatics specific for uptake transporters present in cancer cells can increase the concentration of these drugs in tumour cells. Chemoresistance, effected in part by the action of efflux ABC transporters, can thus be overcome, making tumour cells chemosensitive.

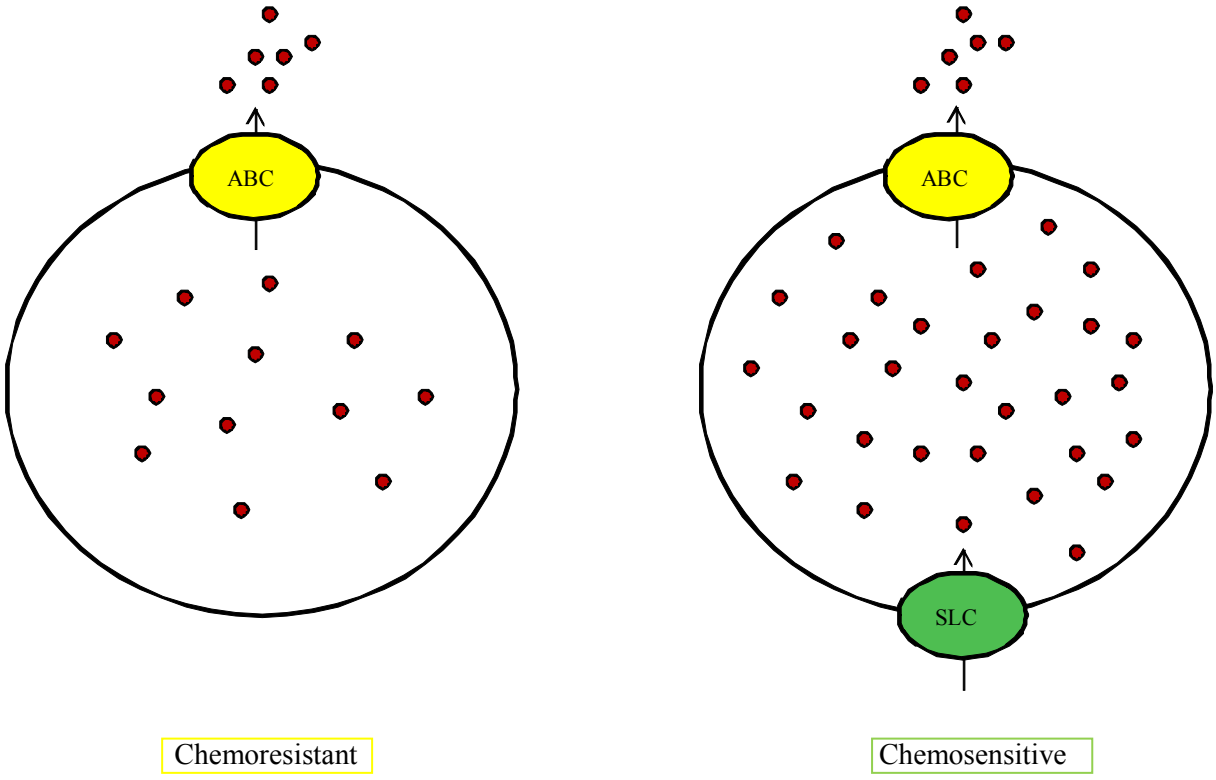

Fig 1.8 Chemoresistance may be overcome by targeting SLC transporters for drug uptake

The aims of this study were threefold: we examined the expression of SLC transporters in lymphoma cell lines and in patients of CLL. Secondly, the interaction of various cytostatics with transporters was determined. Lastly, we investigated the transporter-mediated cytotoxicity of selected drugs in cell lines expressing specific transporters and also in tumour cells.

In an additional project, we generated stably transfected NaDC3 cell line. This cell line will be used for elucidating NaDC3-cytostatics' interactions.

2. MATERIALS

2.1 Cell lines

Cell Line	Provider
Flp-In T-Rex HEK 293	Invitrogen
CHO-OCT1, CHO-OCT2, CHO-K1	Prof. Koepsell, Wuerzburg

All lymphoma cell lines were provided by Prof Wulf, Dept of Haematology and Oncology.

B-lymphoma cell lines:

Karpas-422

Organism	*Homo sapiens* (Human female, 73 years old)
Disease	Lymphoma, follicular, B cell

Raji

Organism	*Homo sapiens* (Human male, 12 years old)
Disease	Burkitt's lymphoma

SUDHL-4

Organism	*Homo sapiens*
Disease	non-Hodkin's lymphoma

L-428

Organism	*Homo sapiens* (Human female, 37 years old)
Disease	Hodkin's lymphoma

T-lymphoma cell lines:

Jurkat

Organism	*Homo sapiens* (Human male, 14 years old)
Disease	Acute lymphoblastic leukaemia

HUT-78

Organism *Homo sapiens*

Disease T cell lymphoma

2.2 Oligonucleotide primers

Sequence specific primers for RT-PCR were obtained from MWG Biotech AG (Matrinsried, Germany) and are listed in Tables 2.1-2.10 below.

Table 2.1 Primers used for the PCR screening of GAPDH.

Gene	Primer	Sequence 5'-3'	size (bp)	Annealing (°C)
GAPDH	GAPDH_334 for	TCACCATCTTCCAGGAGCG	582	58.0
	GAPDH_905 rev	CTGCTTCACCACCTTCTTGA		

Table 2.2 Primers used for the PCR screening of SLC7 family transporters.

Gene	Primer	Sequence 5'-3'	size (bp)	Annealing (°C)
SLC7A5 (LAT1)	LAT1_1082 for	CAATGGGTCCCTGTTCACAT	144	54.0
	LAT1_1225 rev	TAGAGCAGCGTCATCACAC		
SLC7A8 (LAT2)	LAT2_1048 for	CTTCGGAGGACTGGCTGGGT	180	59.5
	LAT2_1227 rev	GTGAGGAGCAATAAGCAGATGGCA		

Table 2.3 Primers used for the PCR screening of SLC10 family transporters.

Gene	Name	Sequence 5'-3'	size (bp)	Annealing (°C)
SLC10A1 (NTCP)	NTCP_332 for	CGGCTGAAGAACATTGAGGCAC	144	58.5
	NTCP_475 rev	AAGGGCACAGAAGGTGGAGC		
SLC10A2 (ASBT)	ASBT_1019 for	ATGCCGCTGTGCCTCCTTATC	104	59.0
	ASBT_1122 rev	GGAACAACGAGAGCAACCAGAGAT		

Table 2.4 Primers used for the PCR screening of SLC13 family transporters.

Gene	Primer	Sequence 5'-3'	size (bp)	Annealing (°C)
SLC13A3 (NaC2/ NaDC3)	NaDC3_1607 for	ACTCCATCGCCTTCGCCTCT	116	59.0
	NaDC3_1723 rev	CTGTGCCCAGGTATTCATAGCCAA		

Table 2.5 Primers used for the PCR screening of SLC16 family transporters.

Gene	Primer	Sequence 5'-3'	size (bp)	Annealing (°C)
SLC16A1 (MCT1)	MCT1_1383 for	TGGAATGCTGTCCTGTCCTC	182	54.5
	MCT1_1564 rev	CTCCTTCTGTGTCTTTCTGGTCCG		
SLC16A7 (MCT2)	MCT2_586 for	CCTCACTATGGGATTCATTACAGG	235	54.5
	MCT2_843 rev	AGCCACACAGGCATTCAAA		
SLC16A3 (MCT4)	MCT4_1132 for	AGCCACACAGGCATTCAAA	180	58.0
	MCT4_1311 rev	GCTCTTTGGGCTTCTTCCTAATGC		

Table 2.6 Primers used for the PCR screening of SLC19 family transporters.

Gene	Primer	Sequence 5'-3'	size (bp)	Annealing (°C)
SLC19A1 (RFT)	RTF_1156 for	TCTGGCTGTGCTATGCGGC	153	59.0
	RTF_1308 rev	TGGTCTTGACGATGGTGGCAAAG		
SLC19A2 (ThTr1)	ThTr_1246 for	GGGTAACATTTGGGTGTGC	174	53.0
	ThTr_1418 rev	ATTAGAGTGAGCAGCGTCTG		

Table 2.7 Primers used for the PCR screening of SLCO family transporters.

Gene	Primer	Sequence 5'-3'	size (bp)	Annealing (°C)
SLCO1A2 (OATP1A2)	OATP-A_484 for	GGATGTGTGGTTATGGGCTTAGGC	258	59.5
	OATP-A_741 rev	AGGCAGGATGGGAGTTTCACCC		
SLCO2B1	OATP-B_582 for	CGCACTTCATCTCGGAGCCATA		

(OATP2B1)	OATP-B_715 rev	GCTTGAGCAGTTGCCATTGGAG	134	59.0
SLCO1B1 (OATP1B1)	OATP-C_1663 for	GGTGAATGCCCAAGAGATGA	165	53.0
	OATP-C_1810 rev	TGAGTGGAAACCCAGTGC		
SLCO3A1 (OATP3A1)	OATP-D_1205 for	ATCCCGAAGGTCACCAAGCAC	205	59.0
	OATP-D_1409 rev	CCAGGAAGATACCCAGACAAGCAC		
SLCO4A1 (OATP4A1)	OATP-E_873 for	CGCCCGTCTACATTGCCATCT	193	58.5
	OATP-E_1065 rev	GCGGTGAAGAAAGCAGCGG		

Table 2.8 Primers used for the PCR screening of SLC22 family transporters.

Gene	Primer	Sequence 5'-3'	size (bp)	Annealing (°C)
SLC22A1 (OCT1)	OCT1_133 for	GCTATGAAGTGGACTGGAACC	216	54.5
	OCT1_481 rev	CAAACAAGAAGCCCGCATTC		
SLC22A2 (OCT2)	OCT2_2695 for	AGTCTGCCTGGTCAATGCT	105	54.5
	OCT2_2798 rev	AGGAATGGCGTGATGATGC		
SLC22A3 (OCT3)	OCT3_1336 for	ACAGTGGCTACATTGGGAAGA	113	54.5
	OCT3_1448 rev	GAACAGAGCGAAACTCCGAA		
SLC22A6 (OAT1)	OAT1_956 for	GGGCACCTTGATTGGCTATGTCTA	243	58.5
	OAT1_1155 rev	TTGGCTCCTTCTTCCCGCTTC		
SLC22A7 (OAT2)	OAT2_841 for	CGCTGGCTTCTGACCCAAGG	222	59.5
	OAT2_1062 rev	TCCGAACCACACCACCACG		
SLC22A8 (OAT3)	OAT3_1223 for	GTCCCAGCCAAGTTCATCACCA	146	59.5
	OAT3_1368 rev	GCCAATACTGTCCTCACGGTCTG		
SLC22A11 (OAT4)	OAT4_510 for	TCCTGGTGGGCTCCTTTAT	134	60.1
	OAT4_623 rev	GCAGTAGATGACGAATGTTGG		

Table 2.9 Primers used for the PCR screening of SLC28 family transporters.

Gene	Primer	Sequence 5'-3'	size (bp)	Annealing (°C)
SLC28A1 (CNT1)	CNT1_1199 for	GGAGGGAGGAAGGAGTGAAACTGA	140	59.0
	CNT1_1317 rev	AAAGTCCAGCACAGCCAGGAAC		
SLC28A2 (CNT2)	CNT2_1173 for	TGTGCTCTCGCCTCATCAAAGC	103	58.5
	CNT2_1254 rev	GGACATTCCTCTCCTTCCCACG		
SLC28A3 (CNT3)	CNT3_267 for	AGTTGAGCAGGATTCTCCAAG	144	54.0
	CNT3_409 rev	CAGATGATGTGCCGAAGAGT		

Table 2.10 Primers used for the PCR screening of SLC29 family transporters.

Gene	Primer	Sequence 5'-3'	size (bp)	Annealing (°C)
SLC29A1 (ENT1)	ENT1_1348 for	CGAGCACGATGCCTGGTTCA	105	58.5
	ENT1_1433 rev	GCTGGCTTCACTTTCTTGGGC		
SLC29A2 (ENT2)	ENT2_807 for	GGAATCAGAGCCAGATGAGCCC	123	59.0
	ENT2_930 rev	GGGAAGACGGACAGGGTGACT		
SLC29A3 (ENT3)	ENT3_601 for	TGAGGAACTCCCAGGCACTGAT	146	59.0
	ENT3_746 rev	GAGCACGAGGAAGATGGTGGC		

2.3 Antibodies

Antibody	Stock concentration	Provider/ Catalogue Number
p53 (DO-1) mouse monoclonal IgG_{2a}	200µg/ml	Santa Cruz Biotechnology/ sc126
actin mouse monoclonal IgG_1	100µg/ml	Dianova/ DLN-07274
Goat anti-mouse IgG	1.0mg/ml	Calbiochem/ 401215

2.4 Plasmid vectors

Vector	Provider/ Catalogue Number
pcDNA5/FRT/TO	Invitrogen/ V6520-20
pDONR221	Invitrogen/ 12536-017
pEF5/FRT/V5-DEST	Invitrogen/ V6020-20
pOG44	Invitrogen/ V6005-20

2.5 Kits

Kit name	Provider/ Catalogue Number
BP Clonase II Enzyme Mix	Invitrogen/ 11789-020
LR Clonase II Enzyme Mix	Invitrogen/ 11791-019
Gateway Vector Conversion System with One Shot ccdB Survival Competent Cells	Invitrogen/ 11828-029
CompactPrep Plasmid Mini Core Kit	Qiagen/ 12745
Nucleospin Plasmid	Macherey Nagel/ 40588.50
M-MuLV Reverse Transcriptase, RNase H minus	AppliChem/ A5211,50000

2.6 Cloning competent cells

Bacteria strains used for maintenance of plasmid constructs are listed below.

Cells	Provider/ Catalogue number	Genotype
One Shot TOP10 Chemically Competent *E.coli*	Invitrogen/ C4040-03	F^- *mcr*A Δ(*mrr-hsd*RMS-*r*BC) ϕ80*lac*ZΔM15Δ l*ac*X74r*ec*A1 *ara*Δ139 Δ (*ara-leu*)7697 *gal*U *gal*K *rps*L (Str^R) *end*A1 *nup*G

One Shot *ccdB* Survival™ T1R Competent Cells	Invitrogen/ C7510-03	F- *mcr*A Δ(*mrr-hsd*RMS-2 *mcr*BC) Φ80*lac*ZΔM15 Δ*lac*X74 *rec*A1 *ara*Δ139 Δ(*ara-leu*)7697 *gal*U *gal*K *rps*L (StrR*end*A1 *nup*G *tonA*::P*trc-ccd*A

2.7 Growth media

All growth media listed here were sterilized by autoclaving

Media	Composition
LB (Luria-Broth)	10 g NaCl, 10 g tryptone, 5 g yeast extract, to 1 L with dd H_2O pH 7.0 with 5N NaOH
DMEM-LG (Dulbecco's Modified Eagle Medium-Low Glucose)	10.03 g DMEM-LG, 3.7 g $NaHCO_3$ to 1 L with dd H_2O
DMEM-HG (Dulbecco's Modified Eagle Medium-High Glucose)	13.44 g DMEM-HG, 3.7 g $NaHCO_3$ to 1 L with dd H_2O
RPMI 1640	10.39 g RPMI-1640, 2 g $NaHCO_3$ to 1 L with dd H_2O

2.8 Solutions and buffers

Solution	Composition
Agarose gel electrophoresis loading buffer (6X)	00.09% bromophenol blue, 60.0% glycerol, 60.00 mM EDTA
Ampicillin stock solution	500 mg/ml in dd H_2O

Ethidium bromide stock solution	10 mg/ml in dd H_2O
Glycine solution	0.10 M glycine-HCl, pH 3
Kanamycin stock solution	50 mg/ml in dd H_2O
MR solution (Mammalian Ringer)	130 mM NaCl, 4 mM KCl, 1 mM $CaCl_2$, 1 mM $MgSO_4$, 20 mM HEPES, 1mM NaH_2PO_4, 18 mM glucose, pH 7.4
Na^+ free MR (Sodium free Mammalian Ringer)	130 mM TMACl, 4 mM KCl,1 mM $CaCl_2$ 1 mM $MgSO_4$, 1mM $TMAPO_4$, 20 mM HEPES, 18 mM glucose, pH 7.4
SDS-PAGE electrophoresis running buffer (10X)	30.30 g Tris base, 144.0 g glycine, 10.0 g SDS, to 1 L with dd H_2O
SDS-PAGE stacking gel buffer	0.5 M Tris-HCL pH 6.8, 0.4 % SDS in dd H_2O
SDS-PAGE separation gel buffer	1.5 M Tris-HCl pH 8.8 0.4 % SDS in dd H_2O
SDS-PAGE sample buffer (2X)	0.125 M Tris-HCl, pH 6.8, 4.0 % SDS 20 % glycerol (v/v), 10 mM DTT 0.02 % bromophenol blue
TAE buffer (10X)	0.4 M Tris acetate, 10 mM EDTA, pH 8.3
Lysis buffer	400 mM NaCl, 1 mM EDTA 10 mM Tris/HCL pH 8, 0.1 % Triton X 100

Western Blot buffer	25 mM Tris base, 192 mM glycine, 20 % (v/v) methanol

2.9 Chemicals and Enzymes

Chemicals were bought from Sigma-Aldrich (Hamburg, Germany), Applichem (Darmstadt, Germany) Merck (Darmstadt, German) and Calbiochem (Gibbstown, USA). Radioactive chemicals were bought from Amersham Bioscience (Freiburg, Germany).

Restriction endonucleases were purchased from New England Biolabs Inc (Beverly, MA, USA) or MBI Fermentas (Vilnius, Lithuania). T4 DNA ligase was purchased from Boehringer Mannheim (Mannheim, Germany).

2.10 Software

Listed below are the software and online servers used to analyze raw sequence data, perform sequence alignments and primer design.

Software

Program	Use	Reference
Chromas	sequence reading program	Technelysium Pty Ltd
Microsoft Excel	evaluation of uptake experiments	Microsoft Corporation
SigmaPlot	statistical analyses	Jandel Corporation
Reference Manager	managing of bibliographic references	Wintertree Software Inc

Online sequence analysis servers

Program	Use	Reference
Entrez Browser	sequence retrieval	http://www.ncbi.nlm.nih.gov/Entrez/
MAP	multiple sequence alignments	http://genome.cs.mtu.edu/map.html
Blast	Sequences alignments	http://www.ncbi.nlm.nih.gov/BLAST/
ClustalW	Sequences alignments	http://www.ebi.ac.uk/clustalw/

2.11 Equipment

Appliance	Model	Manufacturer
Centrifuges	Biofuge fresco	Heraeus (Osterode, Germany)
	5417R	Eppendorf (Hamburg, Germany)
Circulating water baths	D8	Haake (Karlsruhe, Germany)
Gel chamber	Midi	MWG-Biotech (Ebersberg, Germany)
Gel documentation	Gel Print 2000 I	Biophotonics (Ann Arbor, MI, USA)
Blot imaging	LAS 3000 Imager	Fujifilm (Duesseldorf, Germany)
Microplate reader	Model 680	Bio-Rad (Munich, Germany)
Microwave	Privileg 8017	Quelle Schickedanz (Fuerth, Germany)
pH meter	pH-Meter 611	Orion Research Inc (Beverly MA, USA)
Real time PCR system	Mx3005p	Stratagene (Waldbronn, Germany)
Scintillation counter	1500 Tri-Carb	Packard Instrument Co (Meridien, USA)
Shaking incubator	3031	GFL (Burgwedel, Germany)
Spectrophotometer	GeneQuant II	Pharmacia (Uppsala, Sweden)
Thermocycler	PTC-200	MJ Research (Watertown MI, USA)
UV transilluminator	TM40	UVP Inc (Upland, CA, USA)
Vortex	MS1	IKA (Staufen, Germany)

3. METHODS

3.1 Cell culture

3.1.1 Suspension cells

Lymphoma cell lines were grown in 100 ml cell culture flasks at 37°C with 5% CO_2. Cells were grown in supplemented RPMI-1640 media and for passaging the suspension cells, 5 ml of cell culture was diluted with 20 ml medium in the culture flasks.

3.1.2 Adherent cells

CHO and HEK-293 cells were grown in 100 mm culture plates at 37°C with 5% CO_2. Cells were cultivated routinely in culture medium (supplemented DMEM-LG and DMEM-HG, respectively) and passaged 1:5 every third day. Before splitting, medium was removed and cells were rinsed once with PBS. Then, 2.5 ml of pre-warmed EGTA-containing "milieu C" was added per 100 mm culture dishes. After incubation at 37°C for 2-3 minutes (time required for detachment the cells from the plate), 2.5 ml of complete medium per culture dish was added and the cell suspension transferred into a sterile 15 ml Falcon tube. The cells were collected by centrifugation at room temperature at 1000 rpm for 5 minutes. Supernatant was aspirated and cells resuspended 1:2 in fresh complete medium, counted using the Hemacytometer (before counting, 20 µl of cell suspension was diluted with 180 µl of medium for better accuracy) and seeded in the required density. Since the HEK-293 cells come off the plate easily, culture dishes were coated with polylysine (Sigma). Therefore, 500 µl of polylysine solution was pipetted into each well of 24 well plates shortly before seeding, aspirated after a 5 minutes and the plates were allowed to dry before seeding the cells. For transport experiments, cells were plated into the 24 well plates at the density of 2×10^5 cells per well up to 72 hours before the experiment.

3.2 RNA Preparation

Total RNA isolation from cell lines and patient samples was done to carry out RT-PCR and Real-time PCR using the products. TRIZOL Reagent is a mono-phasic solution of phenol and guanidine isothiocyanate. TRIZOL Reagent maintains RNA integrity during sample homogenization, while lysing cells and dissolving cell components. The addition of chloroform to the homogenized sample, followed by centrifugation separates the sample

solution into two phases: aqueous and organic. The aqueous phase contains the RNA and this RNA is recovered by precipitation with isopropyl alcohol.

Homogenization of samples was done in 1 ml TRIZOL. The nucleoprotein complexes were incubated at room temperature for 5 minutes. This was followed by the addition of 0.2 ml chloroform, shaking for 15 seconds and incubation at room temperature for 10 minutes. Centrifugation of the mix was done at 12000 x g, which separated the mixture into the lower red (phenol-chloroform phase) (contains proteins), the interphase (contains DNA) and the colourless upper aqueous phase (contains RNA). The RNA-containing aqueous phase was transferred to a fresh tube and RNA precipitated using 0.5 ml isopropanol per 1 ml TRIZOL. Samples were kept on ice for 15 minutes and centrifuged for 10 minutes at 4°C at 12000 x g. The supernatant was removed and the RNA pellet (formed as a gel like precipitate) washed with 75% ethanol by vortexing and subsequent centrifugation for 8 minutes at 7500 x g at 4°C. The excess isopropanol was removed from the RNA pellet by air drying for 10 minutes and resuspended in RNase free water.

3.3 cDNA Synthesis

Complementary DNA (cDNA) sequences are derived from the coding sequences of specific genes using random primer. The viral RNA-dependent DNA polymerase, called reverse transcriptase, uniquely synthesizes DNA products from primed RNA templates. The first step includes the purification of mRNA. Nonspecific template primers (random primers) may then be used to initiate cDNA synthesis.

2 µg RNA was mixed with 1 µl Random primer and this mixture was made up to 14 µl with dd H_2O, followed by an incubation of 10 minutes at 70°C and a further incubation of 2 minutes at 4°C. Following incubation, a mixture containing 4 µl 5X RT buffer, 1 µl 10 mM dNTPs and 1 µl MuLV enzyme (200 U/ml) was added to each reaction mix. The reaction mix was incubated at 37°C for 1 h, followed by 10 minutes incubation at 70°C to inactivate the MuLV enzyme.

3.4 Polymerase chain reaction

The polymerase chain reaction (PCR) is a three step process which allows the amplification of a specific DNA region. Each cycle consists of: DNA template denaturation, primer annealing, and primer extension. The reaction, carried out in a thermal cycler, involves the denaturation

of the double helix at 94°C, followed by a lowering of temperature to allow the gene specific primers to anneal. The primers chosen are complementary to the flanking region of the target DNA. The annealing temperature is optimized depending on the length and base sequence of the annealing primers. The third step is the extension step in which the heat stable DNA polymerase catalyzes DNA synthesis using the target DNA as template and dNTPs provided in the reaction mix as building units. Extension time depends on the length of the target DNA. Each PCR cycle results in the formation of two new DNA strands identical to the target region defined by the primers.

Each 50 µl reaction mix contained 5 µl of RT-PCR product (template cDNA), 1 µl of each gene specific primer (100 pmol/µl), 8 µl dNTPs (10 mM each), 5 µl buffer (10X buffer), 1 µl *Taq* polymerase (5 U/µl) and 29 µl double distilled water (dd H_2O). PCR conditions used were: 3 minutes at 94°C, 30 cycles of 40 seconds denaturation at 94°C, 50 seconds annealing at the specific annealing temperature, 1 minute extension at 72°C. The 30 cycles were followed by a final step of 5 minutes at 72°C.

3.5 Real-time PCR

Real-time PCR allows the detection of the increase in the amount of DNA as it is amplified. The TaqMan probe used in our studies consists of two fluorophores. While the probe is attached or unattached to the template DNA; and before the polymerase acts, the quencher fluorophore, found at the 3' end of the probe reduces the fluorescence from the reporter fluorophore, found at the 5' end of the probe. Taq polymerase action results in the amplification and subsequent removal of the TaqMan probe from the template DNA. This results in a separation of the quencher from the reporter, allowing the reporter dye to emit its energy, which is then quantified by the computer.

For TaqMan based PCR, the reaction mix included 2X reaction buffer, 20X TaqMan probe, 5 µl of cDNA, nuclease free H_2O to a volume of 25 µl. The thermocycler was programmed as follows: 1 cycle with 2 min at 52°, 10 min at 95°, followed by 40 cycles including 15 s at 95° and 1 min at 61°C. ΔCt evaluation ($C_{T\ target} - C_{T\ reference}$)] was done for the analysis of TaqMan based real-time PCR data. GAPDH was used as an endogenous control (as an active reference). Normalization of gene quantification was done for differences in the amount of total nucleic acid added to each reaction.

3.6 Agarose gel electrophoresis

Agarose gel electrophoresis is a method to separate DNA strands by size. The size of the strands is estimated by comparison to known fragments. Negatively charged DNA molecules are pulled through the agarose matrix using an electrical field. Migration speed of a DNA fragment in the gel is inversely proportional to its size. Increasing the agarose concentration of a gel reduces the migration speed and enables separation of smaller DNA molecules. The central dye used is ethidium bromide, which fluoresces under UV light when intercalated with DNA. DNA fragments run in an ethidium bromide-treated agarose gel enables the visualization of distinct bands under UV light.

For preparing 1% agarose gel, 1.0 g agarose were dissolved in 100 ml TBE buffer by heating the mix in a microwave. The solution was allowed to cool down before adding 3 µl ethidium bromide stock solution (1 mg/ml). The mix was poured in a casting unit and a spacer comb placed. Samples were prepared by adding 5 µl of the agarose gel loading buffer to 20 µl of each sample under test. 5 µl of the appropriate molecular weight marker was loaded alongside each electrophoretic run. The electrophoresis was done at 100 V for approximately 50 minutes after which the DNA bands were visualized under the UV transilluminator.

3.7 Plasmid Purification

A clone positive for the insert was aseptically transferred to 5 ml or to 200 ml sterile LB medium containing the resistance antibiotic (100 µl/ml for ampicillin and 50 µl/ml for kanamycin) and allowed to grow overnight at 37°C, 250 rpm. Plasmids were prepared from the bacterial cultures using the CompactPrep Plasmid Midi Core Kit for midi preps and the Nucleospin Plasmid kit for mini preps.

3.7.1 Plasmid Midi-prep

The CompactPrep Plasmid Midi Core Kit from Qiagen is an anion exchange resin-based plasmid purification kit. Bacterial cells are first lysed through the alkaline lysis method using a combination of NaOH and SDS (Buffer P2). SDS solubilizes the cell membrane lipids and proteins resulting in the release of the cell contents, while NaOH results in DNA and protein denaturation. The addition of acidic potassium acetate (Buffer P3) results in the precipitation of potassium dodecyl sulphate (KDS) where denatured proteins, genomic DNA and cellular debris become entrapped in this salt-detergent complex. Plasmid DNA being smaller and

covalently closed, renatures correctly and remains in the lysate solution as it is neutralized. The resulting supernatant is filtered and loaded on a QIAfilter cartridge. The eluted DNA is washed following which it is loaded to the CompactPrep column. The DNA is bound as a thin layer and is subsequently eluted using Tris.Cl buffer.

A 100 ml overnight bacterial culture was centrifuged at 6000 x g for 15 minutes. The supernatant was decanted and the pellet resuspended in 5 ml of the provided Buffer P1 (ice cold with RNase A). The homogenized lysate was transferred to a fresh 50 ml Starstedt tube and alkaline lysis done by adding 5 ml of Buffer P2 added. The mixture was shaken well and incubated at room temperature for 5 minutes. The lysate was neutralized by adding 5 ml Buffer P3. The lysate was then poured into the barrel of the QIAfilter Cartridge and incubated at room temperature for ten minutes. The lysate from the cartridge was passed into a 50 ml tube. The cleared lysate was washed with 5 ml Buffer BB. This mix was transferred to the CompactPrep column. The DNA was washed with 700 µl Buffer PE. The plasmid DNA was eluted using 200 µl Buffer EB.

3.7.2 Plasmid Mini-prep

The NucleoSpin Plasmid from Macherey-Nagel kit is based on the use of single solution for cell suspension, alkaline lysis as well as for DNA binding to a silica-based membrane. A high-salt buffer is used to allow only DNA to be adsorbed to the silica membrane. Precipitated proteins, RNA and metabolites flow through the column. The bound DNA is eluted in low-salt buffer.

A 5 ml bacterial culture was centrifuged at 11,000 x g for 5 minutes and the supernatant decanted. The pellet was resuspended in 250 µl of the ice-cold lysis buffer (Buffer A1) and the suspension made homogeneous by vortexing. 250 µl Buffer A2 was added to the the homogenized lysate and the mixture incubated for 5 minutes at room temperature, following which 300 µl Buffer A3 was added. Lysate clarification was done by centrifuging the mix for 5 minutes at 11,000 x g and the supernatant loaded onto a NucleoSpin Plasmid Column. The loaded spin column was centrifuged for 1 minute, washed with 600 µl of the diluted wash buffer (Buffer A4) and centrifuged again. The flow through was discarded and the spin column dried by centrifugation at full speed for 1 minute. Elution of the bound DNA was done adding 50 µl of the provided elution buffer, Buffer AE to the centre of the membrane and centrifuging at maximum speed for 1 minute.

3.8 DNA Sequencing

Sequencing was performed by automated dye terminator cycle sequencing method (Applied Biosystems), at a centralized facility within the university. In this method a premix solution, containing four dideoxynucleotides (ddNTPs), each labeled with a different fluorescent dye, and unlabelled deoxynucleotides is mixed with the template DNA and one sequencing primer. The fluorescence of dye-containing polynucleotides was stimulated by 40 mW argon laser (488 nm and 514 nm) and the fluorescent signal was identified by the detector system of the DNA sequencer (automatic sequencer: ABI Prism, Applied Biosystems) and quantified.

300-500 ng DNA were mixed with 10 pmol primer, 6X SeqMix, 5X Buffer and the volume made up to 10 µl with dd H_2O. The sequencing reaction comprised 25 cycles of: 96°C for 30 seconds, 50°C for 50 seconds and 72°C for 4 minutes. Amplification products were precipitated by the addition of 50 µl of 100 % ethanol, 1 µl of 3 M Na acetate and 1 µl of 125 mM EDTA, followed by 5 minutes' incubation. After the incubation, centrifugation of the samples was done for 20 minutes at 14,000 U. Supernatant was discarded carefully, without disturbing the pellet. The product was washed with 250 µl of 70 % ethanol and centrifugation for 10 minutes at 14000 U. Supernatant was removed completely and pellet was air dried and finally resuspended in 30 µl of Hi-Di. The sequence was assembled and analyzed with various software packages, as listed in Section 2.10.

3.9 Generation of stable transfected cell lines

NaDC3- FlpIn T-Rex HEK 293 cell line was prepared using Gateway Cloning Technology. This uses site-specific recombination properties of bacteriophage lambda. Four steps are involved: The first step is the generation of an entry clone where the gene of interest is introduced into a donor vector. The second step includes making a destination vector with a reading frame cassette containing the appropriate recombination sites. The generation of the expression vector involves recombining the donor vector and the destination vector to express the gene of interest, in this case NaDC3. The final step is the stable transfection of the Flp-In T-Rex HEK 293 cells with the generated expression vector.

3.9.1 Generation of the entry clone

Generation of the Entry Clone involved carrying out a BP Reaction, so named because of the attachment B and the attachment P sites involved. The BP Reaction transfers the gene in the

Expression Clone (between *att*B sites) into a Donor vector (containing *att*P sites), to produce a new Entry Clone (*att*L sites) which was selected on Kanamycin plates. This reaction is catalyzed by the BP Clonase mix of recombination proteins. 150 ng of attB-site containing NaDC3 Expression Clone was mixed with 150 ng/µl pDONR 221 and the reaction volume made up to 8 µl with TE buffer (pH 8). 2 µl BP Clonase II enzyme mix was added and the reaction mixture incubated for 1 hour at 25°C. To terminate the reaction, 1 µl Proteinase K was added and sample incubated at 37°C for 10 minutes. The BP reaction was then transformed into One Shot Phage Resistant Cells and plated onto kanamycin (50 µg/ml) plates. Once a gene is flanked by *att*L sites as an Entry Clone, it can be transferred into new expression vectors by recombination with Destination Vectors (via the LR Reaction).

3.9.2 Generation of destination vector

A tetracycline inducible vector was converted into a Destination Vector using the Gateway Vector Conversion System from Invitrogen. 5 µg plasmid vector was digested using *Eco RV* restriction enzyme. Following the removal of 5' phosphates, DNA was adjusted to a final concentration of 50 ng/ µl. Separate ligation mixtures were set up for the three different reading frame cassettes and contained: 50 ng dephosphorylated vector, 2 µl 5X T4 DNA ligase buffer, 2 µl Gateway reading frame cassette (10 ng), 1 µl T4 DNA ligase (I U/µl) and the volume made up to 10 µl with dd H_2O. The ligation mixture was incubated at room temperature for 1 hour, followed by transformation into *ccdB* Survival Competent Cells and finally plated on chloramphenicol (30 µg/ml) plates.

3.9.3 Generation of expression vector

The LR Reaction is a recombination reaction between an Entry Clone and a DestinationVector mediated by the LR Clonase mix of recombination proteins. This reaction transfers DNA segments from the Entry Clone to the Destination Vector, to create an Expression Clone. 150 ng Entry Clone was mixed with 150 ng/µl Destination vector and the volume made up to 8 µl with TE Buffer (pH 8). 2 µl LR Clonase II enzyme mix was added and the reaction mixture incubated for 1 hour at 25°C. To terminate the reaction, 1 µl Proteinase K was added and sample incubated at 37°C for 10 minutes. The LR reaction was then transformed into One Shot Phage Resistant Cells and plated onto selective ampicillin (100 µg/ml) plates.

3.9.4 Transient transfection into Flp-In T-Rex HEK-293 cells

We carried out transient transfection to determine the functionality of the generated expression vector. Flp-In T-Rex HEK- 293 cells were grown overnight at a concentration of 2 x 10^5 cells/ well. Transfection medium was prepared for each well by adding 2 µl Lipofectamine to 48 µl medium without FCS. In another tube, 1 µg plasmid DNA was mixed with medium without FCS to give a final volume of 50 µl. The two tubes were incubated for 5 min at room temperature, followed by mixing the two and further incubation of 20 minutes. 400 µl medium without FCS was added to each well, followed by 100 µl of the transfection mix. Cells were incubated for 4-6 h at 37°C and the medium then changed to that containing FCS. Cells were used for uptake assays the following day.

3.9.5 Stable transfection into Flp-In T-Rex HEK -293 cells

The final step involved introducing the expression vector into Flp-In T-Rex HEK -293 cells. The expression vector containing NaDC3 gene was co-transfected with another plasmid, pOG44, into cells. pOG44 expresses the *Flp recombinase* while the expression vector and the Flp-In cells express the FLP Recombination Target, FRT site. FRT sites serve as recognition and cleavage sites for *Flp recombinase* from pOG44 and allow recombination to occur. The hygromycin resistance gene in the expression vector lacks a promoter and the initiation codon; the action of *Flp recombinase* brings these into the correct frame. The stable cell line is thus resistant to hygromycin B. 6 x 10^5 cells were seeded into one well of a 6-well plate and incubated overnight. Co-transfection of the NaDC3 Expression Vector and pOG44 in 1:9 ratio was done using Lipofectamine. Following transfection, cells were incubated at 37°C for 5 hours and medium changed with that containing 10% FCS. After another overnight incubation, cells were transferred to a 100 mm dish and incubated to enable attachment for 5-6 hours, following which Hygromycin B was added (175 µg/ml). Cells were allowed to grow and medium changed after one week. After another 14 days, stable transfected colonies were picked and transferred to a 96-well plate. When the colonies were confluent, they were further transferred to 24-well, 60 mm dish and ultimately to a 100 mm dish.

3.10 Transformation into competent cells

The process by which exogenous DNA is introduced into bacterial cells is known as transformation. Transformed bacterial cells with plasmids having an appropriate origin of replication recognized by the host DNA polymerases offers a method for plasmid

propagation. Bacteria that are capable of transformation are referred to as competent bacteria. Competency can be induced by a manipulation that causes the outer membrane of the bacteria to partially lose its integrity. Calcium chloride treatment compromises the outer membrane of some *E.coli* strains. The resulting *E.coli* is called chemically competent and can be transformed.

1 µl of the ligation mix were added to 50 µl of partially thawed chemically competent *E.coli*. After incubating the mix for 30 minutes on ice, it was transferred to a 37°C heat block for 30 seconds (heat shock). 250 µl of pre-warmed SOC medium was added to the transformation mix. The mixture was incubated at 250 rpm, 37°C for 60 minutes to allow the expression of the resistance gene under non-selective conditions. 100 µl of the mix was aseptically spread on a pre-warmed agar plate containing the specific antibiotic. The plate was incubated overnight at 37°C to allow the growth of bacteria successfully transformed with the plasmid.

3.11 Transport studies

Adherent CHO or HEK-293 cells were cultured in 24 well plates and grown until 90 -100% confluence. Directly before uptake, cells were washed three times with 1 ml of Mammalian Ringer solution, pre-warmed to 37°C. The transport media was pre-warmed Mammalian Ringer solution, containing radioactively labeled substance (1 µM [^{3}H]MPP or 18 µM [^{14}C]succinate) and the particular cytostatic (100 µM). 200 µl uptake solution was carefully added to each well and cells incubated in the transport media at room temperature for 5 minutes. After incubation, cells were washed with ice cold PBS solution and lysed by the addition of 500 µl 1 N NaOH for 20 min. After complete lysis, the solution was neutralized with 1 N HCl, transferred to scintillation vials and 2.5 ml Lumasafe scintillation solution added to each sample. The [^{3}H] or [^{14}C] content was measured in a scintillation counter (TriCarb 1500 Packard) over 5 minutes.

3.11.1 Apparent K_m determination

Apparent K_m determination was done to determine substrate affinity of specific transporters. The apparent K_m of a substrate is determined in the presence of a competitive inhibitor at a defined concentration.

CHO cells expressing OCT1 and OCT2 were measured for 1 µM [^{3}H]MPP and 20 µM [^{3}H]MPP uptake over 5 min in Mammalian Ringer in the presence of increasing concentrations of unlabelled irinotecan (0-20 µM). For apparent K_m determination of mitoxantrone and paclitaxel for OCT1, concentrations of 0-140 µM unlabelled cytostatic were used.

3.12 Cytotoxicity studies

3.12.1 MTT assay

A colorimetric assay, the MTT assay is used for measuring the activity of the mitochondrial enzyme, mitochondrial reductase, which reduces the yellow MTT (3-(4,5-Dimethylthiazol-2-yl)-2,5-diphenyltetrazolium bromide) to formazan, giving a purple colour. The insoluble formazan is diluted in hydrochloric acid and the absorbance measured using a spectrophotometer. It is used to determine cell cytotoxicity on application of different substances, which would disrupt metabolic functions. Since the reduction of MTT to formazan takes places only by active reductase enzymes, the test is a measure of active, viable (living) cells.

3.12.1.1 Adherent cells

6-well plates were seeded with 0.5 x 10^3 cells and grown 24 hours to 50- 70% confluence. The cells were incubated with desired substances (100 µM irinotecan/ mitoxantrone/ paclitaxel, 2 mM TEA, 100 µM corticosterone, 100 µM irinotecan/ mitoxantrone/ paclitaxel + 2 mM TEA and 100 µM irinotecan/mitoxantrone/ paclitaxel + 100 µM corticosterone) and incubated for 15 minutes at 37°C. Following this incubation, cells were washed with medium and incubated overnight. Cell viability was determined by adding 750 µg/ ml MTT to each well and a further incubation of 2 hours at 37°C. Purple formazan crystals were then diluted in acidified isopropanol (96% isopropanol + 4% 1 N HCl) and absorbance was measured at 595 nm.

3.12.1.2 Suspension cells

2.5 x 10^4 cells/well were seeded in round-bottom 96-well plates (Sarstedt) and incubated overnight. Cells were then treated with different substances (same as for adherent cells) and incubated at 37°C. After 15 minutes incubation, cells were centrifuged (500 rpm, 10 min) and incubated in fresh medium. After 24 h incubation, cells were centrifuged and the pellet

resuspended in MTT solution (750 µg/ ml in each well). Cells were incubated for 2 h at 37°C and the reaction stopped by adding an equal volume of acidified isopropanol. The amount of reduced MTT was assayed by measuring the absorbance at 595 nm using the Microplate Manager, Model 680 (Bio-Rad Laboratories, Inc).

3.12.2 [^{3}H]Thymidine incorporation

The incorporation of [^{3}H]thymidine into cellular DNA is one of the most common cell proliferation assays. Drug effects are quantitated in the thymidine incorporation assay by measuring inhibition of deoxyribonucleic acid (DNA) synthesis by the proliferating cell population following exposure to anticancer drugs.

OCT expressing CHO cells were incubated for 15 min with cytostatics (100 µM irinotecan/ mitoxantrone/ paclitaxel, 2 mM TEA, 100 µM corticosterone, 100 µM irinotecan/ mitoxantrone/ paclitaxel + 2 mM TEA and 100 µM irinotecan/mitoxantrone/ paclitaxel + 100 µM corticosterone). After the incubation, cells were washed twice with medium and incubated 4h at 37°C. Radioactive thymidine was diluted with the medium to a final activity of 0.2-1 µCi/ml. After 15 min incubation at 37°C, cells were fixed with 5% trichloroacetic acid for 30 min at 4°C. The plate was then washed twice with 500 µl of ice cold PBS and once with 500 µl of ice cold 95% ethanol. For the full solubilisation of genomic DNA, the plate was incubated with 500 µl of 1 N NaOH for 2 hours. Following lysis, the solution was neutralized with 500 µl of 1 N HCl and transferred to scintillaion vials together with 2.5 ml of Lumasafe scintillation fluid. Incorporated radioactivity was measured in the scintillation counter (TriCarb 1500 Packard).

3.13 SDS-PAGE

SDS-PAGE is an analytical technique used for the separation of proteins based on their molecular weights. The anionic surfactant sodium dodecyl sulphate and the treatment of samples with reducing agents like dithiothreitol (DTT) or ß-mercaptoethanol, which causes the denaturation of the protein, imparts a uniform negative charge on the protein samples. The separation during electrophoresis thus takes place based on their mass/ charge ratio. A stacking gel is normally loaded onto a separating gel in a ‘discontinuous’ gel, where the pH conditions of the stacking gel results in the samples to stack at the starting point above the separating gel. The protein samples are then resolved in the separating gel due to differences in their molecular weights.

The composition of the stacking and separating gel for two gels is given in Table 3.1. 50-100 µg of the sample was mixed with 5X sample buffer containing β-mercaptoethanol. The samples were boiled at 95°C for 10 minutes and loaded onto the discontinuous SDS polyacrylamide gel cast in miniprotean 3 system. The prestained molecular weight marker (Fermentas) was loaded in a separate lane. The electrophoretic run was allowed to occur at a constant current of 20 mA with maximum voltage set at 300 V.

Table 3.1 Composition of Stacking and Separating gels used for SDS-PAGE (for two gels)

Component	Stacking gel	Separating gel	
	4%	8%	10%
30% acrylamide/bisacrylamide	666 µl	3.17 ml	3.96 ml
dd H_2O	3.04 ml	5.83 ml	5.04 ml
Stacking gel/Separating gel buffer (4x)+ 0.4% SDS	1.25 ml	3.0 ml	3.0 ml
TEMED	5.0 µl	6.0 µl	6.0 µl
10% APS	25.0 µl	60.0 µl	60.0 µl

3.14 Western blotting

Western immunoblotting allows the determination of a single protein from a mixture of proteins and also gives an estimate on the size of the protein. The method relies on the use of a high-quality primary antibody directed against the protein of interest. The primary antibody is detected using an enzyme-conjugated (eg. peroxidase-conjugated) secondary antibody raised against the Fc portion of the primary antibody. When the enzyme substrate is applied, the conjugated peroxidase catalyzes a light emitting reaction that can be visualized after developing an X-ray film exposed to the membrane. A three step process, western immunoblotting involves the separation of a mixture of proteins in SDS-PAGE in the first step. The second step is the transfer of resolved proteins from the gel onto a membrane support (eg. Polyvinylidene difluoride, PVDF) using electrophoresis. The final step involves the incubation of the membrane with specific antibodies and its subsequent detection for the specific protein.

3.14.1 Transferring resolved proteins from the gel to a PVDF membrane

Following electrophoresis, the gels were equilibrated in chilled (4°C) Western blot buffer. A cut-to-size PVDF membrane was briefly immersed in methanol, washed in dd H_2O and then equilibrated in the blotting buffer. The gel and the activated membrane were sandwiched between fiber pads and filter papers previously soaked in blotting buffer. The assembled gel/ blot sandwich was placed in the Bio-Rad blotting cassette holder and placed in the Bio-Rad blotting tank. The tank was filled with the blotting buffer and electrophoresis run at a constant voltage of 100 V for 60 minutes.

3.14.2 Protein detection on Western blots

After completion of transfer, the PVDF membrane was briefly washed in 1X PBS/ 0.05% Tween to remove residual methanol from the blotting buffer. The membrane was incubated for 1 hour in 5% skimmed milk (in 1X PBS/ 0.05% Tween) at room temperature to block nonspecific binding of the antibodies. The primary antibody solution was then applied to the membrane. The 1 ml solution covered the entire membrane, the membrane sealed with parafilm and incubated overnight at 4°C.

Following overnight incubation, the membrane was washed thrice with washing buffer (1X PBS/ 0.05%Tween), at intervals of 10 minutes. Incubation with peroxidase conjugated secondary antibody (in 1X PBS/ 0.05% Tween) was done for 2 hours at room temperature. This was followed by three washing steps at 10 minutes' intervals. For detection, 750 µl ECL solution A/ solution B (1:1) mix were applied to each membrane and incubated for 5 minutes. The blots were developed using the LAS3000 Imager (Fujifilm).

4. RESULTS

4.1 RT-PCR analysis and quantification of transporter expression in lymphoma cell lines and in Chronic Lymphocytic Leukaemia patient samples

As a first, non-quantitative approach, RT-PCR analysis was done for selected transporter proteins. Using previously designed primers, six lymphoma cell lines as well as lymphocytes, termed here "healthy lymphocytes", purified from healthy blood samples (obtained from the blood bank) were used for this analysis. The six lymphoma cell lines used included four B-lymphoma cell lines: Karpas-422, Raji, SUDHL-4 and L-428 and two T-lymphoma cell lines: Jurkat and HUT-78. The cell lines were all kindly provided by Prof G. Wulf at the Dept. of Haematology and Oncology, University Klinikum, Goettingen.

The screening of SLC transporters in six lymphoma cell lines by RT-PCR was followed by real-time PCR analysis to evaluate and quantify the expression of selected transporters in the lymphoma cell lines as well as in samples from patients of Chronic Lymphocytic Leukaemia, CLL. CLL patient samples were divided into groups of seven and each group was used for quantitative analysis of one transporter family. For real-time analysis, the expression in normal, healthy lymphocytes was set to zero and relative expression of samples analyzed after normalization with GAPDH. Mean results were calculated from three independent experiments with two repeats each for the cell lines. For CLL patient samples, mean results were calculated from two independent experiments with two repeats each.

4.1.1 SLC family transporters not expressed in lymphoma cell lines

The six cell lines used did not show any observable expression the following SLC transporters:

LAT2 (SLC7A8)

NTCP (SLC10A1)

ASBT (SLC10A2)

NaDC3 (SLC13A3)

OATP-A (OATP1A2)

OATP-C (OATP1B1)

OCT2 (SLC22A2)

OCT3 (SLC22A3)

OAT3 (SLC22A7)

OAT4 (SLC22A11)

CNT1 (SLC28A1)

CNT2 (SLC28A2)

CNT3 (SLC28A3)

4.1.2 SLC family transporters expressed in lymphoma cell lines

4.1.2.1 Expression of SLC7 family transporters

Each cDNA preparation was controlled using GAPDH amplification.

The L-amino acid transporter 1, LAT1 (SLC7A5), was expressed in all the lymphoma lines tested (Figure 4.1). Three B-lymphoma cell lines, Karpas-422, Raji and L-428 had similar expression levels, also comparable to LAT-1 expression in the two T-lymphoma cell lines, Jurkat and HUT-78. LAT-1 expression in the fourth B- lymphoma cell line, SUDHL-4 was slightly lower than the other cell lines, but this expression level was comparable to healthy lymphocytes, where LAT-1 expression also seemed lower.

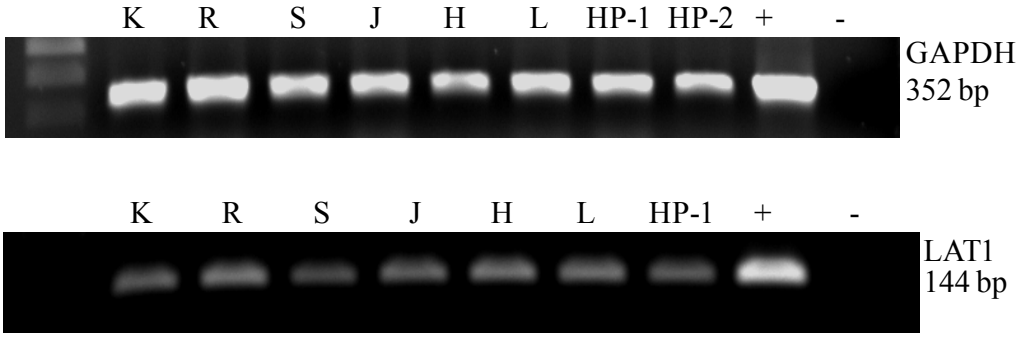

Fig 4.1 RT-PCR screening of SLC7 family transporters in lymphoma cell lines.
K: Karpas-422, R: Raji, S: SUDHL-4, J: Jurkat, H: HUT-78, L: L-428, HP-1: Healthy person sample-1, +: positive control, -: negative control. Also shown is a representative GAPDH amplification, used as cDNA quality control.

4.1.2.2 Expression of SLC16 family transporters

The monocarboxylate transporters exhibited high expression levels in lymphoma cell lines (Figure 4.2). Among the MCT members, the highest expression was observed for MCT1 (SLC16A1), with all six cell lines exhibiting a much stronger expression than in healthy lymphocytes.

MCT2 was expressed at comparatively lower levels than MCT1. While four cells lines, Karpas-422, Raji, Jurkat and HUT-78 exhibited similar expression levels, MCT2 expression was lower in SUDHL-4. The B- lymphoma cell line, L-428 showed an extremely low expression of MCT2. The expression of MCT2 was also lower in healthy lymphocytes than in five cell lines.

Among the cell lines, L-428, Karpas-422 and Jurkat demonstrated the strongest expression of MCT4. SUDHL-4 and HUT-78 had comparable expression to the healthy lymphocytes samples tested. The B-lymphoma cell line, Raji, had a lower expression of MCT4.

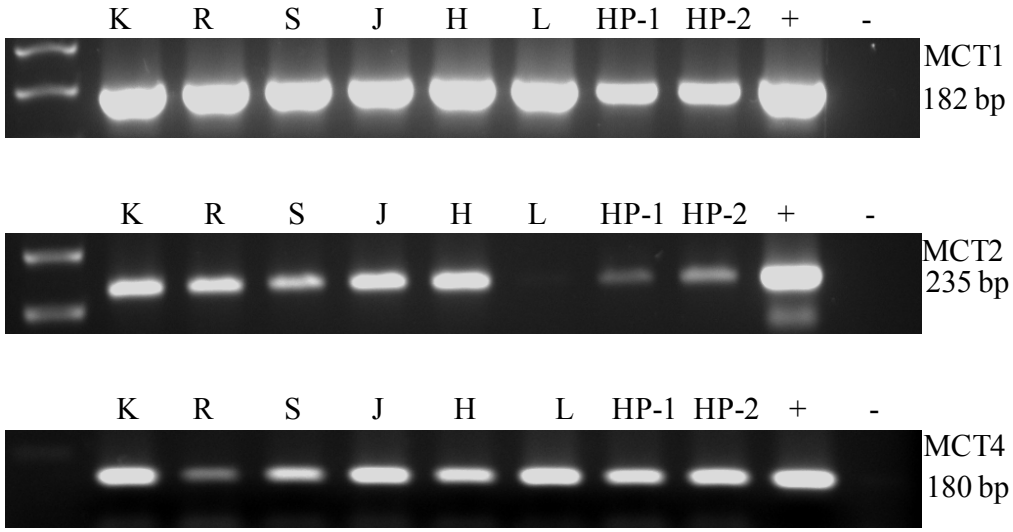

Fig 4.2 RT-PCR screening of SLC16 family transporters in lymphoma cell lines. K: Karpas-422, R: Raji, S: SUDHL-4, J: Jurkat, H: HUT-78, L: L-428, HP-1: Healthy person sample-1, HP-2: Healthy person sample- 2, +: positive control, -: negative control.

Since MCT4 exhibited more expression changes within the cell lines, only MCT4 (SLC16A3) was quantified using real-time PCR in lymphoma cell lines and CLL patient samples. In general, MCT4 was expressed at much higher levels in lymphoma cell lines than in healthy lymphocytes, with Raji and SUDHL-4 being exceptions where the expression was lower. In

healthy lymphocytes, MCT4 appeared at cycle 30 while it appeared at cycles 25, 38, 38, 28, 30 and 23 in Karpas-422, Raji, SUDHL-4, Jurkat, HUT-78 and L-428, respectively. Figure 4.3 shows the ΔCt values after normalization with the housekeeping gene, GAPDH, to correct for differences in the amount of cDNA added to each reaction. There was an 8 cycle difference between Karpas-422 and healthy lymphocytes and thus MCT4 was expressed 256 times higher in Karpas-422 than in healthy lymphocytes. In Raji and SUDHL-4, the expression of MCT4 was slightly downregulated, with the healthy samples expressing more MCT4. In Jurkat and HUT-78, the expression was 64 times that in healthy lymphocytes. The cycle difference between L-428 and healthy lymphocytes was around 10, indicating a very high expression of MCT4 in this cell line.

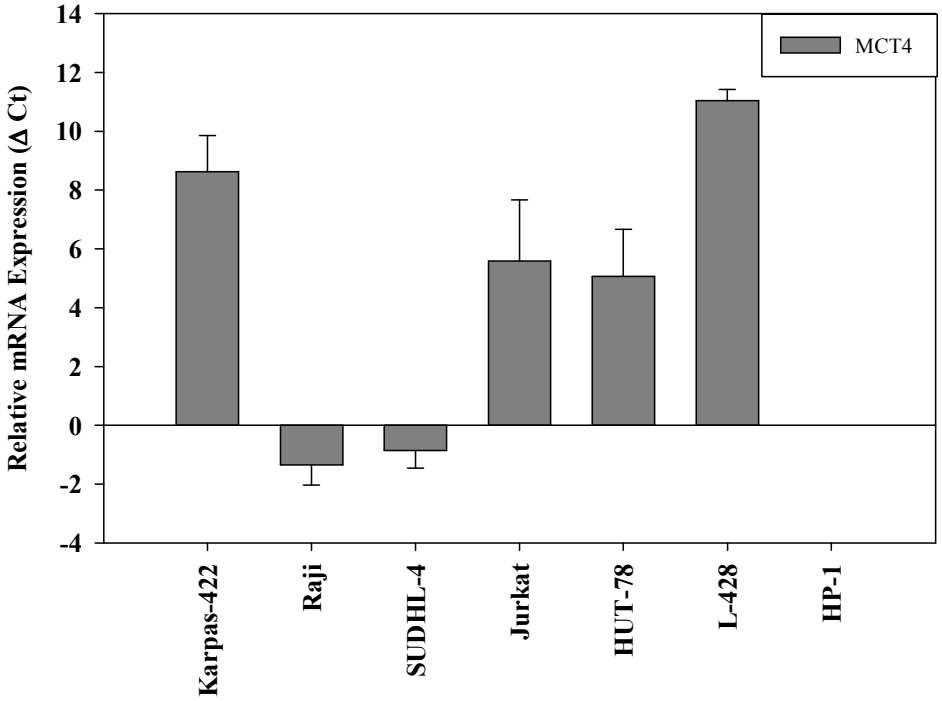

Fig 4.3 TaqMan real-time PCR analysis for MCT4 expression in total RNA extracted from six lymphoma cell lines. MCT4 expression was normalized using GAPDH. Expression in healthy samples obtained from the blood bank was set to 0.

Seven CLL patient samples were analyzed for MCT4 expression (Figure 4.4). In general, MCT4 expression was downregulated in all samples tested. While in the healthy lymphocytes, MCT4 was expressed at cycle 35, in the patient samples tested, MCT4 expression was

between cycles 32- 37. After normalization with GAPDH, there was a 256 times higher expression of MCT4 in healthy lymphocytes than in CLL patient samples. One patient sample, CLL11, did not express MCT4.

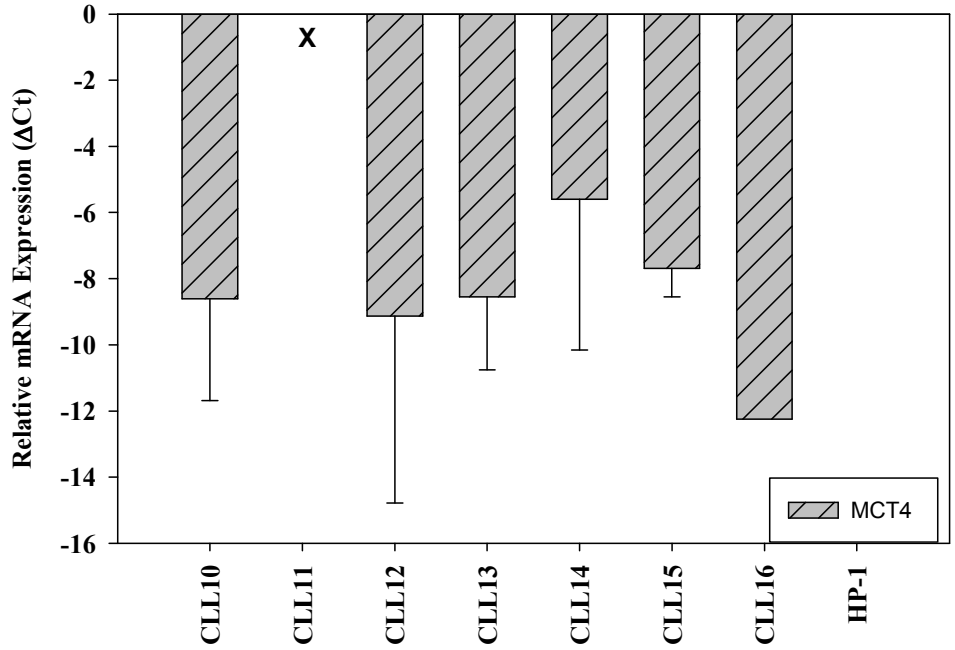

Fig 4.4 TaqMan real-time PCR analysis for MCT4 expression in total RNA extracted from peripheral blood from CLL patients. MCT4 expression was normalized using GAPDH. Expression in healthy samples obtained from the blood bank was set to 0. X denotes no expression of MCT4 in CLL11.

4.1.2.3 Expression of SLC19 family transporters

The folate transporter, RFT (SLC19A1), was expressed in all cell lines tested (Figure 4.5). The expression was the strongest in L-428. The healthy lymphocytes exhibited a relatively lower expression than the cell lines.

Thiamine transporter ThTr1 (SLC19A2) was expressed in all cell lines. However, SUDHL-4 showed a very low expression of ThTr1, while the other five cell lines exhibited a high expression. The expression level in healthy lymphocytes was seemingly lower than the five cell lines.

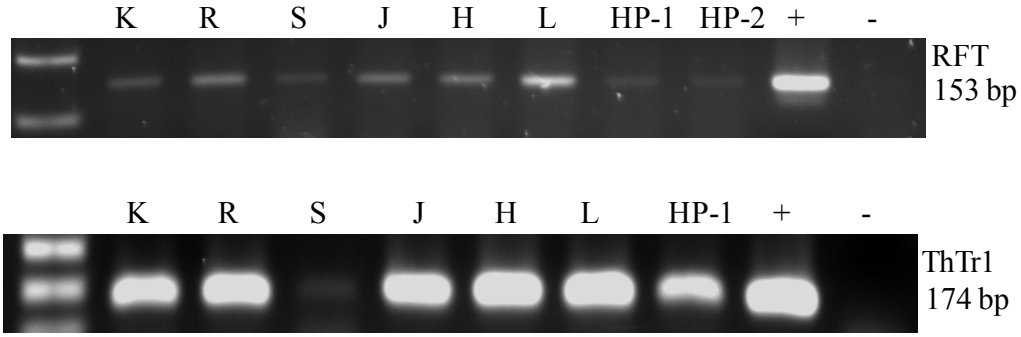

Fig 4.5 RT-PCR screening of SLC19 family transporters in lymphoma cell lines. K: Karpas-422, R: Raji, S: SUDHL-4, J: Jurkat, H: HUT-78, L: L-428, HP-1: Healthy person sample-1, HP-2: Healthy person sample- 2, +: positive control, -: negative control.

4.1.2.4 Expression of SLCO (SLC 21) family transporters

SLCO transporters were differentially expressed in the lymphoma cell lines, as shown in Figure 4.6. OATP-B (OATP2B1) was expressed in only two B- lymphoma cell lines, SUDHL-4 and L-428. Healthy lymphocytes did not express OATP-B.

OATP-D (OATP3A1) was expressed in five cell lines. The expression was the strongest in Jurkat. Raji had a comparatively lower expression of OATP-D. Karpas-422 did not express OATP-D while the expression of the gene in the healthy lymphocytes was very low.

OATP-E (OATP4A1) was expressed in all six cell lines tested. Karpas-422, SUDHL-4, Jurkat and L-428 exhibited comparable levels of expression while HUT-78 exhibited the highest expression of OATP-E. OATP-E expression in Raji was stronger than observed in other B-lymphoma cell lines. In healthy lymphocytes, OATP-E expression was very low.

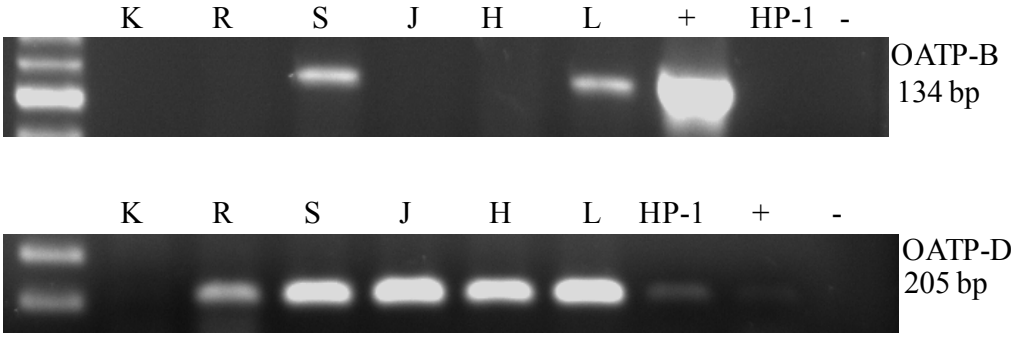

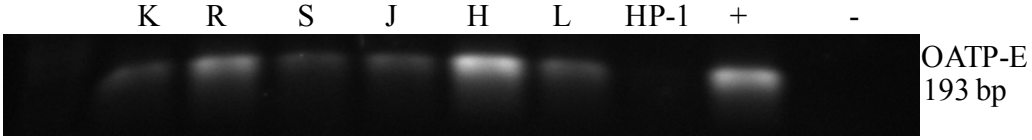

Fig 4.6 RT-PCR screening of SLCO (SLC21) family transporters in lymphoma cell lines. K: Karpas-422, R: Raji, S: SUDHL-4, J: Jurkat, H: HUT-78, L: L-428, HP-1: Healthy person sample-1, +: positive control, -: negative control.

For real-time PCR analysis, we quantified the expression of OATP-B (OATP2B1) and OATP-E (OATP4A1).

OATP-B was expressed at high levels in three B- lymphoma cell lines, Karpas-422, Raji and L-428 (Figure 4.7). While the expression of OATP-B was observed between cycles 25-28 in the three cell lines, there was no expression of OATP-B in healthy lymphocytes even after 40 cycles. The figure shows OATP-B expression in lymphoma cell lines after normalization with GAPDH. The gene was not expressed in SUDHL-4, Jurkat and HUT-78 after 40 cycles.

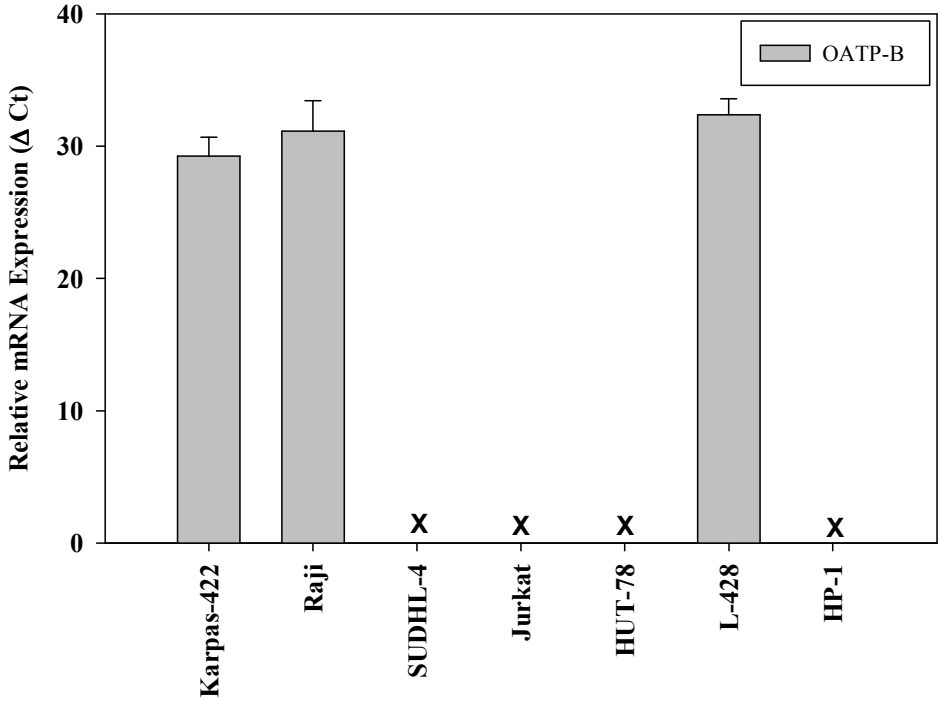

Fig 4.7 TaqMan real-time PCR analysis for OATP-B expression in total RNA extracted from six lymphoma cell lines. OATP-B expression was normalized using GAPDH. No expression of OATP-B was seen in healthy samples. X denotes no expression of OATP-B in the four cell lines.

OATP-E expression was also examined in the six lymphoma cell lines (Figure 4.8). Jurkat showed the strongest expression of the gene with the expression observed at cycle 25. After normalization, Jurkat expressed OATP-E 65000 times higher than healthy lymphocytes, where the gene expression was observed at cycle 34. Karpas-422 and Raji also exhibited more than 4000 times higher OATP-E expression than healthy lymphocytes. The expression of the gene in SUDHL-4, HUT-78 and L-428 was also calculated to be more than 16 times that in healthy lymphocytes. In the cell lines tested, SUDHL-4 showed the lowest expression.

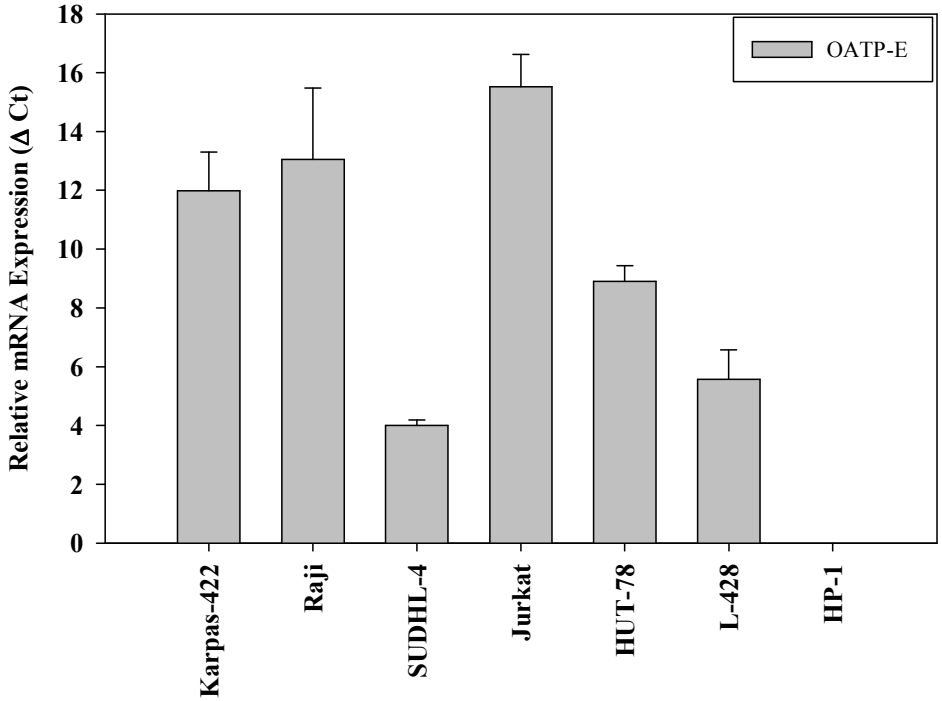

Fig 4.8 TaqMan real-time PCR analysis for OATP-E expression in total RNA extracted from six lymphoma cell lines. OATP-E expression was normalized using GAPDH. Expression in healthy samples obtained from the blood bank was set to 0.

The seven patient samples tested for OATP-B did not show any observable gene expression.

The same set of patient samples was also tested for OATP-E expression (Figure 4.9). While OATP-E was observed at cycle 29 in healthy samples, it appeared between cycles 32 and 37 in the patient samples. Four of the seven patients samples tested exhibited 16 to 256 times lower expression of OATP-E than healthy lymphocytes. Patient samples CLL11 and CLL16

did not express OATP-E after 40 cycles. Patient sample CLL12 showed a slightly higher expression of the gene than healthy samples.

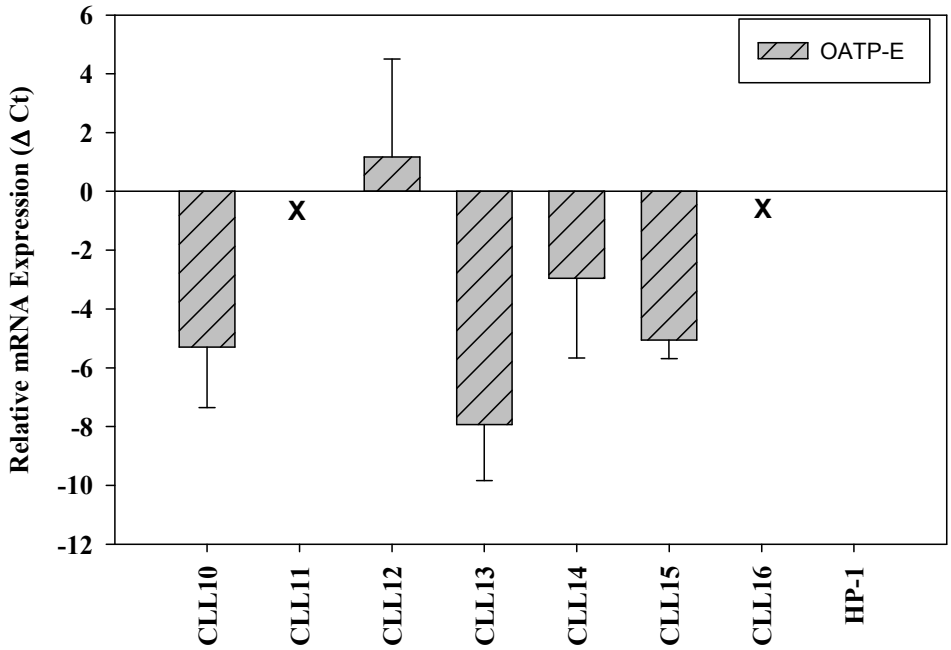

Fig 4.9 TaqMan real-time PCR analysis for OATP-E expression in total RNA extracted from peripheral blood from CLL patients. OATP-E expression was normalized using GAPDH. Expression in healthy samples obtained from the blood bank was set to 0. X denotes no expression of OATP-E in CLL11 and CLL16.

4.1.2.5 Expression of SLC22 family transporters

OCT1 (SLC22A1) was expressed in the six lymphoma cell lines we tested (Figure 4.10). Karpas-422, SUDHL-4 and Jurkat had a seemingly higher expression of the gene. Healthy lymphocytes demonstrated a much lower expression of OCT1 than the cell lines.

Organic anion transporter 1, OAT1 (SLC22A6) was also expressed in all six cell lines, The expression was the strongest for Karpas-422. The expression in Jurkat, HUT-78 and L-428 was comparable to that in healthy lymphocytes.

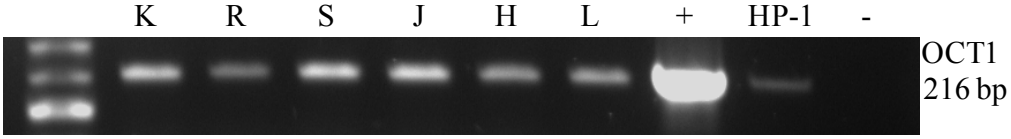

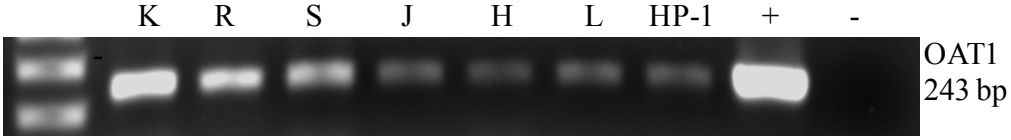

Fig 4.10 RT-PCR screening of SLC22 family transporters in lymphoma cell lines. Of the organic cation transporters tested, only OCT1 (SLC22A1) demonstrated expression in the cell lines. OAT1 (SLC22A6) was the only organic anion transporter expressed. K: Karpas-422, R: Raji, S: SUDHL-4, J: Jurkat, H: HUT-78, L: L-428, HP-1: Healthy person sample-1, +: positive control, -: negative control.

Real-time PCR analysis of OCT1 revealed a higher expression of the gene in five cell lines when compared to healthy lymphocytes (Figure 4.11). The gene was expressed at cycle 35 in healthy lymphocytes while in the cell lines it was expressed at cycles 34-36. SUDHL-4 showed a particularly low expression of the gene and the expression, after normalization, was found to be 256 times lower than in healthy lymphocytes. The other five cell lines demonstrated 16 times higher expression of OCT1 than healthy lymphocytes.

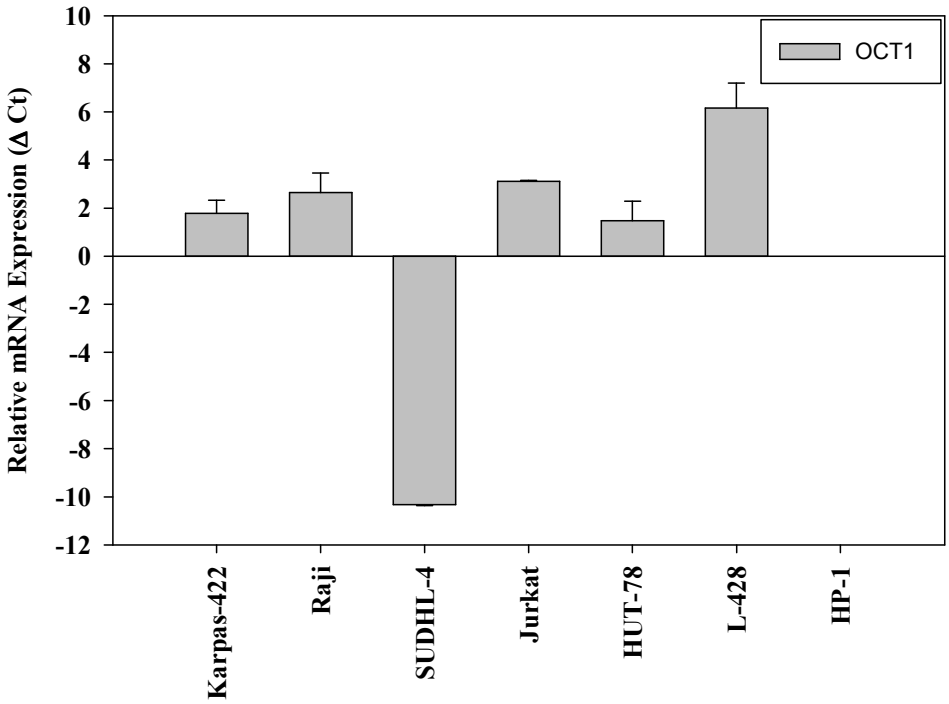

Fig 4.11 TaqMan real-time PCR analysis for OCT1 expression in total RNA extracted from six lymphoma cell lines. OCT1 expression was normalized using GAPDH. Expression in healthy samples obtained from the blood bank was set to 0.

OCT6 was also tested for expression in lymphoma cell lines using real-time PCR (Figure 4.12). The healthy lymphocytes expressed the gene at cycle 33. No expression for OCT6 was seen after 40 cycles in Karpas-422, Raji, SUDHL-4 and Jurkat. In HUT-78 and L-428, OCT6 was expressed at cycles 34 and 36, respectively. Normalization resulted in a cycle difference of 1.5 between the gene expression in the cell lines and healthy lymphocytes, with the two cell lines expressing OCT6 at slightly higher levels.

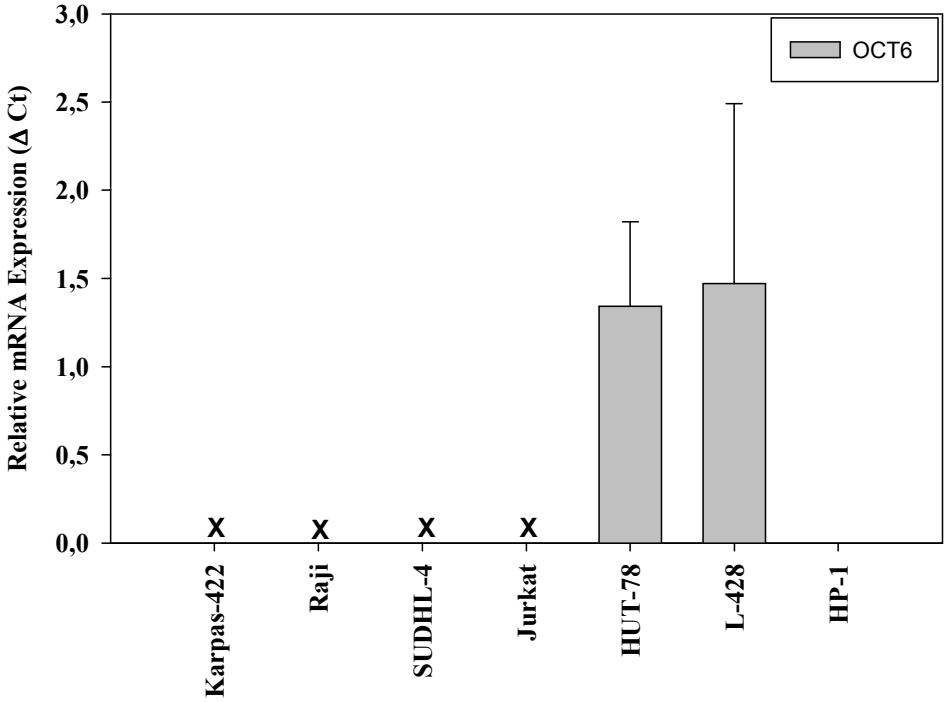

Fig 4.12 TaqMan real-time PCR analysis for OCT6 expression in total RNA extracted from six lymphoma cell lines. OCT6 expression was normalized using GAPDH. Expression in healthy samples obtained from the blood bank was set to 0. X denotes no expression of OCT6 in the four cell lines.

In CLL patient samples, OCT1 expression was expressed at higher levels than in healthy lymphocytes (Figure 4.13). In the healthy lymphocytes, OCT1 was seen at cycle 31 while in the patient samples, expression of OCT1 was seen between cycles 29 and 35. Normalization gave a mean cycle difference of 2 between the seven CLL patient samples and the healthy lymphocytes, with the patient samples exhibiting higher OCT1 expression.

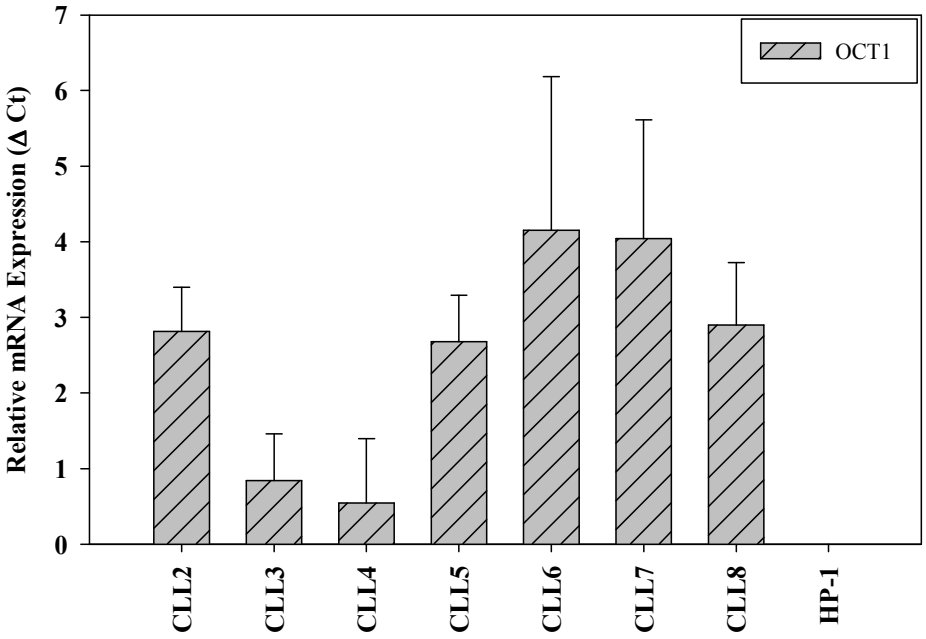

Fig 4.13 TaqMan real-time PCR analysis for OCT1 expression in total RNA extracted from peripheral blood from CLL patients. OCT1 expression was normalized using GAPDH. Expression in healthy samples obtained from the blood bank was set to 0.

OCT6 expression in CLL patient samples was found to be higher than in healthy lymphocytes (Figure 4.14). In one experiment, OCT6 was expressed at cycle 37 in healthy lymphocytes while in the patient samples this number ranged between 34 and 37. Patient sample CLL7 exhibited a lower expression of OCT6 than healthy lymphocytes.

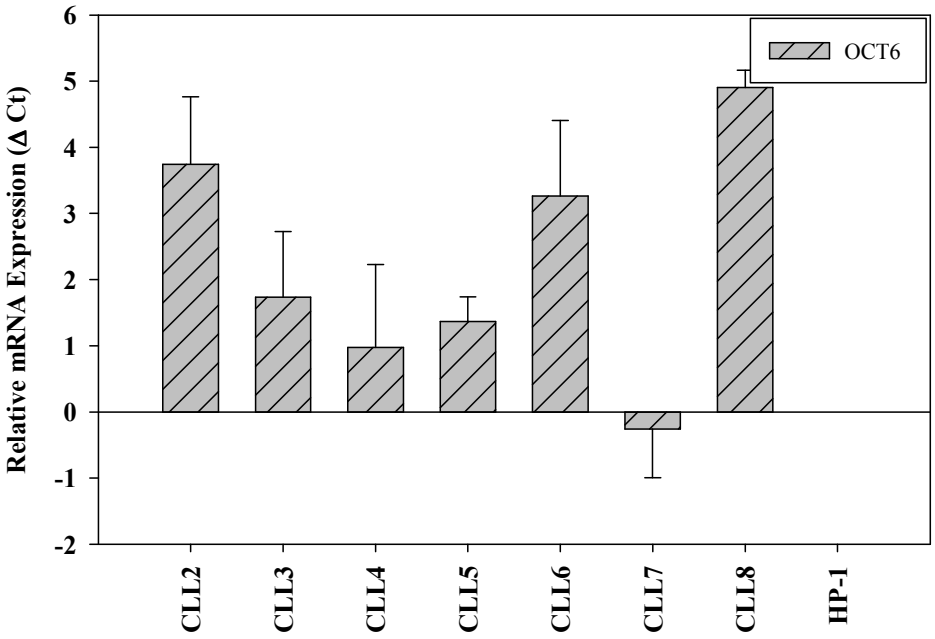

Fig 4.14 TaqMan real-time PCR analysis for OCT6 expression in total RNA extracted from peripheral blood from CLL patients. OCT6 expression was normalized using GAPDH. Expression in healthy samples obtained from the blood bank was set to 0.

Real-time PCR analysis for OAT1 expression in the lymphoma cell lines revealed a higher expression than healthy lymphocytes (Figure 4.15). In the lymphoma cell lines, OAT1 was quantifiable at cycle 32, while this cycle number was 33 in healthy lymphocytes. Normalization with GAPDH revealed at least a four times higher expression in lymphoma cell lines than healthy lymphocytes. The exception was HUT-78 where OAT1 expression was only slightly higher than in healthy lymphocytes.

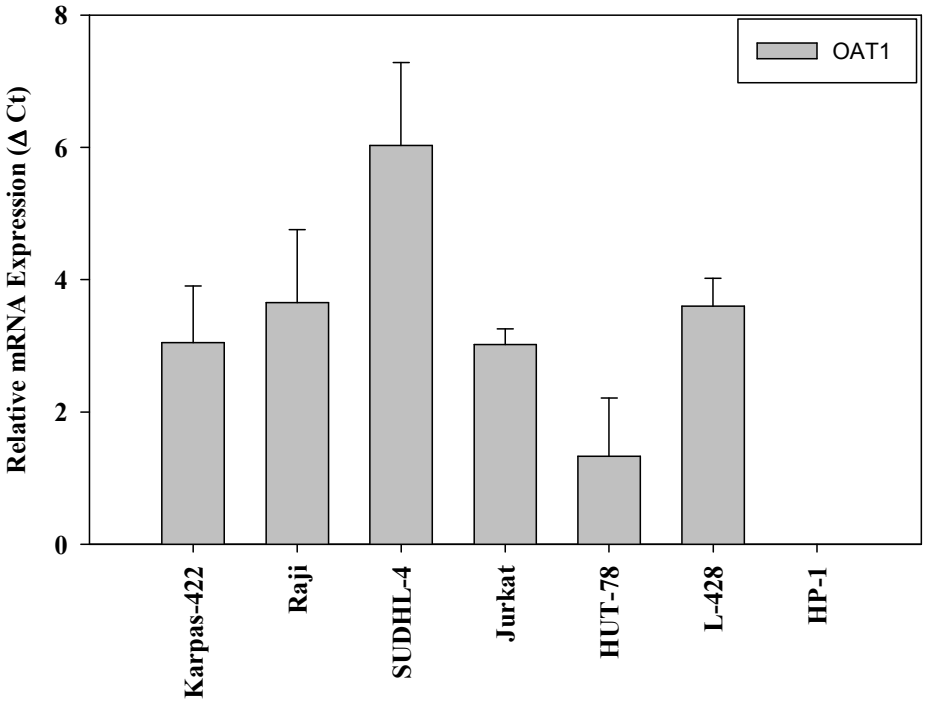

Fig 4.15 TaqMan real-time PCR analysis for OAT1 expression in total RNA extracted from six lymphoma cell lines. OAT1 expression was normalized using GAPDH. Expression in healthy samples obtained from the blood bank was set to 0.

While RT-PCR analysis did not reveal OAT2 expression in the six lymphoma cell lines we tested, OAT2 expression was seen in these cell lines using real-time PCR analysis. Figure 4.16 below shows the mean expression from three different experiments with two replicates each. OAT2 was expressed at cycles 27-32 in the lymphoma cell lines. In healthy lymphocytes, OAT2 expression was seen at cycle 32. Normalization was done with GAPDH and OAT2 expression was seen to be higher in lymphoma cell lines than the control, healthy lymphocytes. The highest expression was seen for SUDHL-4 where the expression was nearly 64 times higher than healthy lymphocytes. The other five cell lines showed 8 to 32 times higher expression of the gene compared to healthy lymphocytes.

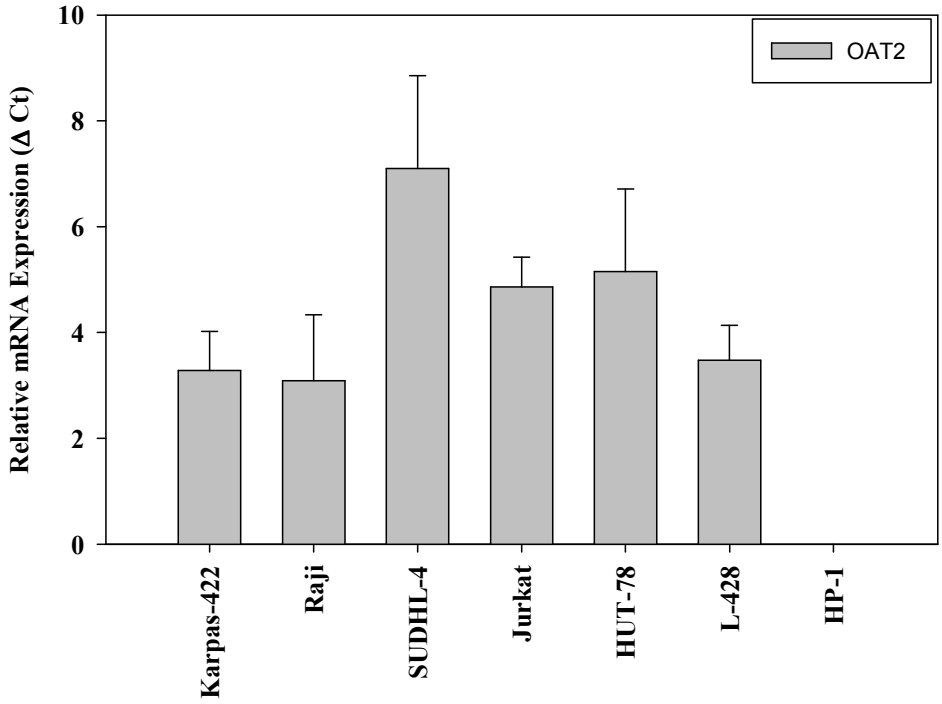

Fig 4.16 TaqMan real-time PCR analysis for OAT2 expression in total RNA extracted from six lymphoma cell lines. OAT2 expression was normalized using GAPDH. Expression in healthy samples obtained from the blood bank was set to 0.

Only OAT1 expression was seen in the seven patient samples tested for organic anion transporter expression (Figure 4.17). While in the healthy lymphocytes OAT1 was quantifiable at cycle 32, the CLL patient samples showed typical cycle values of 35-37. Following normalization with GAPDH, OAT1 expression in CLL patient samples was found to be much lower than that in healthy lymphocytes. A mean ΔCt of -6 was calculated for the CLL patient samples, indicating 64 times lower expression of OAT1 in these samples than in healthy lymphocytes.

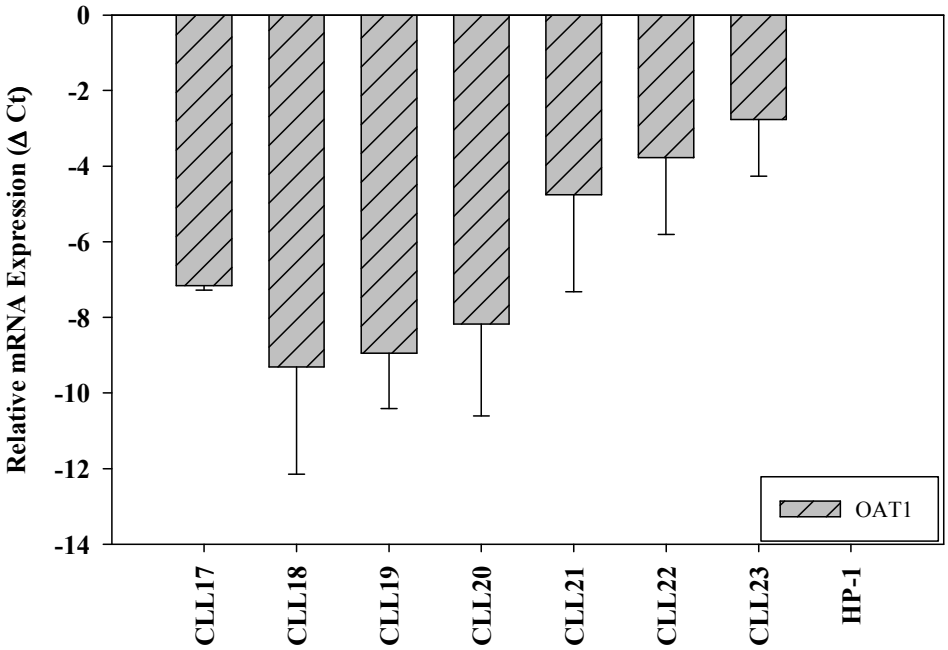

Fig 4.17 TaqMan real-time PCR analysis for OAT1 expression in total RNA extracted from peripheral blood from CLL patients. OAT1 expression was normalized using GAPDH. Expression in healthy samples obtained from the blood bank was set to 0.

4.1.2.6 Expression of SLC29 family transporters

RT-PCR analysis for ENT1 revealed a high expression in all the cell lines tested (Figure 4.18). The healthy lymphocytes showed a slightly lower expression of the gene.

ENT2 expression in the cell lines was much lower. Raji, HUT-78 and L-428 showed similar expression levels and this was comparable to the expression of ENT2 in healthy lymphocytes. Karpas-422 had a lower expression. The lowest expression was seen in Jurkat while SUDHL-4 did not express ENT2 at all.

ENT3 was expressed in all the six lymphoma cell lines tested. Karpas-422 showed a lower expression of the gene while the other five cell lines as well as the healthy lymphocytes' samples had comparable ENT3 expression.

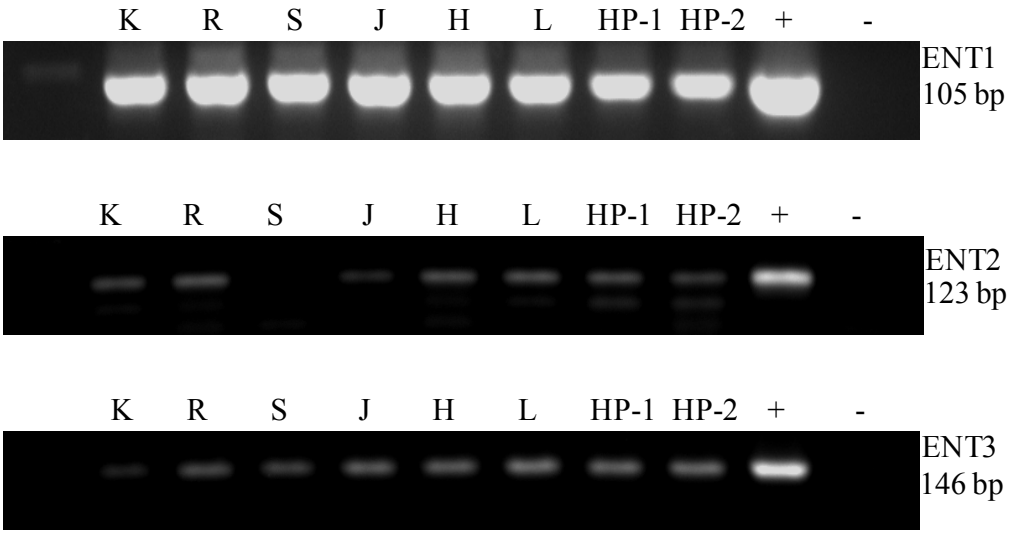

Fig 4.18 RT-PCR screening of SLC29 family transporters in lymphoma cell lines with all three transporters tested being expressed in the six cell lines. K: Karpas-422, R: Raji, S: SUDHL-4, J: Jurkat, H: HUT-78, L: L-428, HP-1: Healthy person sample-1, HP-2: Healthy person sample- 2, +: positive control, -: negative control.

Consistent with RT-PCR results, ENT1 was expressed at higher levels than normal in five cell lines, with the exception of the T-lymphoma cell line, Jurkat which exhibited a lower ENT1 expression (Figure 4.19). ENT1 was typically expressed between cycles 26-28 in the lymphoma cell lines while in healthy lymphocytes, it was expressed at cycle 32. For Jurkat, this cycle number was 35. Normalization with GAPDH was done and a mean ΔCt of 5 was calculated for the five cell lines. In Jurkat, ENT1 expression was nearly 16 times lower than in healthy lymphocytes.

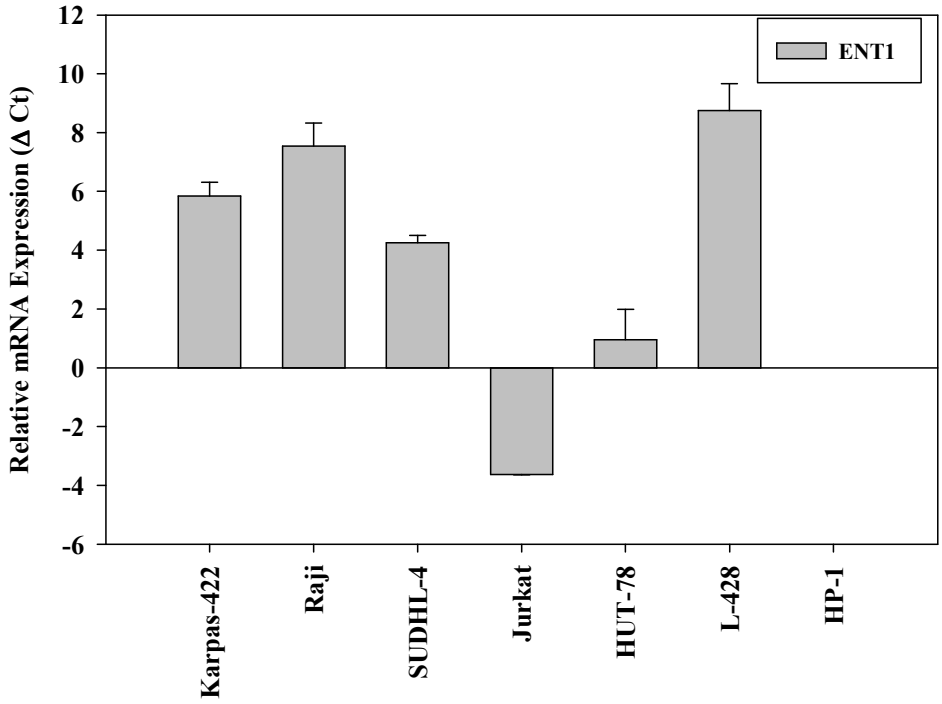

Fig 4.19 TaqMan real-time PCR analysis for ENT1 expression in total RNA extracted from six lymphoma cell lines. ENT1 expression was normalized using GAPDH. Expression in healthy samples obtained from the blood bank was set to 0.

ENT2 was expressed at very high levels in five of the six cell lines tested (Figure 4.20). Consistent with the RT-PCR data, no expression of ENT2 was seen in SUDHL-4. In the other five lymphoma cell lines, ENT2 was typically expressed between cycles 26-30. In healthy lymphocytes, ENT2 was expressed at cycle 33. Normalization with GAPDH revealed more than 16 times higher expression in the lymphoma cell lines than healthy lymphocytes. Raji demonstrated the highest ENT2 expression, with nearly 128 times higher expression of the gene compared to the control, healthy lymphocytes.

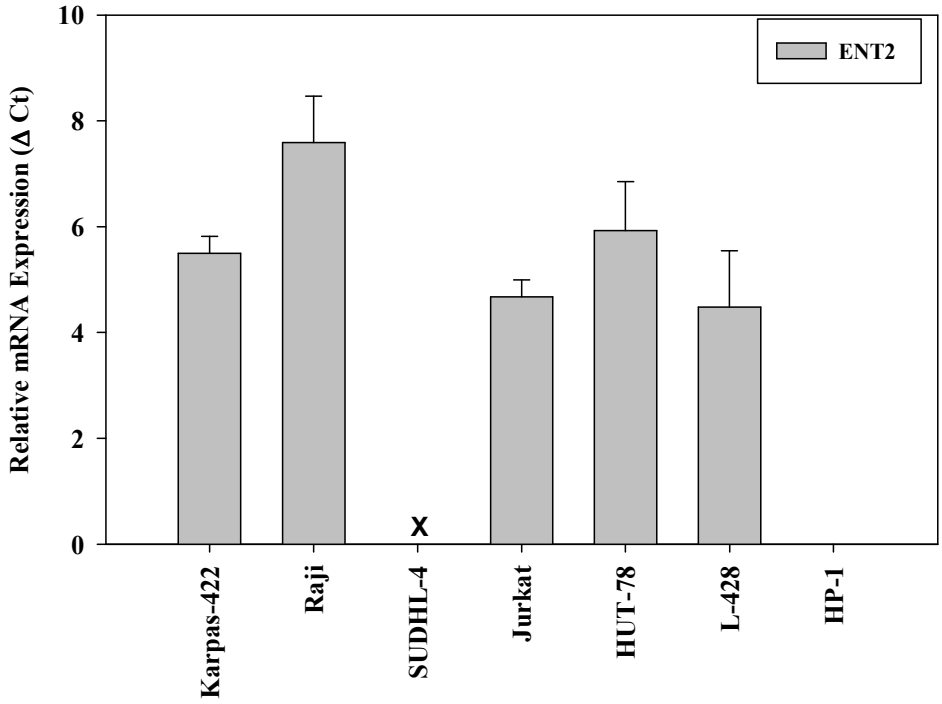

Fig 4.20 TaqMan real-time PCR analysis for ENT2 expression in total RNA extracted from six lymphoma cell lines. ENT2 expression was normalized using GAPDH. Expression in healthy samples obtained from the blood bank was set to 0. X denotes no expression of ENT2 in SUDHL-4.

ENT3 was also seen to be expressed higher in the lymphoma cell lines than in healthy lymphocytes (Figure 4.21). While no expression of ENT3 was seen in SUDHL-4, the five cell lines showed expression at cycles 28-30. The healthy lymphocytes showed an expression of ENT3 at cycle 32. After normalization ENT3 was seen to be typically expressed 16 to 64 times higher in five lymphoma cell lines than in healthy lymphocytes. The highest expression was seen in Raji.

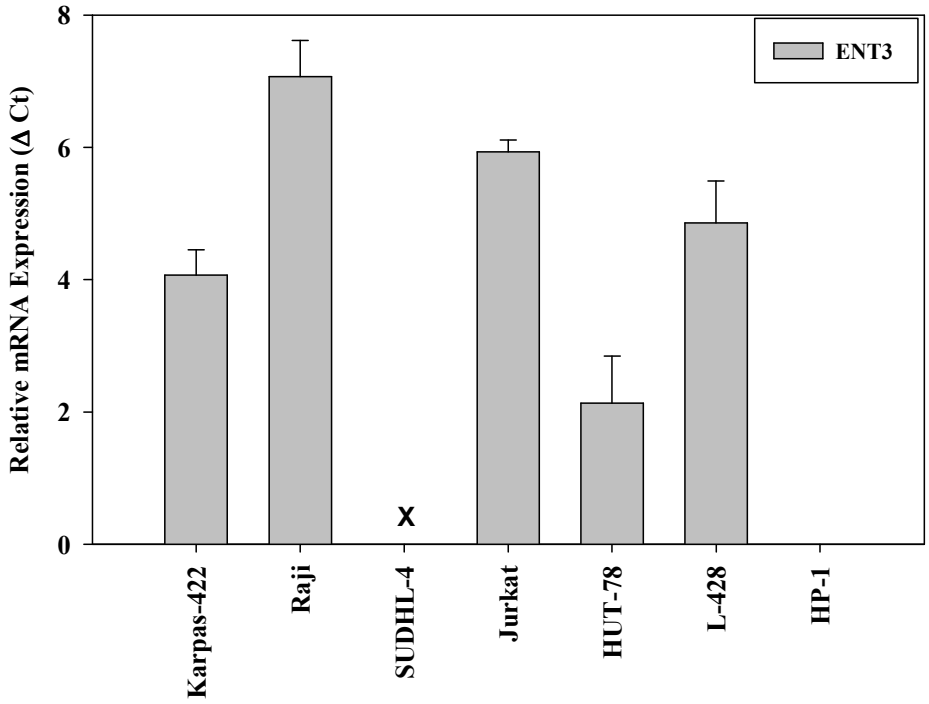

Fig 4.21 TaqMan real-time PCR analysis for ENT3 expression in total RNA extracted from six lymphoma cell lines. ENT3 expression was normalized using GAPDH. Expression in healthy samples obtained from the blood bank was set to 0. X denotes no expression of ENT3 in SUDHL-4.

ENT1 expression in seven CLL patient samples was analyzed using real-time PCR (Figure 4.22). One patient sample, CLL26, did not show ENT1 expression even after 40 cycles. In the other patient samples tested, ENT1 appeared at cycles 31-37, in healthy lymphocytes at cycle 26. ENT1 was typically expressed 64 times lower in patient samples compared to healthy lymphocytes.

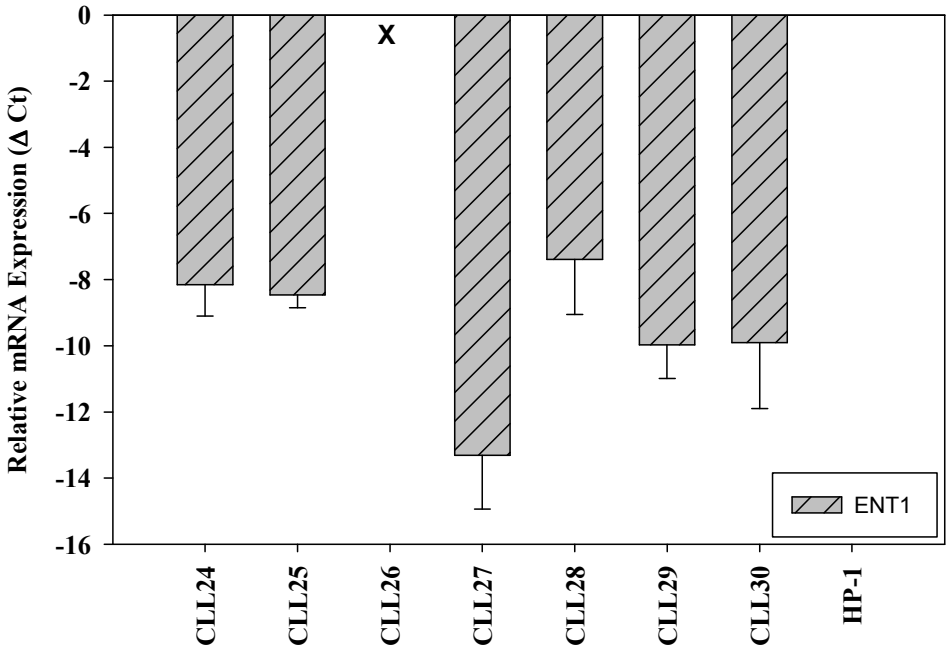

Fig 4.22 TaqMan real-time PCR analysis for ENT1 expression in total RNA extracted from peripheral blood from CLL patients. ENT1 expression was normalized using GAPDH. Expression in healthy samples obtained from the blood bank was set to 0. X denotes no expression of ENT1 in CLL26.

ENT2 expression was also much lower in CLL patient samples than in healthy lymphocytes (Figure 4.23). CLL26 did not show ENT2 expression at all while in the other six patient samples, a mean ΔCt of -9 was calculated, indicating a much lower expression of the gene in these samples. In the healthy lymphocytes, ENT2 expression was seen at cycle 34 while this number was between 35-38 in patient samples.

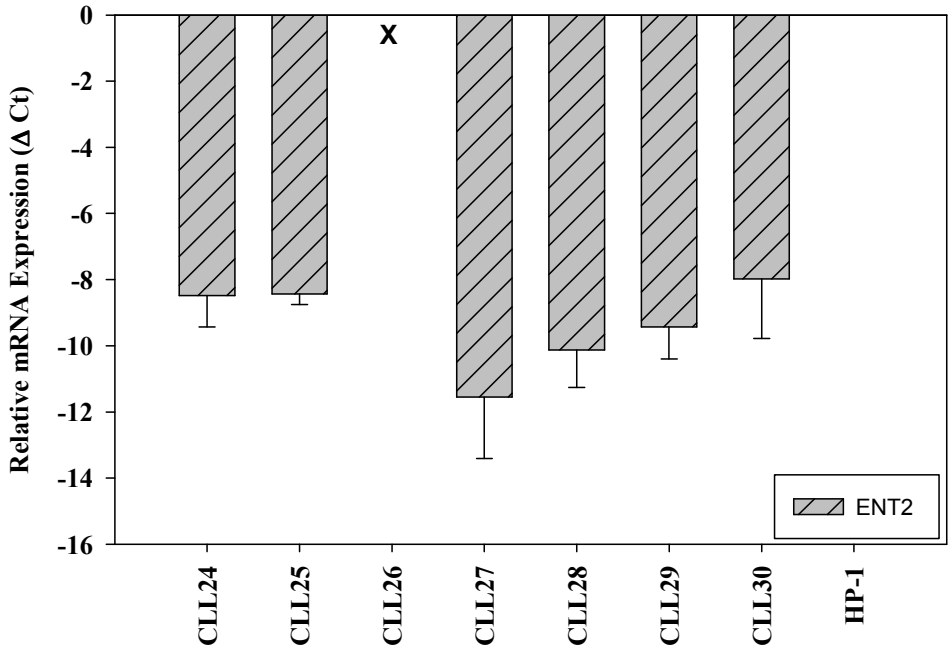

Fig 4.23 TaqMan real-time PCR analysis for ENT2 expression in total RNA extracted from peripheral blood from CLL patients. ENT2 expression was normalized using GAPDH. Expression in healthy samples obtained from the blood bank was set to 0. X denotes no expression of ENT2 in CLL26.

ENT3 expression was not seen in patient sample CLL26 (Figure 4.24). The other patient samples tested gave a mean ΔCt value of -7, indicating a nearly 128 times lower expression of ENT3 in CLL patient samples than in healthy lymphocytes. In healthy lymphocytes, ENT3 expression was seen at cycle 34 while in CLL patient samples, this number ranged within 31-38.

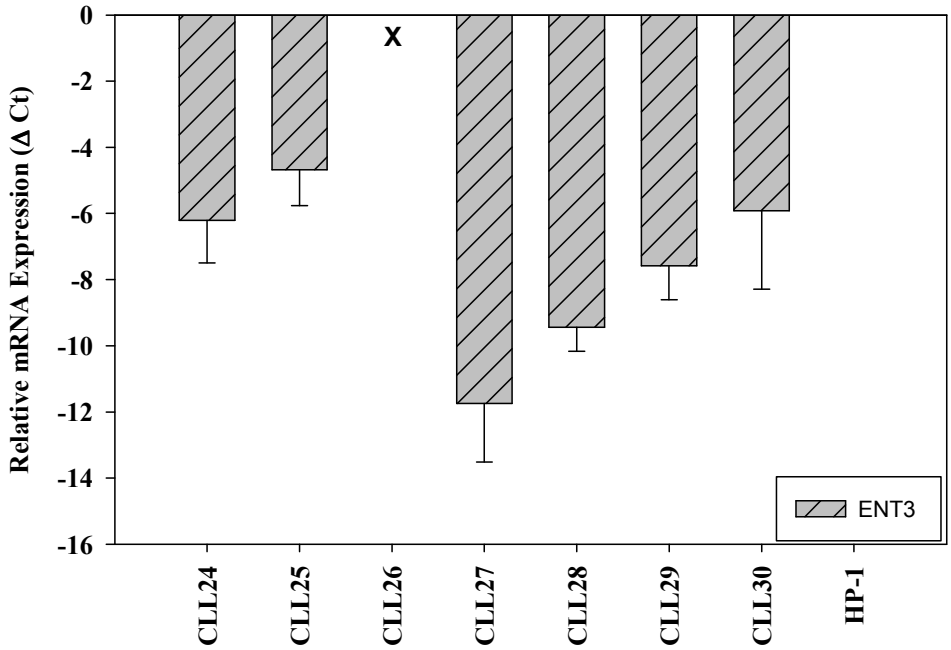

Fig 4.24 TaqMan real-time PCR analysis for ENT3 expression in total RNA extracted from peripheral blood from CLL patients. ENT3 expression was normalized using GAPDH. Expression in healthy samples obtained from the blood bank was set to 0. X denotes no expression of ENT3 in CLL26.

4.1.3 Expression of ABC transporters

All investigated members of the ABC family were expressed in the lymphoma cell lines (Figure 4.25). MDR1 was expressed at the highest levels. Only one B-lymphoma cell line, SUDHL-4 did not express MDR1. HUT-78 and L-428 had nearly comparable expression to that in normal lymphocytes. The expression was slightly lower in Karpas-422 and Raji and still lower in Jurkat.

MRP1 was consistently expressed in lymphoma cell lines. Strongest expression of MRP1 was observed in HUT-78 and L-428 and this was again comparable to MRP1 expression in healthy lymphocytes. SUDHL-4 demonstrated a much lower expression of MRP1 than the other cell lines tested. Karpas-422, Raji and Jurkat had comparable expression of the gene.

MRP2 showed a high expression in L-428. Karpas-422 and Jurkat had comparable expression of the gene while HUT-78 demonstrated a relatively lower expression. Raji, SUDHL-4 and the healthy lymphocytes did not show MRP2 expression.

MRP4 was expressed at very low levels in the cell lines. While Raji and SUDHL-4 demonstrated negligible gene expression, the expression of MRP4 in Karpas-422, Jurkat and HUT-78 was nearly comparable to that in healthy lymphocytes. L-428 showed a slightly stronger expression of MRP4 than healthy lymphocytes.

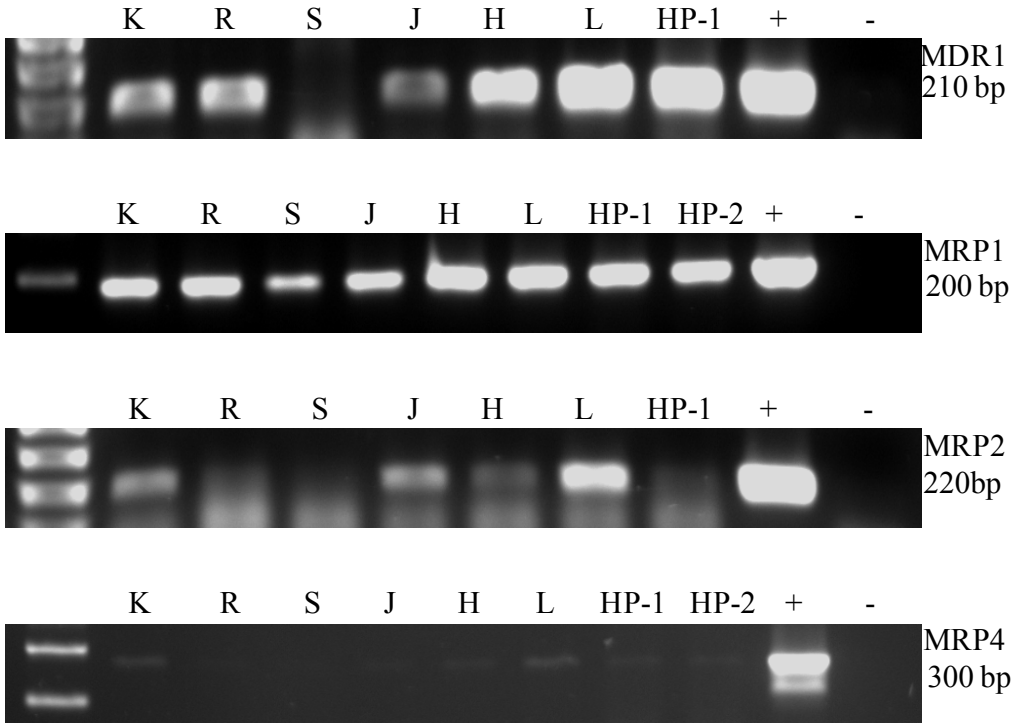

Fig 4.25 RT-PCR screening of ABC transporters in lymphoma cell lines K: Karpas-422, R: Raji, S: SUDHL-4, J: Jurkat, H: HUT-78, L: L-428, HP-1: Healthy person sample-1, HP-2: Healthy person sample- 2, +: positive control, -: negative control.

4.2 OCT1 and OCT2 mediated MPP uptake in cells

MPP^+, 1-methyl-4-phenylpyridinium, is a known substrate of Organic Cation Transporters (31). To ensure that our cells expressed functional proteins, we measured radiolabelled MPP uptake in CHO cells, stably expressing OCT1 and OCT2 (Figure 4.26). The uptake of 20 nM [^{3}H]MPP in CHO-OCT1 was 123.8 ± 0.41 fmol/5 min, which was 14 fold higher than CHO control cells (8.45 ± 0.86 fmol/5 min, P<0.0001). OCT1 mediated [^{3}H]MPP uptake was significantly inhibited by 50 μM unlabelled (cold) MPP (25.38 ± 0.50%, P<0.0001) and 100 μM unlabelled MPP (20.64 ± 0.44%, P<0.0001). OCT2 mediated [^{3}H]MPP was 60.25 ± 2.57 fmol/5 min and this was again significantly inhibited by 50 μM unlabelled MPP (21.08 ± 1.56%, P< 0.0001) and 100 μM unlabelled MPP (17.88 ± 0.47%, P< 0.0001). The addition of

500 µM unlabeled MPP resulted in complete abolishment of [^{3}H]MPP uptake by both OCT1 and OCT2.

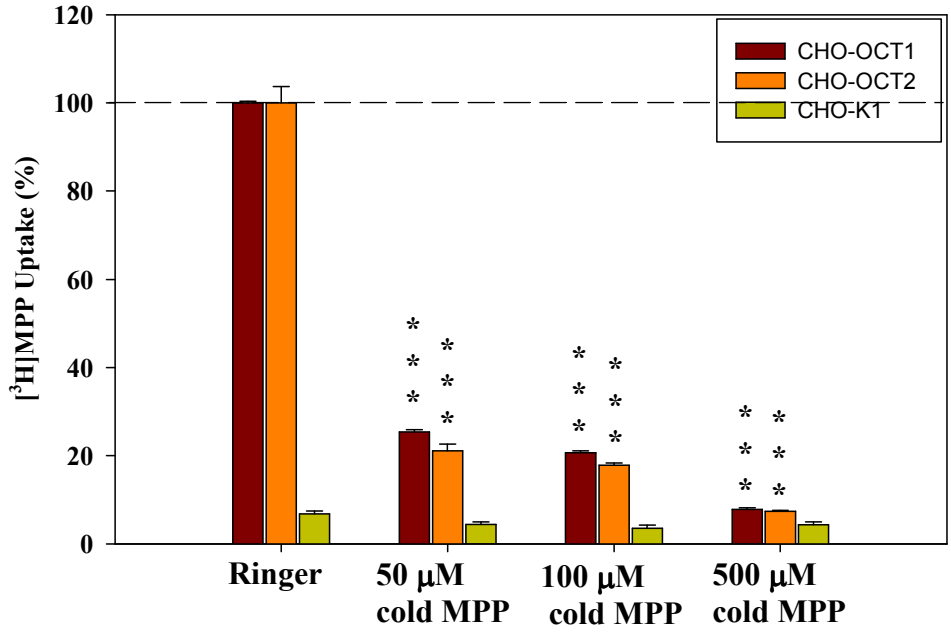

Fig 4.26 Inhibition of [^{3}H]MPP uptake into OCT1 and OCT2 cells. Cells were incubated with 20 nM [^{3}H]MPP alone or in addition with 50 µM, 100 µM and 500 µM unlabelled MPP for 5 minutes. Data are means of three independent experiments with four repeats each.
***P< 0.0001

4.2.1 Cis-Inhibition of OCT1 and OCT2 mediated MPP uptake by cytostatics

The interaction of cytostatics with OCT1 and OCT2 was determined by inhibition of [^{3}H]MPP uptake by these cells. Several groups of cytostatics were tested for their interaction with OCT1 and OCT2, and thus the inhibition of OCT-mediated MPP uptake.

4.2.1.1 Cis-Inhibition of OCT1 and OCT2 mediated MPP uptake by alkylating drugs

We tested 7 alkylating drugs for their interaction with OCT1 and OCT2. Ifosphamide and trofosphamide significantly reduced MPP uptake by OCT1 to 71.45 ± 4.37%, P< 0.0001 and 55.74 ± 6.34%, P< 0.0001, respectively (Figure 4.27). Bendamustine also effected OCT1 mediated MPP uptake and reduced it to 75.84 ± 9.24% (P< 0.05). The inhibition of MPP uptake by OCT1 was reduced to 76.72 ± 18.32% by melphalan. Cyclophosphamide, treosulfan and chlorambucil stimulated MPP uptake by OCT1 to 111.47 ± 7.79%, 101.07 ± 5.74% and 110.18 ± 5.45%, respectively. This increased MPP uptake, however, was not

significant. Treosulfan also resulted in a slightly increased MPP uptake by the control cells (18.02 ± 3.52%), but this was not significant.

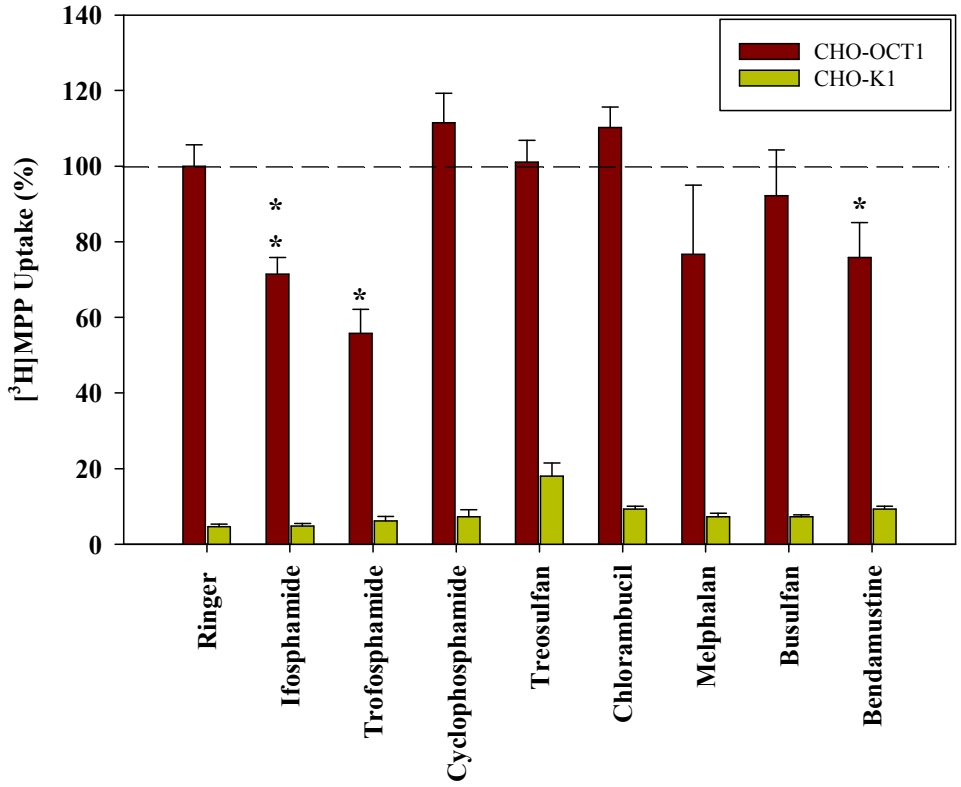

Fig 4.27 Inhibition of [^{3}H]MPP uptake by alkylating agents (100 µM each) in CHO-OCT1 cells. The control set (without inhibitor) was set at 100 %. Data are means of three independent experiments with four repeats each. * P< 0.05, **P< 0.01

MPP uptake by OCT2 was significantly inhibited by ifosphamide, cyclophosphamide, busulfan and bendamustine to 51.21 ± 7.74%, P< 0.0001; 71.68 ± 9.23%, P< 0.05; 49.10 ± 6.60%, P< 0.0001 and 54.13 ± 10.59%, P< 0.001, respectively (Figure 4.28). Treosulfan and chlorambucil also inhibited OCT2 mediated MPP uptake and reduced it to 83.84 ± 10.75% and 77.70 ± 12.68%, respectively. This observed inhibition was not significant. Trofosphamide and melphalan did not affect OCT2 mediated MPP uptake.

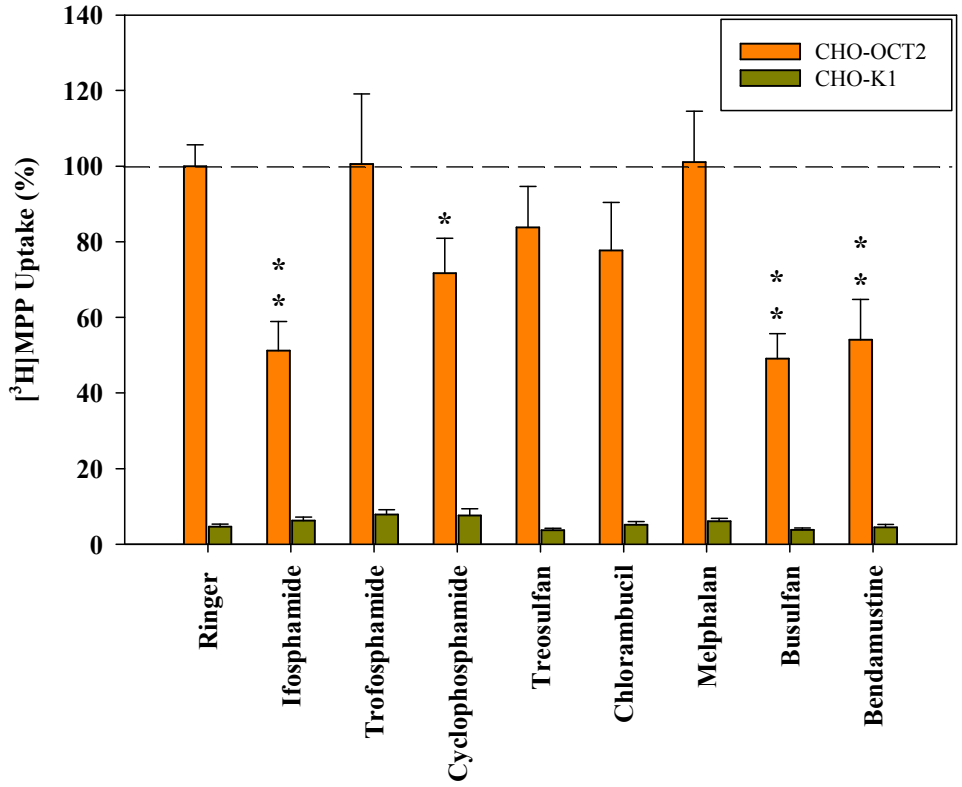

Fig 4.28 Inhibition of [^{3}H]MPP uptake by alkylating agents (100 µM each) in CHO-OCT2 cells. The control set (without inhibitor) was set at 100 %. Data are means of three independent experiments with four repeats each. * P< 0.05, **P< 0.01

4.2.1.2 Cis-Inhibition of OCT1 and OCT2 mediated MPP uptake by antimetabolites

None of the antimetabolites tested inhibited MPP uptake by OCT1 (Figure 4.29). However, the sugar analog, cytosine arabinoside did result in a stimulation of MPP uptake to 145.10 ± 13.83%, P< 0.001. Cladribine also resulted in a slightly increased MPP uptake by OCT1 cells to 109.66 ± 6.04%, but this change was not significant. The control cells showed a non-significant increase in MPP uptake on treatment with antimetabolites, particularly on treatment with cytosine arabinoside and gemcitabine.

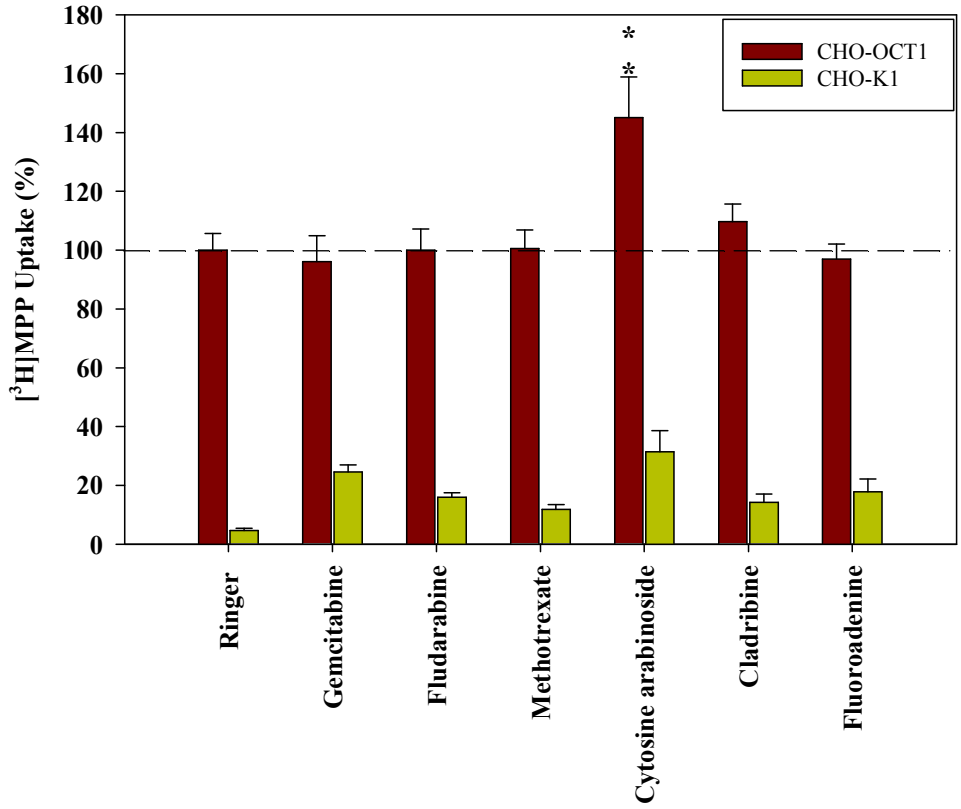

Fig **4.29 Inhibition of [^{3}H]MPP uptake by antimetabolites (100 µM each) in CHO-OCT1 cells.** The control set (without inhibitor) was set at 100 %. Data are means of three independent experiments with four repeats each. **P< 0.01

OCT2 mediated MPP uptake was non-significantly inhibited by fluoroadenine and fludarabine to 85.98 ± 4.51% and 86.72 ± 15.97%, respectively (Figure 4.30). Methotrexate, cytosine arabinoside and cladribine did not affect MPP uptake by OCT2. Gemcitabine, however, increased MPP uptake in OCT2 cells to 114.17 ± 13.46 and in control cells to 14.81 ± 2.56%. However, the increase observed in both the cells lines was not significant.

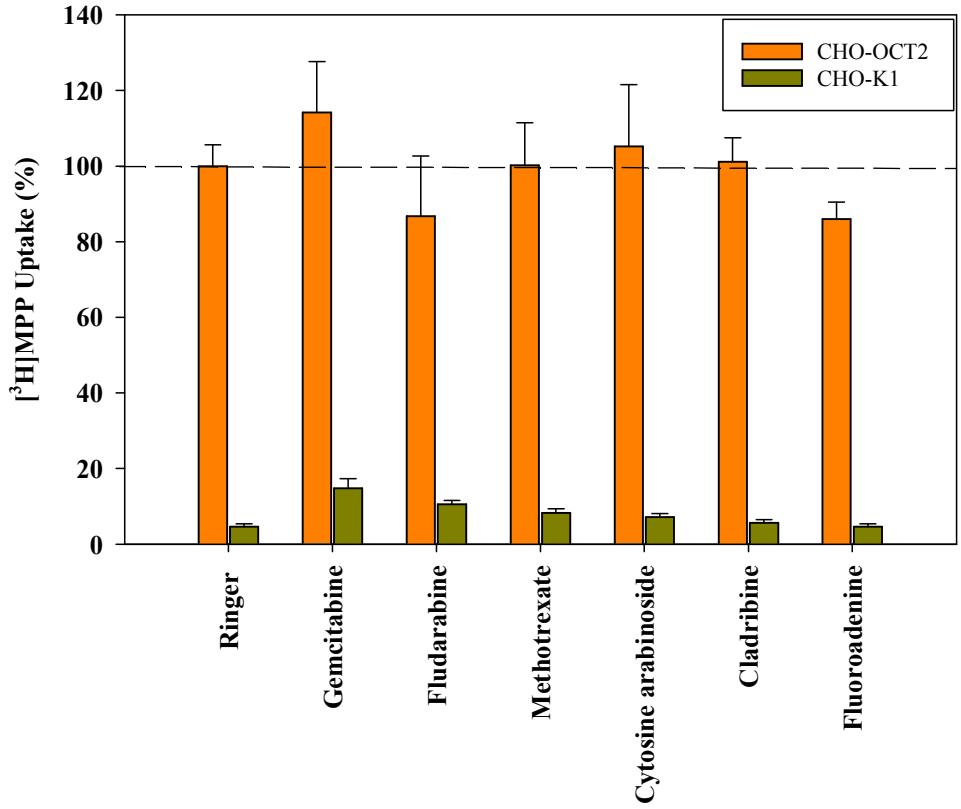

Fig 4.30 Inhibition of [^{3}H]MPP uptake by antimetabolites (100 µM each) in CHO-OCT2 cells. The control set (without inhibitor) was set at 100 %. Data are means of three independent experiments with four repeats each.

4.2.1.3 Cis-Inhibition of OCT1 and OCT2 mediated MPP uptake by topoisomerase inhibitors

Two of the three topoisomerase inhibitors tested, mitoxantrone and irinotecan, dramatically reduced [^{3}H]MPP uptake by OCT1 cells, inhibiting the uptake to 25.42 ± 2.01% ($P < 0.0001$) and 16.65 ± 1.88% ($P < 0.0001$), respectively (Figure 4.31). Etoposide also inhibited MPP uptake by OCT1 to 79.33 ± 5.59%, but this inhibition was not significant. Control cells demonstrated a higher MPP uptake than normal on irinotecan treatment to 15.17 ± 1.75%. This increased uptake by the control cells was not significant.

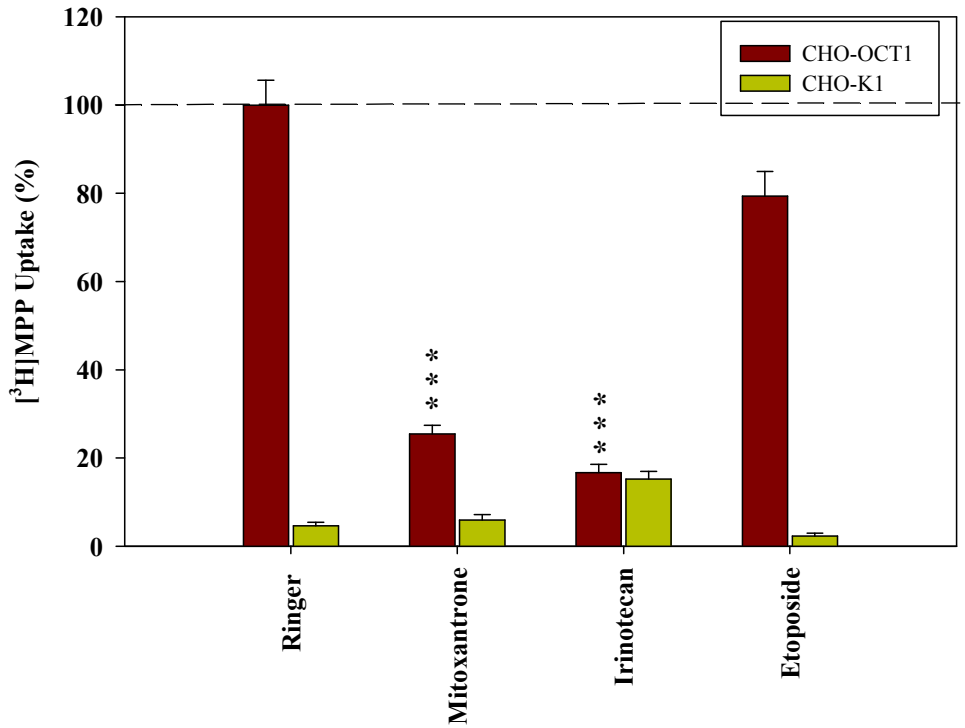

Fig 4.31 Inhibition of [^{3}H]MPP uptake by topoisomerase inhibitors (100 µM each) in CHO-OCT1 cells. The control set (without inhibitor) was set at 100 %. Data are means of three independent experiments with four repeats each. ***P< 0.0001

Since the OCT1 mediated MPP uptake was strongly inhibited by mitoxantrone and irinotecan, we measured the affinity of OCT1 for these two cytostatics. We performed apparent K_m (K_i) analysis.

Three experiments were performed for the kinetic analysis of OCT1 for mitoxantrone. Increasing concentrations of mitoxantrone (0-140 µM) were used with 1 µM and 20 µM [^{3}H]MPP for the assay. A representative example is shown below (Figure 4.32) and the K_i was determined to be 85.2 µM.

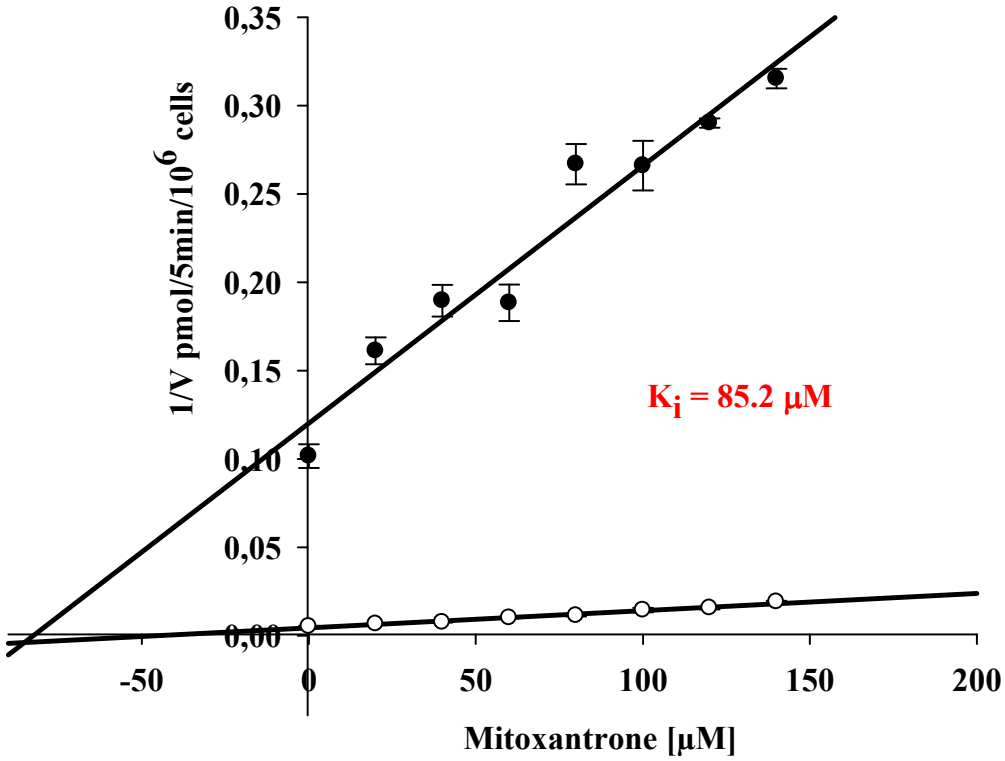

Fig 4.32 Dixon plot studies on OCT1 expressing CHO cells showing an interaction of mitoxantrone with OCT1 giving a K_i of 85.2µM. Uptake experiments were carried out with ● 1µM and ○ 20µM MPP with different concentrations of mitoxantrone. A representative experiment is shown. Data are means ±SEM of three data repeats.

For the determination of irinotecan kinetics, OCT1 was assayed for 1 µM [^{3}H]MPP uptake and 20 µM [^{3}H]MPP uptake over 5 minutes in the presence of increasing concentrations of unlabelled irinotecan (0-20 µM). Figure 4.33 shows a representative example of Dixon plot analysis in OCT1 and in this experiment, the K_i was determined to be 1.73 µM.

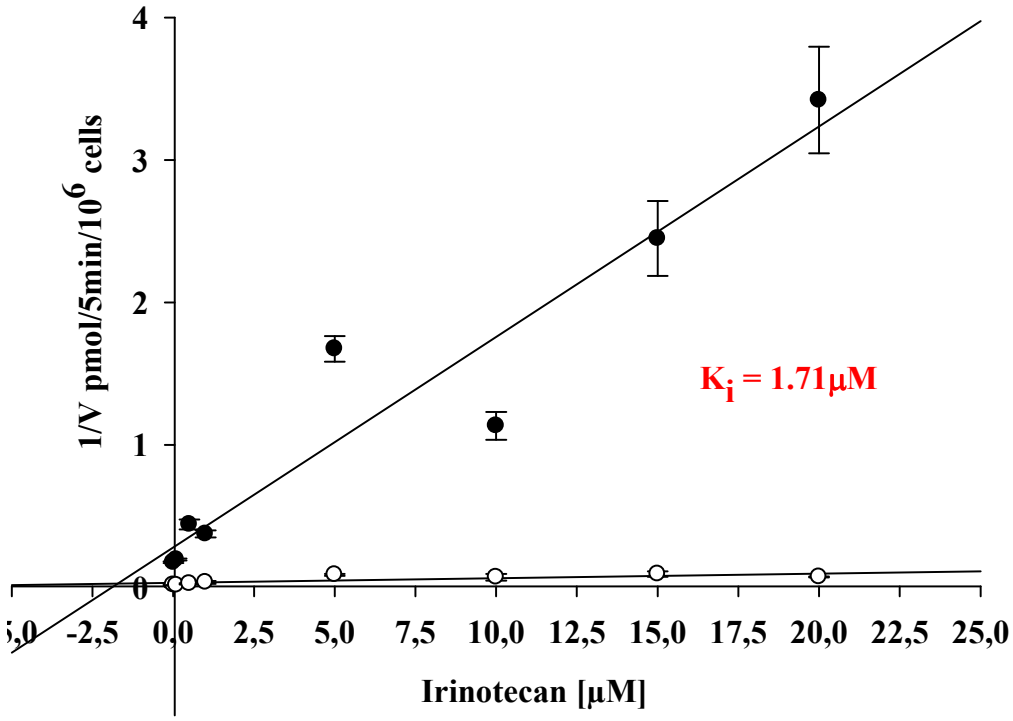

Fig 4.33 Dixon plot studies on OCT1 expressing CHO cells showing an interaction of irinotecan with OCT1 giving a K_i of 1.73 µM. Uptake experiments were carried out with ● 1µM and ○ 20µM MPP with different concentrations of irinotecan. A representative experiment is shown. Data are means ±SEM of three data repeats.

Mitoxantrone and irinotecan effected a reduced MPP uptake by OCT2 cells to 58.72 ± 14.96%, P< 0.05 and 28.51 ± 3.30%, P< 0.0001, respectively (Figure 4.34). Etoposide also inhibited MPP uptake by OCT2 to 70.07 ± 4.87%, but this inhibition was not significant.

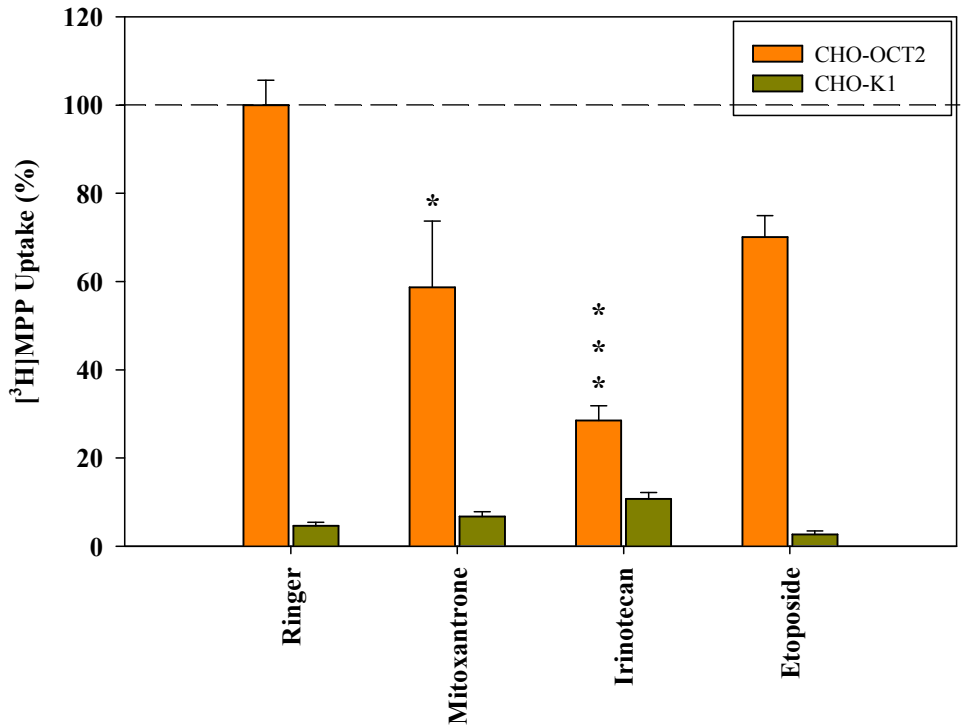

Fig 4.34 Inhibition of [^{3}H]MPP uptake by topoisomerase inhibitors (100 µM each) in CHO-OCT2 cells. The control set (without inhibitor) was set at 100 %. Data are means of three independent experiments with four repeats each. * P< 0.05, ***P< 0.0001

We looked for the affinity of OCT2 for irinotecan using an indirect method for calculating the apparent K_m value. Three separate experiments were made using increasing concentrations of unlabelled irinotecan (0-20 µM). 1 µM [^{3}H]MPP uptake and 20 µM [^{3}H]MPP uptake over 5 minutes was measured and the K_i value for irinotecan was calculated to be 86.3 µM. Figure 4.35 gives a representative example of Dixon plot studies on OCT2 for irinotecan.

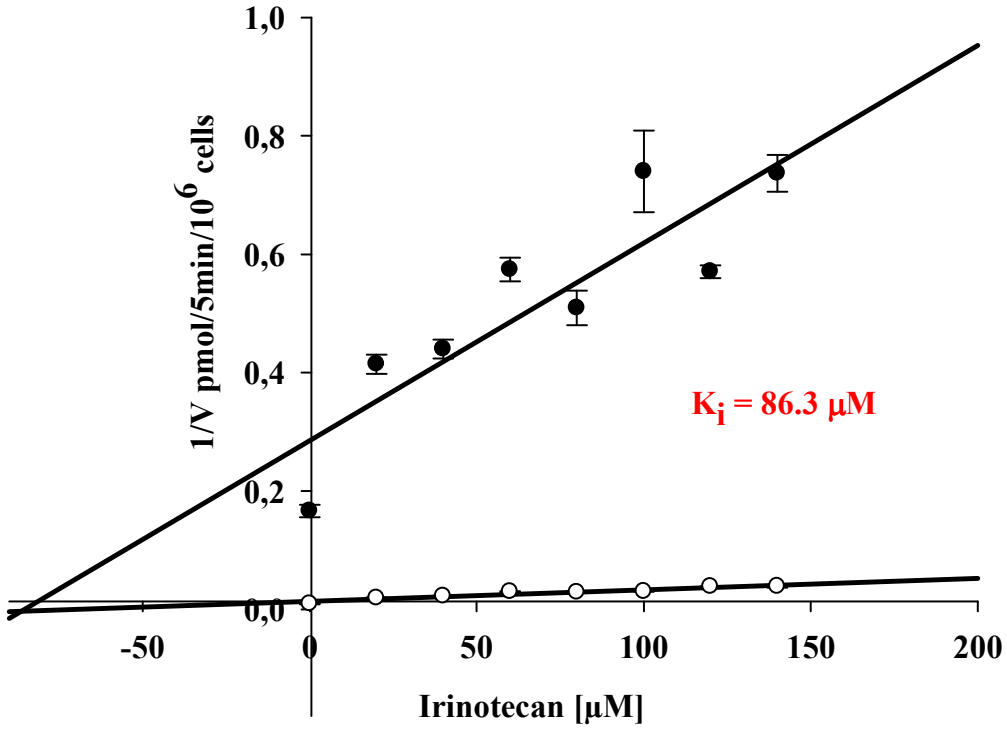

Fig 4.35 Dixon plot studies on OCT2 expressing CHO cells showing an interaction of irinotecan with OCT2 giving a K_i of 86.3 µM. Uptake experiments were carried out with ● 1µM and ○ 20µM MPP with different concentrations of irinotecan. A representative experiment is shown. Data are means ±SEM of three data repeats.

4.2.1.4 Cis- Inhibition of OCT1 and OCT2 mediated MPP uptake by cytostatics acting on mitotic spindle

Paclitaxel and vinblastine significantly inhibited OCT1 mediated [^{3}H]MPP uptake and reduced it to 28.54 ± 5.31%, P< 0.0001 and 55.42 ± 9.63%, P< 0.0001, respectively (Figure 4.36). Vincristine did not affect MPP uptake by OCT1. The control cells exhibited an increased MPP uptake on treatment with vincristine and vinblastine to 14.93 ± 1.56% and 16.36 ± 2.33%, respectively. This increase, however, was non-significant.

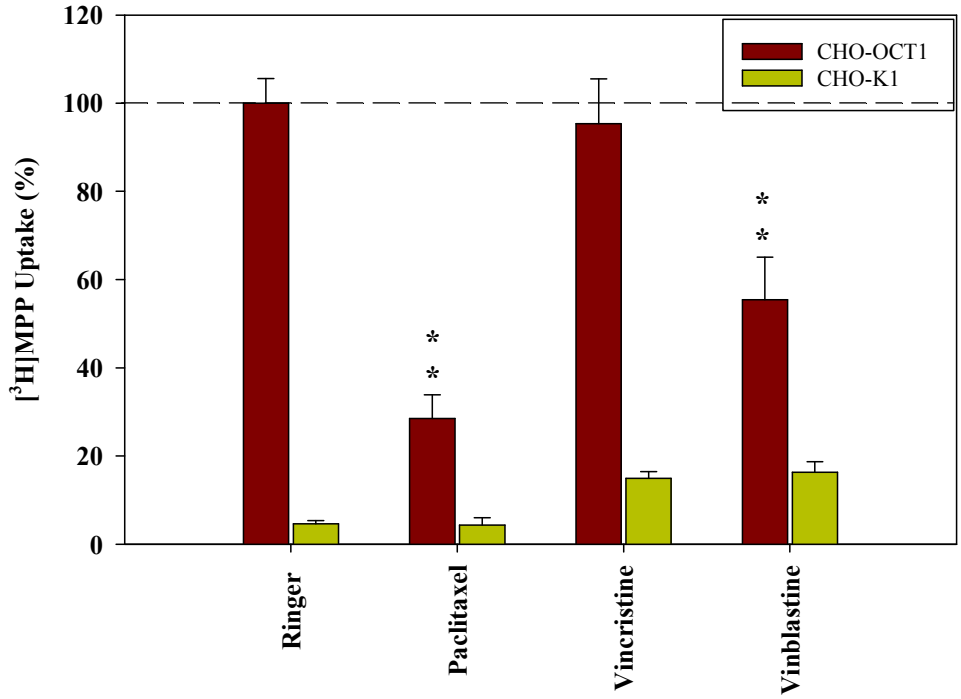

Fig 4.36 Inhibition of [^{3}H]MPP uptake by cytostatic agents acting on mitotic spindle (100 µM each) in CHO-OCT1 cells. The control set (without inhibitor) was set at 100 %. Data are means of three independent experiments with four repeats each. **P< 0.01

Dixon plot analysis was done to determine the affinity of OCT1 for paclitaxel. OCT1 was assayed for 1 µM and 20 µM [^{3}H]MPP uptake over 5 minutes in the presence increasing concentrations of paclitaxel (0- 140 µM). The K_i was calculated to be 50.1 µM from the representative experiment shown in Figure 4.37.

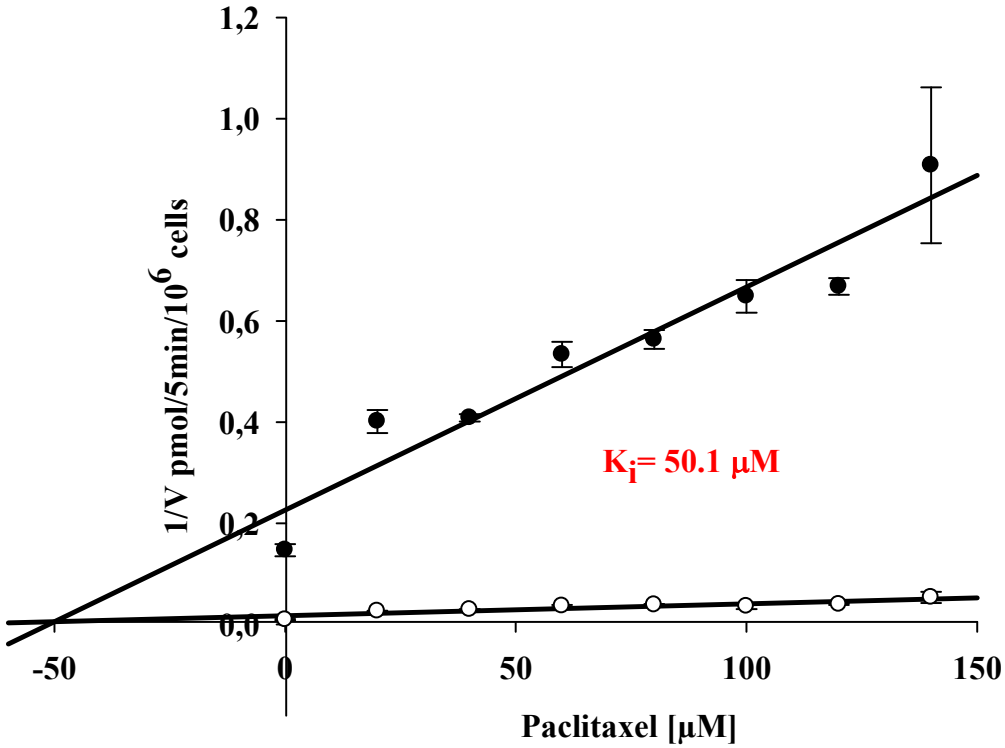

Fig 4.37 Dixon plot studies on OCT1 expressing CHO cells showing an interaction of paclitaxel with OCT1 giving a K_i of 50.1µM. Uptake experiments were carried out with ● 1µM and ○ 20µM MPP with different concentrations of paclitaxel. A representative experiment is shown. Data are means ±SEM of three data repeats.

OCT2 mediated MPP uptake was significantly inhibited by paclitaxel to 51.23 ± 8.13%, P< 0.001 (Figure 4.38). Vincristine did not affect MPP uptake by OCT2 but vinblastine resulted in an increased OCT2 mediated MPP uptake to 118.88 ± 15.73%. This increased MPP uptake in the presence of vinblastine was non- significant.

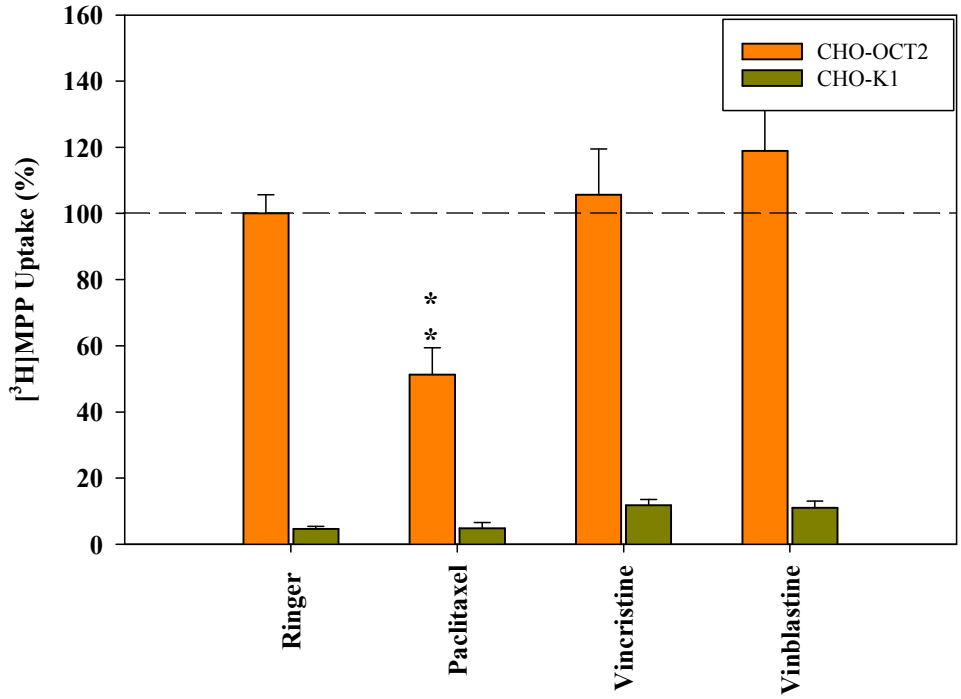

Fig 4.38 Inhibition of [^{3}H]MPP uptake by cytostatic agents acting on mitotic spindle (100 µM each) in CHO-OCT2 cells. The control set (without inhibitor) was set at 100 %. Data are means of three independent experiments with four repeats each. **P< 0.01

4.2.1.5 Cis-Inhibition of OCT1 and OCT2 mediated MPP uptake by cytostatics acting on steroid hormone receptors

Prednisone inhibited OCT1 mediated [^{3}H]MPP uptake to 74.71 ± 4.14% (P< 0.001) while clodronic acid resulted in slight stimulation of [^{3}H]MPP uptake (111.97 ± 3.96%, P< 0.05), as shown in Figure 4.39.

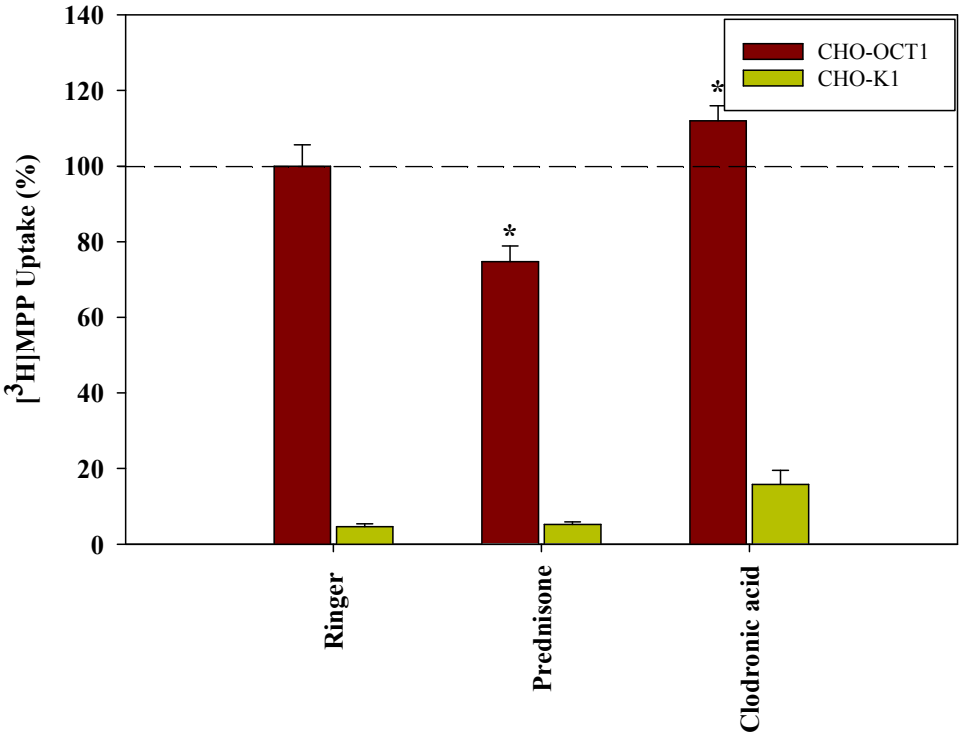

Fig 4.39 Inhibition of [^{3}H]MPP uptake by drugs acting on steroid hormone receptors (100 µM each) in CHO-OCT1 cells. The control set (without inhibitor) was set at 100 %. Data are means of three independent experiments with four repeats each. * P< 0.05

OCT2 mediated [^{3}H]MPP uptake was also significantly inhibited by 100 µM prednisone (65.85 ± 9.01%, P< 0.001). Clodronic acid did not affect MPP uptake by OCT2 cells (Figure 4.40).

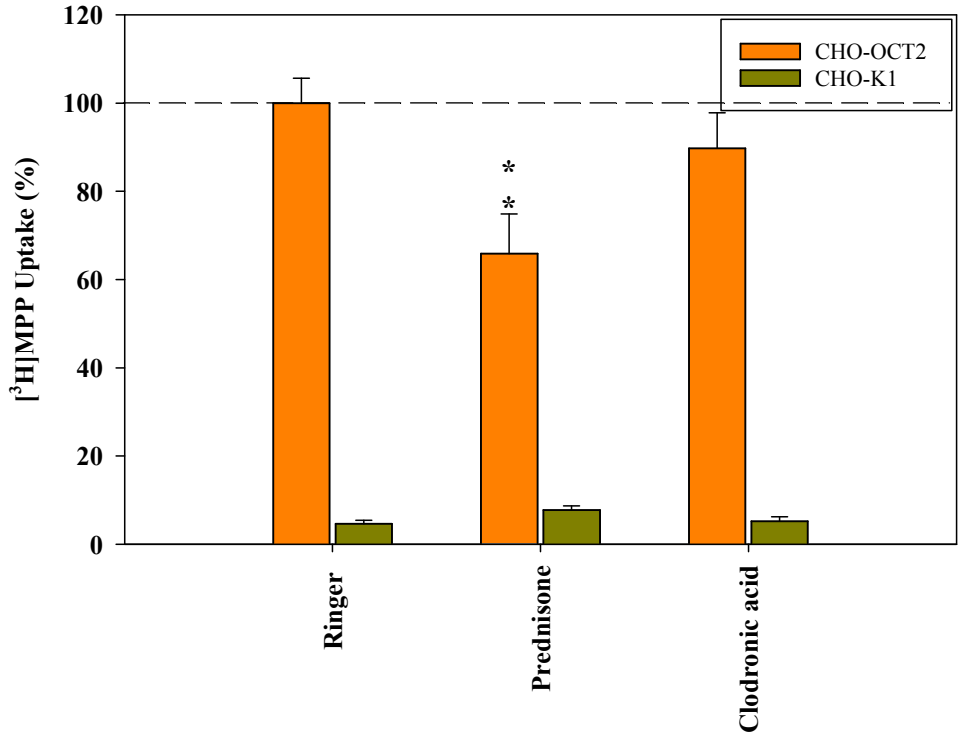

Fig 4.40 Inhibition of [^{3}H]MPP uptake by drugs acting on steroid hormone receptors (100 µM each) in CHO-hOCT2 cells. The control set (without inhibitor) was set at 100 %. Data are means of three independent experiments with four repeats each. **P< 0.01

4.3 Transporter mediated transporter sensitivity

For elucidating the role of OCT1 and OCT2 in the uptake of cytostatics and their resultant cytotoxicity, we performed MTT assays in stably transfected CHO cells expressing OCT1 and OCT2, as well as in two B-lymphoma cell lines: L-428, with high OCT1 expression, and SUDHL-4, with no OCT1 expression. Cells were treated with the cytostatic alone and together with TEA, a known substrate of OCTs and corticosterone, an inhibitor of OCTs. An incubation time of only 15 minutes was used to ensure that the effects observed were transporter mediated and not due to any other factors (like passive diffusion).

4.3.1 Evaluation of OCT1 and OCT2 mediated cytotoxicity of irinotecan using the MTT assay

Figure 4.41 demonstrates the cell viability assay performed in OCT1 and OCT2 expressing CHO cells on treatment with irinotecan. Irinotecan, which specifically interacts with OCT1

and OCT2, resulted in a decrease in cell viability after 15 minutes of cytostatic treatment. The decrease in cell viability was 30 ± 4.5%, P <0.05; and 23 ± 3.3%, P< 0.001, in OCT1 and OCT2 cells, respectively. Treatment with TEA and corticosterone alone did not affect OCT2. In OCT1 cells, however, incubation with TEA and corticosterone increased cell viability to 112.33 ± 8.84% and 112.45 ± 7.66%, respectively. The observed increase in cell viability was not significant. Treatment of OCT1 and OCT2 cells with irinotecan and TEA simultaneously, demonstrated a reversal in reduced cell viability seen with irinotecan alone with no observable differences from that of the control set (104.27 ± 10.71% and 99.71 ± 1.98%, respectively). Similar results were obtained on simultaneous treatment of cells with irinotecan and corticosterone, with cell viability comparable to that of the control conditions. OCT1 expressing cells exhibited a cell viability of 113.77 ± 6.44% and OCT2 cells 100.57 ± 0.45%. Mock cells (non- transfected CHO-K1 cells) did not exhibit changes in cell viability under the different conditions tested.

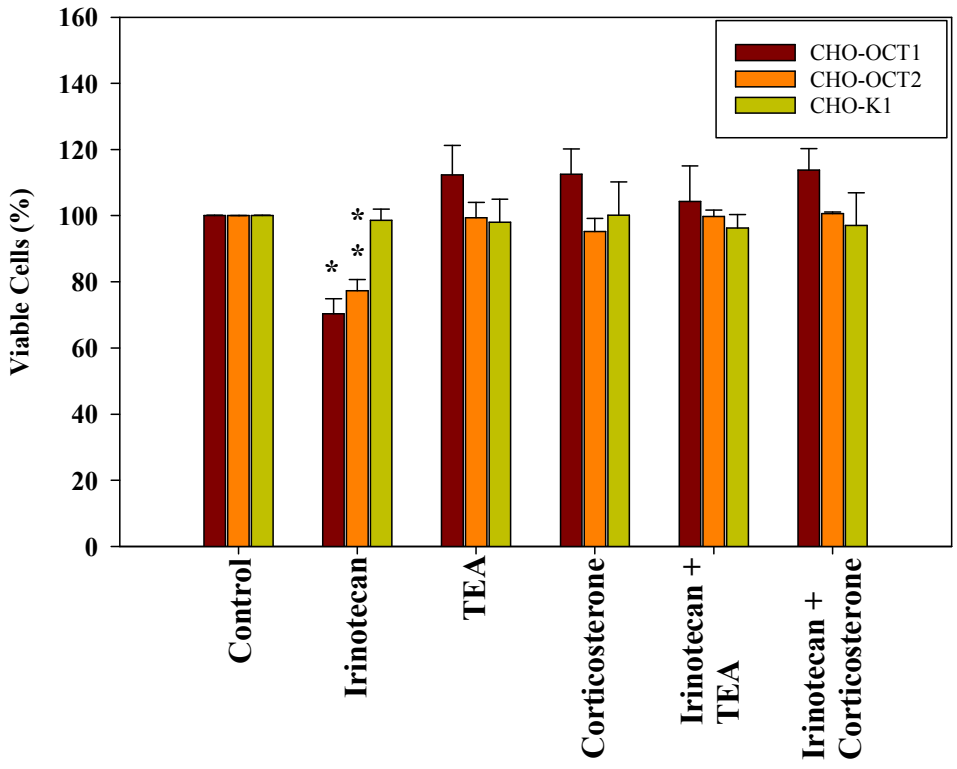

Fig 4.41 OCT1 and OCT2 mediated cytotoxicity of irinotecan was determined using the MTT assay. Cells were treated with 100 µM Irinotecan for 15 min, washed with PBS and incubated in cell culture medium for an additional 24 h at 37 °C. Irinotecan toxicity on CHO-OCT1 and CHO-OCT2 was reversed by the addition of TEA and corticosterone. Data are means of three independent experiments with four repeats each. *P<0.05, **P< 0.01

The MTT assay for irinotecan on B-lymphoma cell lines is shown in Figure 4.42. L-428 demonstrated a decrease in cell viability by 15.7 ± 1.84% (P< 0.0001) on irinotecan treatment alone. On treatment of cells with irinotecan and TEA simultaneously, L-428 cells showed a very slight reversal in decreased cell viability to 14 ± 2.45% (P< 0.0001). When corticosterone and irinotecan were applied to cells simultaneously, L-428 cells demonstrated a decrease of only 12.91 ± 2.88% (P< 0.001). SUDHL-4, not expressing OCT1 or OCT2, demonstrated no observable effects on cell viability under any condition tested.

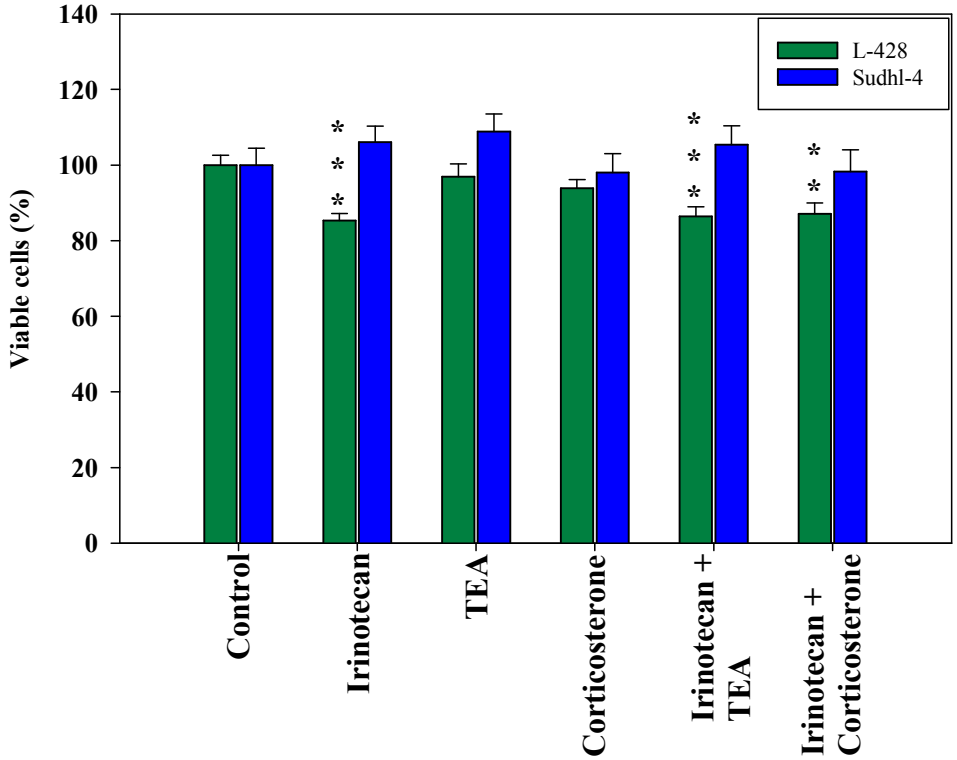

Fig 4.42 OCT1 mediated cytotoxicity of irinotecan was determined using the MTT assay in the B- lymphoma cell line, L-428. SUDHL-4, with no observed expression of OCT1, was used as a control. Cells were treated with 100 µM irinotecan for 15 min, washed with PBS and incubated in cell culture medium for an additional 24 h at 37 °C. Data are means of three independent experiments with four repeats each. **P<0.01, ***P< 0.0001

4.3.2 Evaluation of OCT1 mediated cytotoxicity of mitoxantrone using the MTT assay

The effect of the topoisomerase inhibitor mitoxantrone on cell viability was examined in OCT1 expressing cells (Figure 4.43). Cells were treated with 100 µM mitoxantrone alone and together with 2 mM TEA and 100 µM corticosterone. On mitoxantrone treatment alone, OCT1 expressing cells exhibited reduced cell viability by 40.8 ± 2.54%, P< 0.001. Mock cells

also demonstrated decreased cell viability by 8.44 ± 7.8 % although this was not significant. On treatment with mitoxantrone and TEA together, cell viability was reduced by only 3.2 ± 2.6% and this change from mitoxantrone cytotoxicity was significant. Mitoxantrone and corticosterone treatment of cells resulted in a significant reversal of the decrease in cell viability by 14.3 ± 3.22% in OCT1 cells.

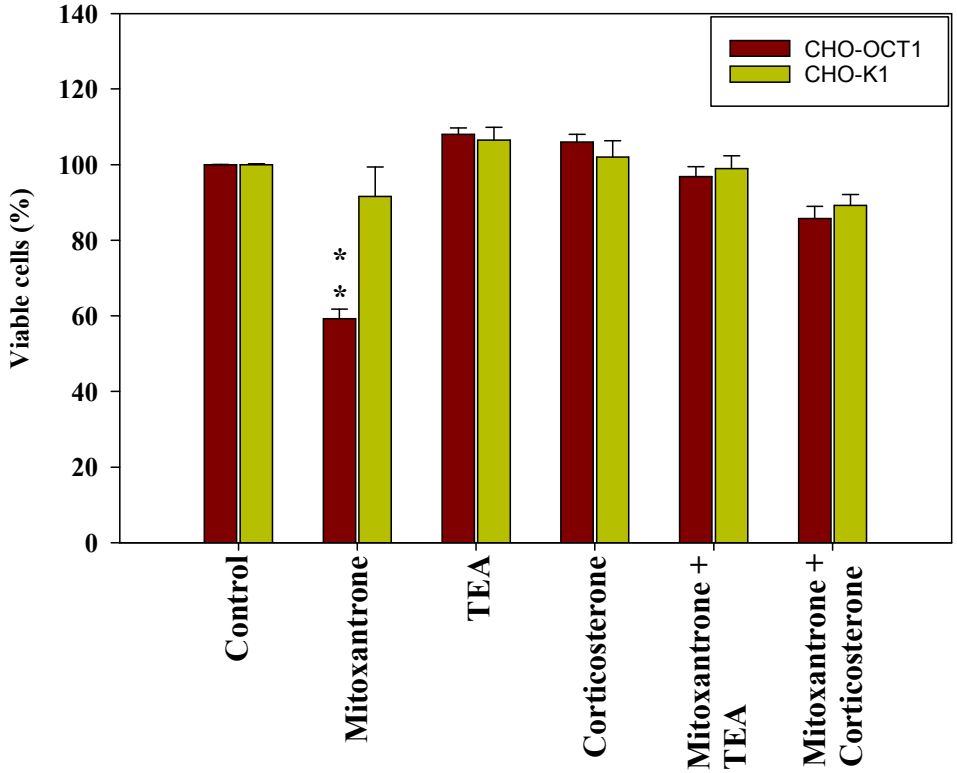

Fig 4.43 OCT1 mediated cytotoxicity of mitoxantrone was determined using the MTT colorimetric assay. Cytotoxicity of mitoxantrone was tested by incubating the cells with 100 µM cytostatic for 15 min, followed by washing with PBS and an overnight incubation in cell culture medium at 37 °C. Data are means of three independent experiments with four repeats each. **P< 0.01

The decrease in cell viability observed in the two B-lymphoma cell lines was more dramatic, with mitoxantrone treatment alone effecting a decrease in cell viability by 45.87 ± 2.69%, P< 0.0001 and 65.45 ± 3.49%, P< 0.0001 in L-428 and SUDHL-4 cells, respectively (Figure 4.44). The observed decrease in cell viability in both cell lines could not be reversed on simultaneous treatment with TEA and corticosterone. On simultaneous application of mitoxantrone and TEA, the cell viability decreased to 54.87 ± 3.74%, P< 0.0001 in L-428 and to 33.04 ± 3.17%, P< 0.0001 in SUDHL-4. The decrease in cell viability observed on

treatment with mitoxantrone and corticosterone was 55.46 ± 3.93%, P< 0.0001 and 26.95 ± 2.25%, P< 0.0001 in L-428 and SUDHL-4, respectively.

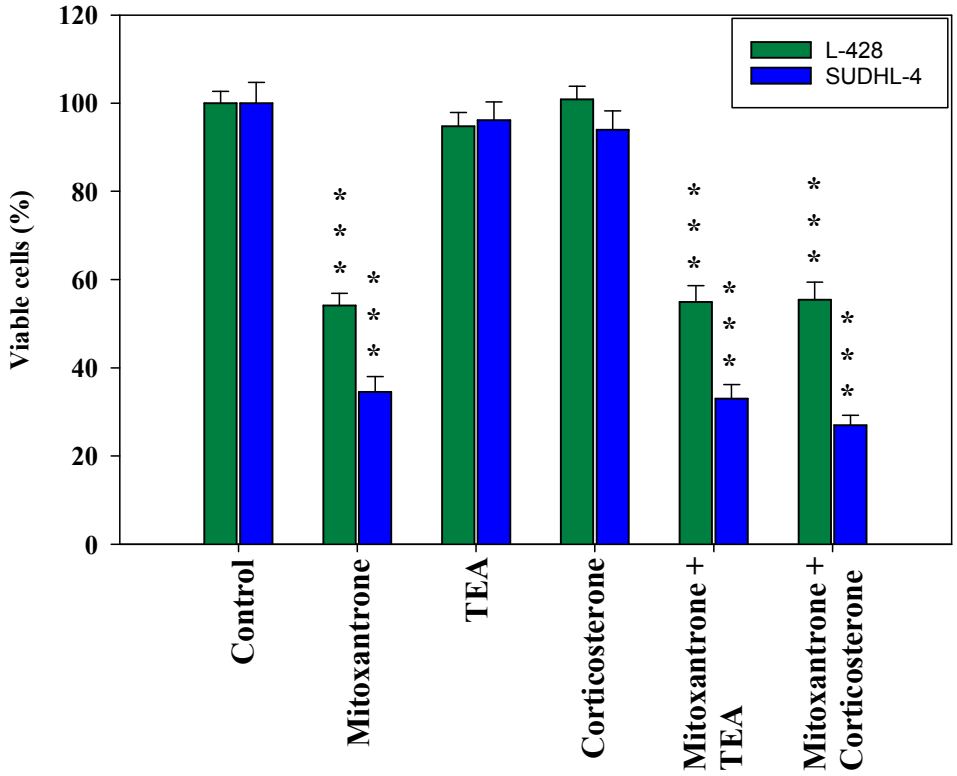

Fig 4.44 OCT1 mediated cytotoxicity of mitoxantrone was examined using the MTT assay in the B- lymphoma cell lines, L-428 and SUDHL-4. Cells were treated with 100 µM mitoxantrone for 15 min, washed with PBS and incubated in cell culture medium for an additional 24 h at 37 °C. Mitoxantrone cytotoxicity was not reversed on simultaneous incubation with TEA and corticosterone. Data are means of three independent experiments with four repeats each. ***P< 0.0001

4.3.3 Evaluation of OCT1 mediated cytotoxicity of paclitaxel using the MTT assay

Treatment of OCT1 expressing cells with 100 µM paclitaxel effected a 30.67 ± 3.29%, P< 0.05 decrease in cell viability (Figure 4.45). This was significantly reversed on simultaneous treatment with paclitaxel and TEA, and paclitaxel and corticosterone to 106.79 ± 1.3% and 99.02 ± 3.41%, respectively. OCT1 expressing cells also exhibited increased cell viability when treated with TEA and corticosterone (110 ± 2.39%, P< 0.05 and 113.12 ± 0.89%, P< 0.05, respectively). No significant changes in cell viability of mock cells were observed.

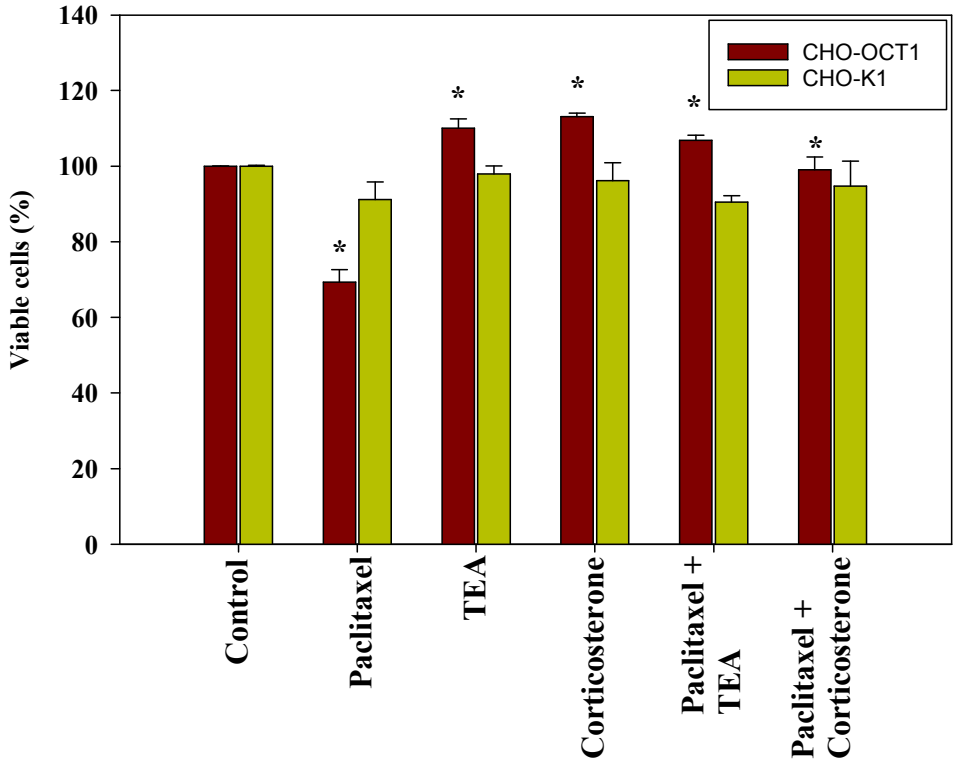

Fig 4.45 Cell viability test for OCT1 expressing cells after paclitaxel treatment. The test was performed using the MTT colorimetric assay. Cells were treated with 100 µM of the cytostatic for 15 min, washed with PBS and incubated overnight in cell culture medium at 37 °C. Data are means of three independent experiments with four repeats each. * P< 0.05

In B-lymphoma cells lines treated under similar conditions, SUDHL-4 did not show any changes in cell viability (Figure 4.46). OCT1 expressing L-428, however, exhibited a decrease in cell viability by 45.71 ± 4.5% on paclitaxel treatment alone. Treatment of L-428 with paclitaxel and TEA resulted in a significant recovery of cells (47%) with the reduced cell viability of only 18.44 ± 5.39%. The recovery of cells on incubation with paclitaxel and corticosterone was also highly significant, with the decrease in cell viability calculated to be only 9.96 ± 5.66%.

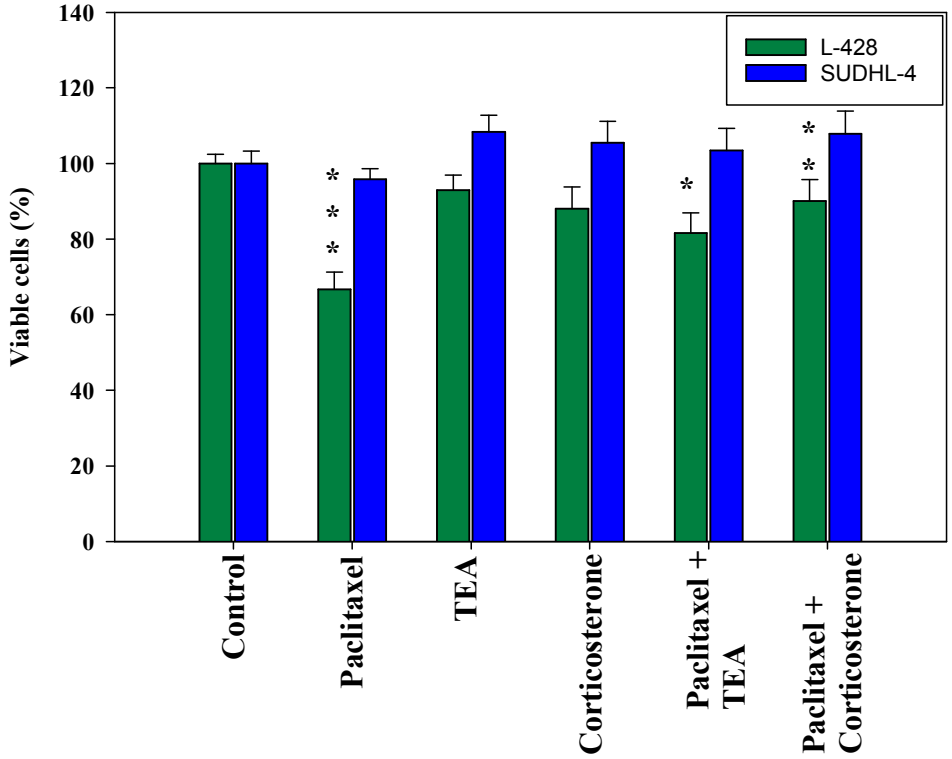

Fig 4.46 OCT1 mediated cytotoxicity of paclitaxel was determined using the MTT assay in the B- lymphoma cell line, L-428. SUDHL-4, with no observed expression of OCT1, was used as a control. Cells were treated with 100 µM paclitaxel for 15 min, washed with PBS and incubated in cell culture medium for an additional 24 h at 37 °C. Paclitaxel toxicity in L-428 was partially reversed by the addition of TEA and corticosterone. Data are means of three independent experiments with four repeats each. * P< 0.05, **P<0.001, ***P< 0.0001

4.4 p53 expression analysis

The tumour suppressor, p53, is responsible for the transcriptional activation of a series of proteins involved in apoptosis. This protein is present at low levels in resting cells, but exposure to DNA- damaging agents stabilizes and activates p53. We looked for changes in p53 expression by quantifying the expressed protein under different conditions (control, 100 µM specific cytostatic, 2 mM TEA, 100 µM corticosterone, cytostatic + TEA, cytostatic + corticosterone). Cells were incubated in different conditions for 15 min and allowed to recover for 1 h at 37°C. Western blots for p53 expression analysis were probed with mouse anti-p53 (1:1000) and with mouse anti-actin (1:1000) for normalization.

4.4.1 Evaluation of p53 expression on irinotecan treatment

Western blot analysis revealed that 15 minutes treatment of OCT1 and OCT2 expressing cells with irinotecan did not result in an elevation of steady state levels of the p53 protein (Figure 4.47). No changes were seen in irinotecan treated cells from untreated cells.

The control cells also exhibited a constant p53 expression under various conditions.

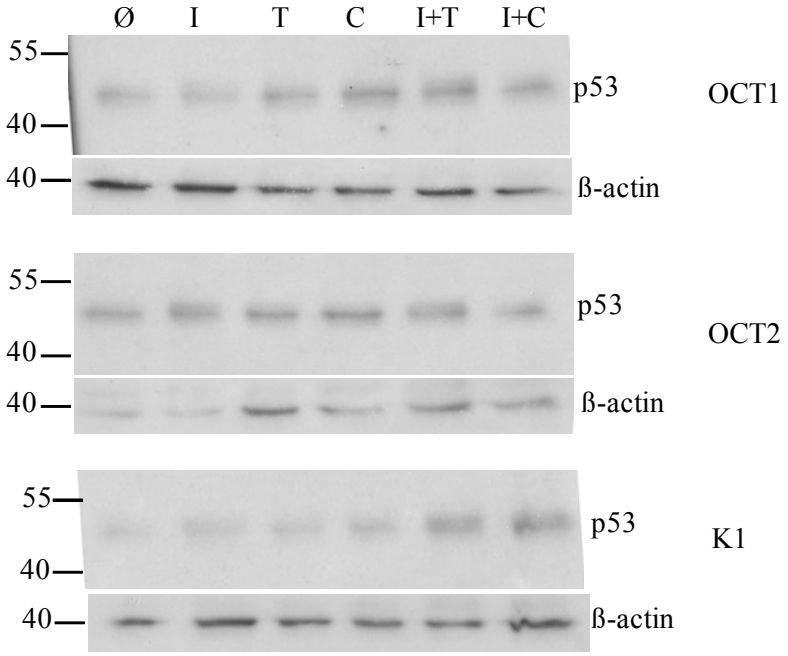

Fig 4.47 p53 expression on irinotecan treatment in OCT1 and OCT2 expressing cells. Cells were treated with normal media ø, irinotecan I, TEA T, corticosterone C, irinotecan+TEA I+T and irinotecan+corticosterone I+C, for 15 minutes. Following 1 h recovery, cells were lysed and gels run.

4.4.2 Evaluation of p53 expression on mitoxantrone treatment

Treatment of OCT1 cells with mitoxantrone gave a slight shift in the p53 protein band. This upward shift in the signal for p53 was also seen in samples treated with mitoxantrone together with TEA and corticosterone (Figure 4.48).

The control cells revealed a steady state expression of p53 with no changes under any condition tested. A slightly higher expression of p53 with mitoxantrone alone could be due to higher protein loaded for this sample as demonstrated by a slightly stronger actin signal.

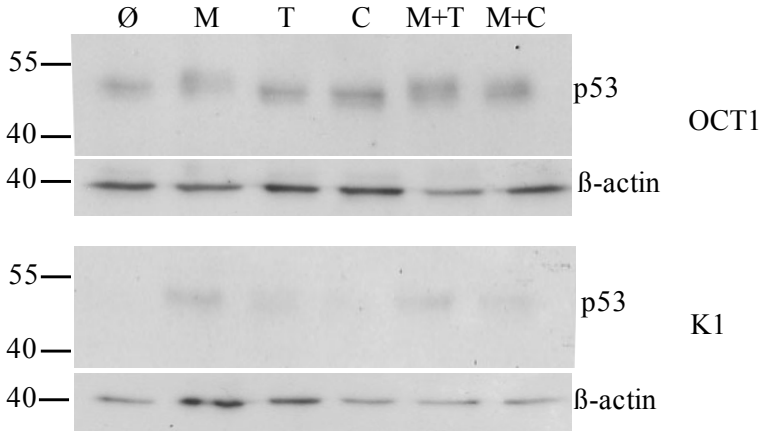

Fig 4.48 p53 expression on mitoxantrone treatment in OCT1 expressing cells. Cells were treated with normal media ø, mitoxantrone M, TEA T, corticosterone C, mitoxantrone+TEA M+T and mitoxantrone+corticosterone M+C, for 15 minutes. Following 1 h recovery, cells were lysed and gels run. Blots were probed for p-53 expression using mouse anti-p53 (1:1000).

4.4.3 Evaluation of p53 expression on paclitaxel treatment

p53 expression in OCT1 cells on paclitaxel treatment alone did not change from control conditions (Figure 4.49). However, TEA and corticosterone treatment of OCT1 cells gave much weaker p53 signals.

The control cells exhibited a constant p53 expression under different conditions. Paclitaxel in the presence of corticosterone gave a weaker signal for p53, but this can be explained by a slightly lower protein loading for this sample as evidenced by the actin blot.

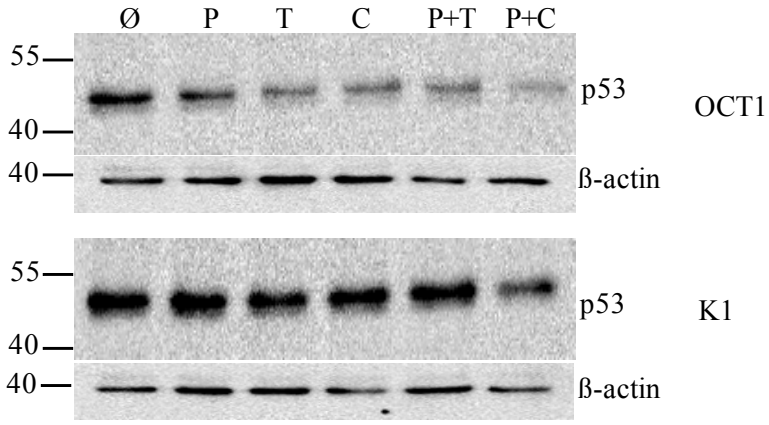

Fig 4.49 p53 expression on paclitaxel treatment in OCT1 expressing cells. Cells were treated with normal media ø, paclitaxel P, TEA T, corticosterone C, paclitaxel+TEA P+T and paclitaxel+corticosterone P+C, for 15 minutes. Following 1 h recovery, cells were lysed and gels run. Blots were probed for p-53 expression using mouse anti-p53 (1:1000).

4.5 Uptake of [^{14}C]succinate by NaDC3- FlpIn T-Rex HEK 293

To determine whether the NaDC3 cell line generated expressed the functional protein, we measured the uptake of radiolabelled succinate, a known substrate of NaDC3 (Figure 4.50). The stably transfected cells expressing NaDC3 exhibited an uptake of 93920.30 ± 2351.61 fmol/ 5 min, which was 95% higher than mock cells (2922.02 ± 751.48 fmol/ 5 min). This uptake was reduced to 10.33 ± 0.67%, P< 0.0001 (9704.45 ± 629.77 fmol/5 min) by the addition of 1 mM cold succinate. Lithium is known to inhibit transport via NaDC3 and the addition of 10 mM lithium into the transport medium reduced the uptake of succinate by 51.88 ± 4.04%, P< 0.0001 (46226.22 ± 3798.23 fmol/ 5 min). Since NaDC3 relies on Na^+ to effect transport, we also checked for transporter activity in the absence of Na^+ in transport medium. Na^+ free transport medium effectively abolished NaDC3 activity (4106.58 ± 599.80 fmol/ 5 min).

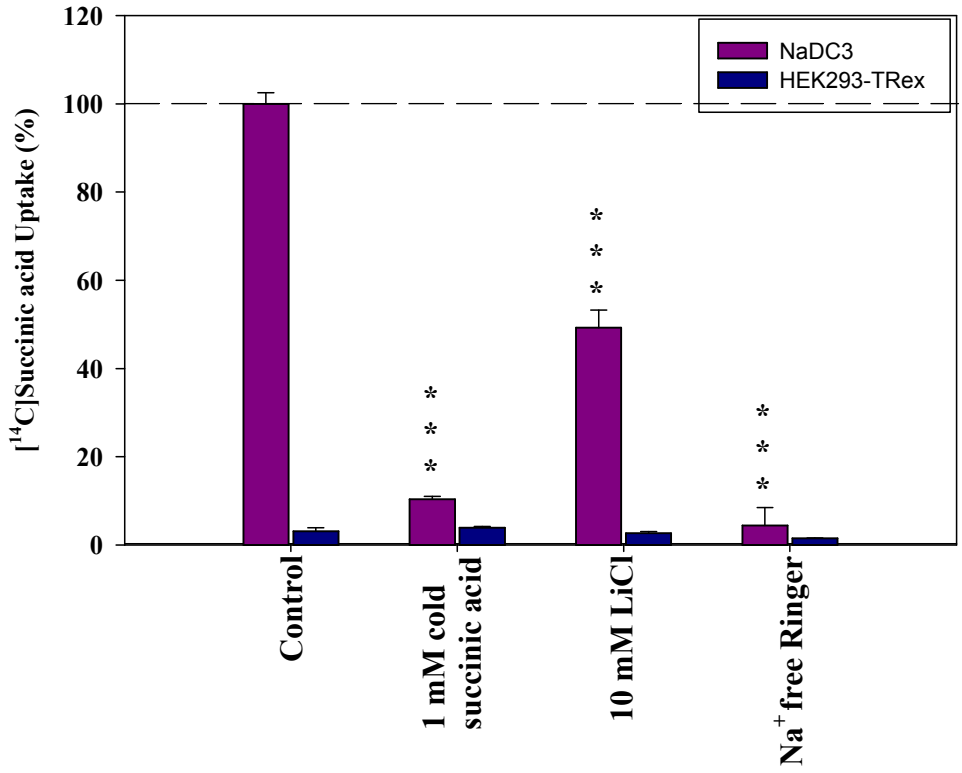

Fig 4.50 [^{14}C]succinate uptake by NaDC3. The uptake was significantly inhibited by unlabelled succinate, in the absence of sodium in the uptake medium and in the presence of lithium. Data are means of three independent experiments with four repeats each.
***P< 0.0001

4.6 Cis-Inhibition of NaDC3 mediated [^{14}C]succinate uptake

The interaction of cytostatics with NaDC3 was determined by inhibition of [^{14}C]succinate uptake by these cells (Figure 4.51). Twelve cytostatics were tested and succinate uptake was significantly inhibited by 100 µM methotrexate to 76.1 ± 1.16%, P< 0.05. Another antimetabolite, gemcitabine, also reduced succinic acid uptake by NaDC3 by 30.5 ± 0.78%, P< 0.001. Nearly 20% inhibition of succinate uptake by NaDC3 was also observed with busulfan, irinotecan, paclitaxel, fludarabine, mitoxantrone, cladrabine and fluoroadenine; but this inhibition was not significant. Prednisone stimulated uptake of succinate by NaDC3 to 105.4 ± 1.40%. However this observed stimulation of succinate uptake was not significant.

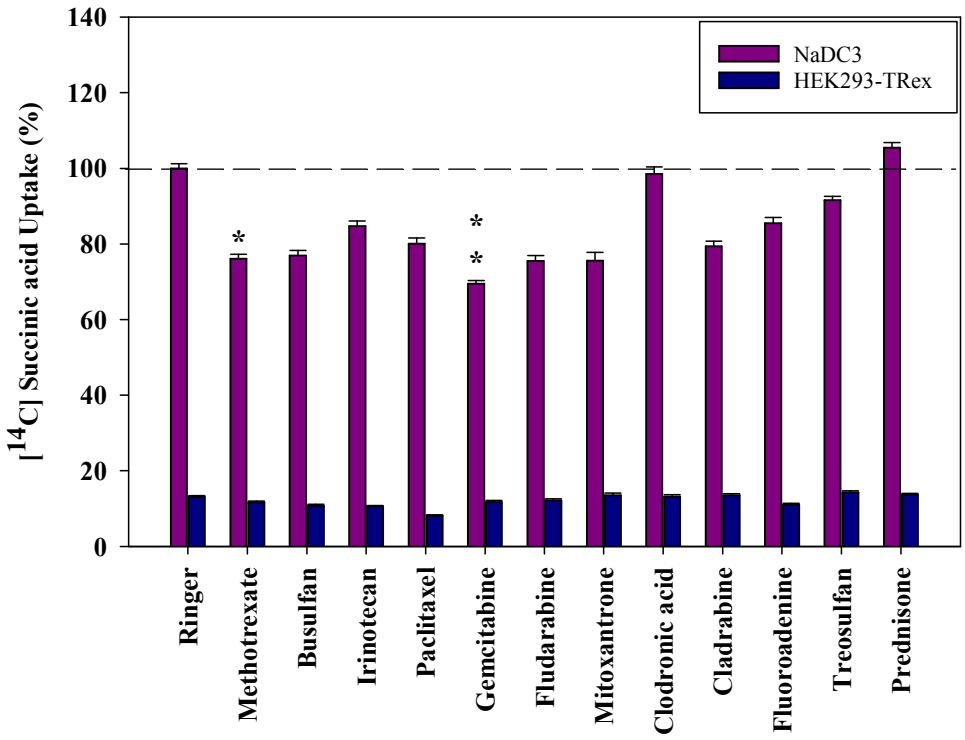

Fig 4.51 Inhibition of NaDC3 mediated [^{14}C]succinate uptake by various cytostatics (100 µM). Cells expressing hNaDC3 were incubated in transport medium for 5 min. All experiments were standardized by setting the control (without cytostatic) to 100 %. Data are means of three independent experiments with three repeats each. * P< 0.05, **P< 0.01

The inhibition observed with methotrexate and gemcitabine was much lower than 50% and therefore, the drug kinetics with NaDC3 were not examined further.

5. DISCUSSION

The successful treatment of cancer involves an effective uptake of chemotherapeutic agents into cancer cells, mediated by transporter proteins. An increased expression of drug exporting proteins, like MDR1 and MRPs results in chemoresistance of cancer cells. This chemoresistance could possibly be overcome by using cytostatics specific for certain uptake transporters present in tumour cells. Although there has been a growing interest in SLC transporters over the years, not much is known about the interaction of tumour treating drugs with these transporters. Therefore, the aims of the present study were to examine the expression of SLC transporters in lymphoma cell lines and in CLL patient samples, the interaction of cytostatics with specific transporters; and finally, the transporter mediated cytostatic effect of these drugs on tumour cells.

In recent years, ATP-binding cassette (ABC) transporters related to multidrug resistance (MDR), such as P-glycoprotein (MDR1) and ABCG2 (breast cancer resistance protein/mitoxantrone resistance protein) have emerged as key factors that regulate the intracellular concentrations of many therapeutics. Drug transporters may be overexpressed in cancer cells reducing intracellular drug concentrations (117). For example, MDR1 has been shown to reduce doxorubicin access to nuclear targets in cells (106). MDR1 and MRP1 were expressed at high levels in all lymphoma cell lines we tested. Since chemoresistance is mediated in part by the efflux of cytostatics by these transporters, the expression levels of ABC transporters in cancer cells should be considered during tumour therapy.

5.1 Expression of uptake transporters belonging to the SLC family in lymphoma cell lines and CLL patient samples

Total cell RNA was purified from six lymphoma cell lines and from the peripheral blood of CLL patient samples. Following reverse transcription, PCR was carried out. As a target of cytostatics, expression levels of different SLC transporter families were analyzed.

The ubiquitous system L transporters, LATs (SLC7) mediate the transfer of large, neutral amino acids across plasma membranes (59). LATs occur ubiquitously in the body and the tissue distribution of LAT1 suggests that it is expressed in growing cells, a fact that may be utilized in transporting drugs into cells. Melphalan, used in chronic lymphocytic leukaemia treatment, is also known to be transported by LAT1 into the cells (124). We observed a high expression of LAT1 in all six cell lines tested, which may make these cells sensitive to

cytostatic analogs of L-amino acids. However, our results demonstrated a high expression of LAT1 in healthy lymphocytes as well. This high expression of LAT1 in healthy cells makes the use of LAT1 specific cytostatics difficult since it would result in the death of healthy cells.

The SLC10 transporters, NTCP and ASBT are essential in maintaining the enterohepatic circulation of bile acids. NTCP mediates the transport of bile acid in the liver while ASBT transports bile acid through the membrane in the intestine (68;79). SLC10 transporters can provide an effective means of cellular uptake of bile-conjugated drugs for therapy and NTCP is a known transporter of the drug-conjugate chlorambucil-taurocholate (67). However, we did not observe SLC10 transporter expression in our cell lines and thus these transporters are not viable for use in transporter-specific tumour therapy for lymphomas.

The SLC13 family transporters are found in plasma membranes of mammalian cells. NaDC3 is found in kidneys, placenta, liver and brain. Substrates include dicarboxylates essential in the citric acid cycle, like α-ketoglutarate (88). In the brain, NaDC3 mediates the transport of N-acetylaspartate, and benzylpenicillin is also known to interact with NaDC3 (15). Transport of cytostatics by NaDC3 has not been reported so far, although the presence of this transporter in brain and kidneys makes it a viable target for selective therapy of brain and kidney tumours. The expression of NaDC3 was not seen in lymphoma cell lines and therefore cannot be a target for limiting tumour cell growth.

The monocarboxylate transporters belonging to the SLC 16 family, MCTs, are expressed ubiquitously in the human body (45;93) and catalyze the transport of monocarboxylates including lactate and pyruvate (46). The interaction of MCT2 with ifosphamide metabolites has also been reported (20) and the transport of other drugs like valproic acid may also be mediated by MCTs (53). MCT1 and MCT4 require CD147 for proper cell surface expression and function. CD147 is a member of the immunoglobulin superfamily and is also up-regulated in aggressive tumours (119). The interaction of MCTs with cytostatics makes them important candidates in the uptake of cancer treating drugs and their resultant cytotoxicity. MCT1, MCT2 and MCT4 were all expressed at high levels in lymphoma cell lines. MCT1 and MCT4 were also expressed at high levels in healthy lymphocytes. MCT2 was expressed at lower levels in healthy lymphocytes and may be considered in mediating ifosphamide based therapy. However, MCT transporters are very important for cell survival and this makes these transporters unsuitable for transporter-mediated therapy. Real time analysis of MCT4

expression in CLL patient samples also revealed a much lower MCT4 expression than in healthy lymphocytes, thus negating this transport for use in tumour therapy.

The folate/thiamine transporter family, SLC19, includes the reduced folate transporter (RFT). RFT expression is seen in all human tissues, although it is much higher in absorptive tissues like intestine, kidney and placenta. RFT mediates the cellular influx of folate and its derivatives. The transporter also mediates the transport of the antineoplastic methotrexate. Mutations in RFT can lead to chemoresistance to antifolates like methotrexate (35). The thiamine transporter, ThTr1, is expressed ubiquitously and may be used to transport thiamine-conjugated drugs. RFT and ThTr1 were found to be expressed at slightly higher levels in the lymphoma cell lines than in healthy samples, making these transporters candidates for antifolate cytostatic therapy.

Organic anion transporting polypeptides, OATPs, belong to the SLCO family of transporters and are expressed in a variety of tissues, including intestine, liver, kidney and brain (64). These mediate the uptake of a broad range of compounds into the cells, including bile salts, hormones and steroid conjugates (35). OATPs play a critical role in drug absorption, distribution and excretion. Due to their wide tissue distribution and broad substrate spectrum, altered protein localization and transport characteristics can contribute to interindividual variations of drug effects. Bamet-UD, a cisplatin derivative, is transported by OATP-A (13) and SN-38, the active metabolite of irinotecan, has been shown to interact with OATP-C (85). OATP8 transports cytostatics like methotrexate and paclitaxel (108). OATP-B was found to be expressed in only B-lymphoma cell lines with no expression seen in healthy cells. Therefore, this transporter could be used for specifically targeting B-lymphoma cells. However, in CLL patient samples, OATP-B expression was not observed at all, thus opposing the use of OATP-B specific cytostatics in treatment. OATP-D was also expressed at much higher levels than normal in the lymphoma cell lines and may be a candidate for transporter therapy. OATP-E was expressed at higher levels than normal in the cell lines but was expressed at much lower levels in CLL patient samples. Therefore, OATP-E cannot be considered for use in tumour therapy.

The SLC22 family includes the organic cation transporters, OCTs. Expressed in many tissues like the kidney, liver and the blood-brain barrier, OCTs transport positively charged endogenous substrates (epinephrine, norepinephrine) and exogenous substrates (MPP, TEA) (17). OCTs are also involved in drug distribution and are known to mediate drug transport

across the blood-brain barrier (105). Cisplatin, a platinum based cytostatic, is specifically transported by OCT2 (26). Recently, our lab has demonstrated the involvement of OCT3 in the uptake of three cytostatics- irinotecan, melphalan and vincristine and the OCT3 mediated cytotoxicity of these drugs in Renal Carcinoma cell lines (107). OCT6 has been shown to transport doxorubicin, used in carcinoma therapy (87). Using real time analysis, we found that OCT1 was expressed at higher levels in lymphoma cell lines than in healthy lymphocytes. In CLL patient samples too, OCT1 was expressed at much higher levels than in healthy lymphocytes, making it a prime candidate for transporter mediated tumour therapy. OCT6 was also expressed at much higher levels in lymphoma cell lines as well as in CLL patient samples than normal. OCT6 can thus be considered for tumour therapy.

Organic anion transporters, OATs, are located at boundary epithelia and play an important role in distribution and excretion of drugs. The antimetabolite cytostatic, methotrexate, is known to be transported by OAT1, 2, 3 and 4 (118). OAT2 is also known to transport the cytostatic 5-fluorouracil (61). Unpublished studies in our group have demonstrated the interaction of chlorambucil with OAT1, 3 and 4; and a specific interaction of bendamustine with OAT3 (PD Dr. Yohannes Hagos, personal communication). While OAT1 was expressed at higher levels than normal in the lymphoma cell lines, much lower expression than normal was observed for OAT1 in CLL patient samples. The same was true for OAT2 where the expression was high in lymphoma cell lines but no expression was observed in CLL patient samples. Thus, OAT transported drugs cannot be considered for therapy in this case, since the application of these cytostatics may result in major side effects rather than efficient tumour treatment.

The sodium-coupled concentrative nucleoside transporters of the SLC 28 family, CNTs, transport nucleosides and nucleoside analogs actively into cells. CNTs are pharmacologically important as they transport many clinically relevant drugs. CNT1, which is expressed in the liver, kidney and small intestine, is a known transporter of cytotoxic cytidine analogs cytarabine and gemcitabine, used in the treatment of tumours (40). CNT3, occurring ubiquitously in the body, transports many anticancer nucleoside analogs like cladribine, gemcitabine and fludarabine (98;99). However, no observable expression of CNTs was seen in the lymphoma cell lines thus making these transporters unsuitable for use in tumour therapy.

Most mammalian cells express equilibrative nucleoside transporters (ENTs) belonging tot he SLC 29 family. ENTs play key roles in nucleoside and nucleobase uptake (42). ENTs are implicated in the cellular uptake of nucleoside analogues used in cancer treatment and also in the treatment of viral diseases. ENT2 has a great capacity to transport clinically important drugs used in HIV therapy, like 3'-azido-3'-deoxythymidine (AZT) (125). ENTs, in particular ENT1, play a critical role in the uptake of many cytotoxic nucleoside analogues like cladribine, cytarabine, fludarabine and gemcitabine (28). High ENT1 expression may contribute to the selectivity of nucleoside chemotherapy for malignant cells and the *in vitro* sensitivity of acute lymphoblastic leukaemia cells to cladribine has been attributed to these transporters (28). Conversely, a lowered expression of these transporters may contribute to drug resistance for cytotoxic nucleoside analogues. Expression measurement of these transporters can thus provide a valuable tool in guiding cancer therapy. While the ENT expression was high in the lymphoma cell lines tested, lower than normal expression was seen in CLL patient samples. Nucleoside analogs (eg. fludarabine) are successfully used in CLL therapy; however, the cytotoxic effect of these drugs may not be ENT-dependent.

The transporter expression studies made by us in CLL patient samples may be limited by the improper collection of patient samples and the handling thereafter (eg. freezing of samples). In addition, results may be affected by the medical history of patients. Substrate induction for transporters has been shown previously (81). It is possible that changes in transporter expression take place as a result of cytostatics used in the treatment regimen. Understanding the expression changes in transporters can also potentially help in generating safer treatment regimen by predicting changes in drug pharmacokinetics.

5.2 Interaction of cytostatics with OCT1 and OCT2

The electrogenic organic cation transporters 1 and 2 are expressed in the liver, kidney, brain and the intestines (63); and translocate a variety of organic cations with widely differing molecular structures. Substances transported by the OCT transporters include organic cations and weak bases which are positively charged at physiological pH. Non-charged compounds may also be transported, as has been demonstrated for cimetidine transport (63). 1-Methyl-4-phenylperidinium (MPP) and tetraethylammonium (TEA) are model cations transported by OCT1, OCT2 and OCT3. The OCT transporters are inhibited by a variety of compounds which may not be transported themselves. Inhibitors of OCT transport include cations like

tetrapentylammoniun, noncharged compounds like corticosterone and anions like probenecid (63).

The high expression of OCT1 in lymphoma cell lines as well as in CLL patient samples makes it a suitable candidate for drug targeting. OCT1 and 2 mediated transport for drugs like the antidiabetic metformin and the antimalarial drug quinine has been previously reported. OCT1 also transports antivirals like aciclovir and ganciclovir. Among the cancer treating drugs, cisplatin has been identified as an OCT2 substrate and its transport demonstrated (63).

To confirm the functionality of OCT1 and OCT2 in stable transfected cells, we performed experiments with the known substrate of organic cation transporters, MPP. Using increasing concentrations of [^{3}H]MPP, we determined 20 nM MPP to be efficiently transported in OCT1 and OCT2 cells. [^{3}H]MPP uptake was inhibited by the addition of cold MPP (50-500 μM) to the transport medium. The high ratio of hot and cold MPP in the transport medium results in a very low uptake of radiolabelled (hot) MPP uptake.

We next performed a series of experiments to test the inhibition potency of cytostatics for OCT1 and OCT2 mediated [^{3}H]MPP uptake. The interaction of cytostatics with OCT3 was previously studied in our group and demonstrated the interaction of irinotecan, vincristine and melphalan with OCT3 (107). For our experiments, we selected substances covering the major groups of cytostatics used in chemotherapy. Among the 22 cytostatics we tested, irinotecan, mitoxantrone and paclitaxel inhibited OCT1 mediated [^{3}H]MPP uptake by more than 50%. In OCT2 expressing cells, irinotecan effectively inhibited more than 50% [^{3}H]MPP uptake. Irinotecan, thus, interacts with OCTs 1, 2 and 3 while paclitaxel and mitoxantrone interact with only OCT1.

The interaction of these three cytostatics was analyzed using Dixon plot studies. Irinotecan interacted with OCT1 in a competitive manner while the interaction of mitoxantrone and paclitaxel with OCT1 was non-competitive. OCT1 showed a high affinity for irinotecan, with a K_i value of only 1.73 μM. The observed affinity of OCT1 was relatively low for mitoxantrone and paclitaxel, with calculated K_i values of 85.2 μM and 50.1 μM, respectively. The interaction of irinotecan with OCT2 was also analyzed and was determined to be mixed inhibition. OCT2 showed a much lower affinity for irinotecan with a K_i value of 86.3 μM. While irinotecan may be transported by OCT1, results for mitoxantrone and paclitaxel suggest that these two cytostatics do not occupy the substrate recognition site and are not transported.

Similarly, the results with OCT2 suggest that while the transporter interacts with irinotecan, it does not transport the cytostatic. However, deviations from the classical competitive inhibition have been observed and we cannot exclude the transport of mitoxantrone and paclitaxel by OCT1 and that of irinotecan by OCT2.

Although the lymphoma cell lines we tested demonstrated a strong OCT1 expression, it was not possible to carry out uptake studies in these suspension cells. High background of radioactivity was measured during uptake in suspension cells which interfered with the measurement of incorporated radioactivity. The methodology for uptake measurements in suspension cells involved the use of silicon oil which should theoretically draw the non-incoporated radioactivity. However, a high background of radioactivity was measured even after the removal of the silicon oil. The elimination of the oil itself was rather inefficient with small amounts present in the samples, adding to the measured radioactivity.

5.2.1 Transporter mediated cytotoxicity of irinotecan

OCT1 and OCT2 mediated [^{3}H]MPP uptake was efficiently inhibited by the addition of irinotecan to the transport media in stably transfected cells. Irinotecan is a topoisomerase I inhibitor and is used as a first-line therapy in metastatic colorectal cancer in combination with other drugs (103). Irinotecan is converted by hydrolysis to its active metabolite, SN-38, which undergoes glucuronide conjugation to the pharmacologically inactive SN-38 glucuronide, SN-38G (56). As a topoisomerase I inhibitor, SN38 inactivates topoisomerase I enzyme activity, leading to a ‘locking’ of topoisomerase I on DNA. The topoisomerase I-DNA complex formed blocks DNA duplication and RNA transcription.

SN-38 treatment makes cells sensitive to other cytostatics and irinotecan cytotoxicity is dependent on the concentration of active SN-38 in cells. This SN-38 concentration in cells is modulated by the hydrolase enzyme responsible for the hydrolysis of irinotecan to SN-38 as well as the glucuronosyltransferase which converts SN-38 into its inactive form (56). The concentration of SN-38 is also dependent on the efflux of the irinotecan metabolite out of cells by MDR1 while the influx may be regulated by specific uptake transporters.

In the MPP uptake inhibition experiments, we demonstrated an interaction of irinotecan with OCT1 and OCT2. To test whether the expression of OCT1 and OCT2 affected cell proliferation on treatment with irinotecan, we carried out MTT assays. Cell proliferation was significantly inhibited in OCT1 and OCT2 expressing CHO cells treated with irinotecan

compared to control cells that do not express OCT1 or OCT2. To prove that the cytotoxic effect of irinotecan is dependent on OCT1 and OCT2 activity, we inhibited irinotecan uptake into our cells by 2 mM TEA. TEA, tetraethylammonium, is a substrate of OCTs and the OCT mediated transport into cells has been previously demonstrated (63). OCT1 and OCT2 expressing CHO cells which were treated with irinotecan in the presence of TEA did not demonstrate lowered cell viability. Treatment with irinotecan in the presence of 100 µM corticosterone, an inhibitor of OCT-mediated uptake, did not affect cell viability in OCT1 and OCT2 expressing cells. These results suggest that irinotecan is indeed transported by OCT1 as well as OCT2 and can explain the lowered cell viability in OCT expressing cells.

To test whether irinotecan could be used in the treatment of lymphomas expressing OCT1 or OCT2, we performed similar experiments using two B-lymphoma cell lines. Our previous studies on expression of OCTs revealed a high OCT1 expression in the B-lymphoma cell line L-428 while no expression for OCT1 was observed in SUDHL-4 cells. OCT2 expression was not observed in any cell line. Since irinotecan transport is also mediated by OCT3 in renal carcinoma cell lines and the resultant cytotoxicity demonstrated previously (107); we tested OCT3 expression in lymphoma cell lines and found no observable expression of OCT3. Irinotecan cytotoxicity tests revealed a comparatively higher sensitivity in OCT1 expressing L-428. This sensitivity to irinotecan, read as lowered cell viability of L-428 cells, was slightly inhibited on treatment with irinotecan in the presence of TEA and corticosterone. In the OCT deficient cell line, SUDHL-4, no effect on cell viability was observed. These results again suggest that OCT1 is responsible for the transport of irinotecan into cells and the selective lowering of cell viability in OCT1 expressing L-428 cells may be explained by the cytotoxic action of irinotecan on these cells.

The relatively lower degree of the reversal in cytotoxicity on the application of irinotecan in the presence of TEA and corticosterone may be due to the uptake of irinotecan by some other transporter. Studies in our lab have demonstrated the interaction of MATE1 with irinotecan and SN-38 (the active metabolite of irinotecan) has also shown to be a substrate for OATP8 (OATP1B3) (123). It may be worthwhile to investigate the expression of MATE1 and OATP8 in our lymphoma cell lines.

The reduction in cell viability observed in both, the stably transfected CHO cells expressing OCT1 and OCT2, as well as in the lymphoma cell line, L-428, was less than 60 %. This could be explained by the relatively short incubation time of only 15 minutes. Cells were incubated

for only 15 minutes under different conditions to ensure that the observed effects were due to active uptake and thus transporter dependent. Cytotoxicity assays are usually done by exposing cells to various drug concentrations for 24-72 h (66). However, using this short incubation time, we could theoretically rule out diffusion of the drug into cells. Another possible reason for the relatively lower reduction in cell viability seen in our experiments is the efflux of irinotecan by the ABC transporters. We tried inhibiting the efflux of irinotecan by applying verapamil, MDR inhibitor, to our cells. However, the inhibition of MDR proved toxic to cells and lowered cell viability was observed for OCT expressing as well as non-expressing cells even in the absence of irinotecan. Therefore, verapamil was not used in further experiments.

We also carried out [^{3}H]thymidine incorporation experiments as a measure of inhibition of DNA synthesis in irinotecan treated OCT1 and OCT2 expressing stably transfected cells. However, in our experiments we could not demonstrate a clear inhibition of cell proliferation using this method. One possible reason for the absence of clear DNA synthesis inhibition could be the incorporation of radioactivity from [^{3}H]thymidine into macromolecules other than DNA (58).

As an additional readout of irinotecan cytotoxicity on our cells, we screened the expression of p53 by treated cells. The p53 tumour suppressor is a critical transcription factor. It controls cell growth and induces apoptosis during cellular stress (65). Transactivation of target genes under the control of p53 is an essential step in stress response (120). We carried out experiments on stably transfected OCT1 and OCT2 cells treated with irinotecan, in the presence and absence of TEA and corticosterone. p53 expression under different conditions was examined and we found that after 15 minutes of treatment, steady state levels of p53 did not change. Irinotecan, via its active metabolite, SN-38, has been demonstrated to significantly increase the expression of p53 and its phosphorylation, alongwith increased expression of apoptosis-inducing proteins, Bax, caspase-9 and caspase-3 (111). The increased expression of p53 was observed by Takeba et al. after 24 h treatment with irinotecan. The absence of elevated p53 levels in treated cells may be due to the absence of immediate activation of apoptosis after only 15 minutes of treatment. The active efflux of irinotecan by MDR1 may also account for the absence of changes in p53 levels seen in our experiments. The increased expression of MDR1 has previously been shown to inhibit irinotecan-induced apoptosis (112). To test the role of p53 dependent cellular response to DNA damage, it would

be worthwhile to examine the expression of p53 regulated genes like p21. Alternatively, the cells may exhibit a p53-independent response to irinotecan treatment. Although the mechanism is not clear, our experiments demonstrate that despite the failure of irinotecan to induce programmed cell death, it does reduce cell viability in OCT1 and OCT2 treated cells, as shown using the MTT assay.

We suggest that the sensitivity of cells to irinotecan is dependent on OCT1. A positively charged compound, irinotecan shares partial structural similarity to MPP, the OCT substrate. This similarity to MPP structure may explain the interaction and suggested transport of irinotecan by OCT1. TEA and MPP binding in OCT1 is mediated by amino acids in the fourth transmembrane helix, an area located in the large cleft (16). This large cleft is easily accessible for organic cations, and may also recognize irinotecan. With a high affinity of OCT1 for irinotecan, the cytotoxicity of this cytostatic may be used in tumour cells expressing OCT1.

Since the lymphoma cell lines available to us did not express OCT2, we could not confirm an OCT2 mediated irinotecan sensitivity on lymphoma cells. However, OCT2 may also play a role in irinotecan sensitivity as demonstrated by experiments on stably transfected cells. The comparatively lower affinity of OCT2 for irinotecan may be explained by differences in the substrate recognition regions of OCT1 and OCT2. Further experiments are needed to confirm irinotecan uptake by OCT2 and its usefulness in therapy.

5.2.2 Transporter mediated cytotoxicity of paclitaxel

OCT1 mediated [^{3}H]MPP uptake was inhibited in CHO cells by the addition of paclitaxel to transport media. Paclitaxel is active against a broad range of cancers like lung cancer, and head and neck cancer. It is used in palliative therapy of ovarian and breast cancers resistant to chemotherapy (102) . This taxane works by promoting the polymerization of tubulin (104). Polymers of tubulin form microtubules which are responsible for the formation of the mitotic spindle during cell division. Microtubules are also involved in interphase functions, like maintenance of shape, motility and intracellular transport (33). Paclitaxel inhibits the disassembly of microtubules at subnanomolar concentrations. At higher concentrations, paclitaxel increases the mass and number of microtubules. Paclitaxel induced microtubules are particularly stable and dysfunctional, causing cell death by disrupting normal microtubule dynamics required for cell division and interphase functions (102).

Some tumours express alpha- and beta-tubulin with an impaired ability to polymerize. Polymerization of tubulin in these tumour cells is very slow and is normalized by the application of paclitaxel (102). Resistance to paclitaxel may also be due to the activity of drug-efflux pumps like MDR1. The organic anion transporting polypeptide 8, OATP8 is a known transporter of paclitaxel and polymorphisms in the gene encoding this transporter may play crucial roles in the elimination of paclitaxel from cells (108). SLC transporters are also exchangers and OATP-8 may also contribute to chemoresistance in this case by exporting drugs out of the cell.

Our experiments showed an interaction of paclitaxel with OCT1 by significantly inhibiting MPP uptake by OCT1 expressing cells. To test whether this inhibition of [^{3}H]MPP uptake was actually due to transport of the cytostatic into cells, we measured the decrease in cell proliferation on application of paclitaxel. Stably transfected CHO cells expressing OCT1 were incubated with paclitaxel and this resulted in a 30 % lowered cell viability. To confirm the OCT1 dependent activity of paclitaxel on cells, we incubated cells with paclitaxel in the presence of TEA, a substrate of OCTs and corticosterone, an inhibitor of OCTs. Cell viability was not reduced in these samples.

The B-lymphoma cell lines, L-428 and SUDHL-4, were also tested for OCT1 mediated cytotoxicity of paclitaxel. The OCT1 expressing L-428 demonstrated reduced cell viability by 35 % while SUDHL-4, which does not express OCT1, was not affected. The reduced cell viability was partially reversed on application of the OCT1 substrate TEA together with paclitaxel. The OCT inhibitor corticosterone also effectively reversed the lowered cell viability seen in OCT1 expressing L-428 with paclitaxel alone. These results indicate that OCT1 mediates the uptake of paclitaxel into cells and its resultant cytotoxic action.

The relatively lower reduction in cell viability in the MTT assays can be explained by the short incubation time of cells under different conditions and also due to the export of paclitaxel out of the cells by MDR1. Paclitaxel is a known substrate of MDR1 (78). The inhibition of MDR1 was done by the application of verapamil, but this proved toxic to OCT1 expressing as well as non-expressing cells. Therefore, experiments were carried out without inhibiting MDR1.

[^{3}H]Thymidine incorporation experiments in stably transfected OCT1 cells were again inconclusive with no clear reduction in cell viability of treated OCT1 cells. This may again be

due to high background levels of non-incorporated [^{3}H]thymidine, similar to [^{3}H]thymidine incorporation in irinotecan treated cells explained in the previous section.

Previous studies have shown that microtubule inhibiting cytostatics activate the expression of p53 in cells (122). We examined the induction of p53 expression in OCT1 cells on paclitaxel treatment. We did not observe any changes in p53 expression under different conditions but this may be due to the short treatment time. It is possible that prolonged exposure to the cytostatic may result in higher p53 levels and thus induce immediate apoptosis. The maintenance of steady state p53 levels on paclitaxel treatment may also indicate that these levels are sufficient in activating cell cycle arrest, giving the cell time to repair the damage and thus avoid genetic instability.

We hypothesize that paclitaxel transport and the resultant cytotoxicity is mediated by OCT1. OCT1 is also present in the bronchi of humans and OCT1 mediated paclitaxel transport can account for type I hypersensitivity reactions like bronchospasms that most patients experience on treatment with paclitaxel (102). There have also been reports of corticosteroid treatment to relieve this hypersensitivity (102) which may partially act by blocking the OCT1 mediated transport of the drug.

An interaction of paclitaxel with OCT2 was also demonstrated but since the inhibition of MPP uptake affected was less than 50 %, this transporter was not studied for paclitaxel uptake studies. Nevertheless, OCT2 mediated paclitaxel transport is a viable area of study. Due to its expression in neurons, OCT2 transport of paclitaxel may also explain peripheral neuropathy observed in paclitaxel treated patients. While the expression of OATP8 in our cells was not tested, there are no reports to suggest that it is expressed in these cells. However, the role of OATP8 in paclitaxel uptake by these cells and its effect on cell death cannot be ruled out. One member of the OATP family, rat Oatp2, has been shown to function as a bidirectional organic solute transporter (74). It may well be that OATP8 functions as a paclitaxel-paclitaxel exchanger, although the affinities for this bidirectional transport may be different. Studies in our lab have also demonstrated the interaction of paclitaxel with OATP-B (Mr. Ronny Eckhardt, personal communication) and OATP-B mediated paclitaxel effects have yet to be elucidated.

5.2.3 Cytotoxicity of mitoxantrone is not OCT1 specific

The addition of mitoxantrone to transport media resulted in a strong inhibition of OCT1 mediated [^{3}H]MPP uptake. Mitoxantrone is widely used against acute leukaemia, non-Hodgkin and Hodgkin lymphomas, melanoma, liver cancer, prostate cancer, bladder cancer, and head and neck cancer (75). A topoisomerase II inhibitor, mitoxantrone induces DNA strand breaks (10;24). Structurally related to anthracycline antibiotics, mitoxantrone has been shown to be adsorbed by the plasma membranes of living cells (32). The breast cancer resistance protein, BCRP (ABCG2) facilitates the efflux of mitoxantrone from cancer cells (84).

Mitoxantrone demonstrated an exceptionally high inhibition of MPP uptake by OCT1 cells and we therefore checked for OCT1 mediated transport of this cytostatic. Using MTT assays, we determined the effect of mitoxantrone on OCT1 expressing cells. Cell viability of these cells was reduced by 40 % while no effect was seen in mock cells.

However, both the B-lymphoma cell lines tested for mitoxantrone sensitivity demonstrated reduced cell viability. The cell viability was reduced by more than 40 % in L-428 which expresses OCT1. SUDHL-4, which did not demonstrate any observable OCT expression, showed more than 60 % decrease in cell viability on mitoxantrone treatment. In both cell lines, this effect on mitoxantrone treatment was not reversible with TEA or corticosterone.

These results lead us to conclude that mitoxantrone cytotoxicity seen in these cells is clearly not OCT1- specific. According to published data, mitoxantrone uptake into cells is not carrier mediated, but may occur due to simple diffusion and this may explain the cytotoxic effects seen in all cells treated with mitoxantrone (18). However, Pan and colleagues have recently demonstrated the role of influx transporters in mitoxantrone accumulation in cells. It has been suggested that mitoxantrone permeability in cells is not only affected by passive diffusion but also by an influx transporter (90). A lowered accumulation of mitoxantrone was observed at lower temperatures, similar to the uptake of the cytostatic imatinib, which was also found to be temperature dependent (113). OCT1 influx system has been suggested to play a role in imatinib transport. A putative mitoxantrone uptake transporter may belong to the SLC transporter family. With a positive charge at physiological pH, mitoxantrone may be transported by OCTs or OCTNs. However, mitoxantrone may not be selective substrate for OCTs, as demonstrated in our experiments. The cation and carnitine transporters 1 and 2,

OCTN1 and OCTN2, are expressed in lymphocytes (63) and mitoxantrone uptake in the studied B-lymphoma cell lines may be attributed to OCTN- mediated transport. The interaction of drugs like levofloxacin with OCTN2 has been demonstrated (50).The uptake of L-carnitine, OCTN2 substrate is trans-stimulated by intracellular TEA (86). The uptake of TEA by OCT1 into cells may thus trans-stimulate OCTN2 mediated uptake of mitoxantrone into cells. The expression analysis of OCTN in our cell lines was not done and additional studies are needed to ascertain the influx transporter involved in mitoxantrone uptake.

The expression of p53 in OCT1 cells on treatment with mitoxantrone revealed a slightly higher molecular weight band. This may well be a post translationally modified, for example, a phosphorylated form of p53. These up-shifted bands were also observed when mitoxantrone was applied to cells in the presence of TEA and corticosterone. Phosphorylation of p53 is regarded as the first step of p53 stabilization (65). These higher molecular weight bands may represent stabilized p53 in the cell which could then induce apoptosis. This would also support the high reduction in cell viability observed in the B-lymphoma cell lines on mitoxantrone treatment. It would be important to check the expression of p53 regulated factors that are functional in programmed cell death to confirm whether mitoxantrone cytotoxicity can really induce p53 activation.

5.3 Interaction of cytostatics with NaDC3

NaDC3 is a high affinity Na^+/dicarboxylate transporter, encoded by SLC13A3 gene. With a broad tissue distribution, NaDC3 is found in renal proximal tubule cells, liver, brain and placenta (88). NaDC3 is responsible for transporting a range of substrates, including long chain or branched dicarboxylates. Substrates of NaDC3 include α-ketoglutarate and heavy metal chelators like dimercaptopropane-1-sulfonate (14). NaDC3 also mediates the high affinity transport of N-acetylaspartate in the brain (36). The transport of substrates by NaDC3 is sodium-dependent and is electrogenic. Interaction with monovalent organic anions like benzylpenicillin has also been demonstrated (15). Human NaDC3 transport is inhibited by millimolar concentrations of lithium (121).

NaDC3 is an important regulator of oxidative metabolism, but the pathophysiological implications and the mechanisms of expression of this high affinity Na^+/dicarboxylate transporter are poorly understood. The use of the generated cell line in studying potential

interaction partners may help in making the physiological and pathological roles of NaDC3 clearer.

Following the generation of stable transfected NaDC3 cell line, we examined the interaction of NaDC3 with various cancer treating drugs. Only methotrexate and gemcitabine inhibited NaDC3 mediated succinate uptake significantly. However, the inhibition achieved was less than 50 % and therefore these interactions were not studied further.

5.4 Conclusions and outlook

In the present study, we investigated the expression of uptake transporter proteins in cancer cells and the transporter mediated cytotoxic effects of cytostatics. The lymphoma cell lines studied demonstrated a variable expression of uptake transporters. The high expression of OCT1 in these cells could potentially be used for treatment with cytostatics like irinotecan and paclitaxel. The use of cytostatics specifically transported by OCT1 could help target these cancer cells better and thus, result in an effective treatment regimen. The lymphoma cell lines studied also expressed a variety of efflux ABC transporters. Inhibiting the efflux action of these pumps while simultaneously applying OCT1 specific drugs is one way of overcoming chemoresistance in cancer cells.

The use of transporter-mediated cancer therapy has immense potential. Studying transporter expression in cancer cells, before as well as during, therapy can help tailor therapy to suit individual needs, while minimizing serious side effects.

6. Appendix

6.1 Vector maps

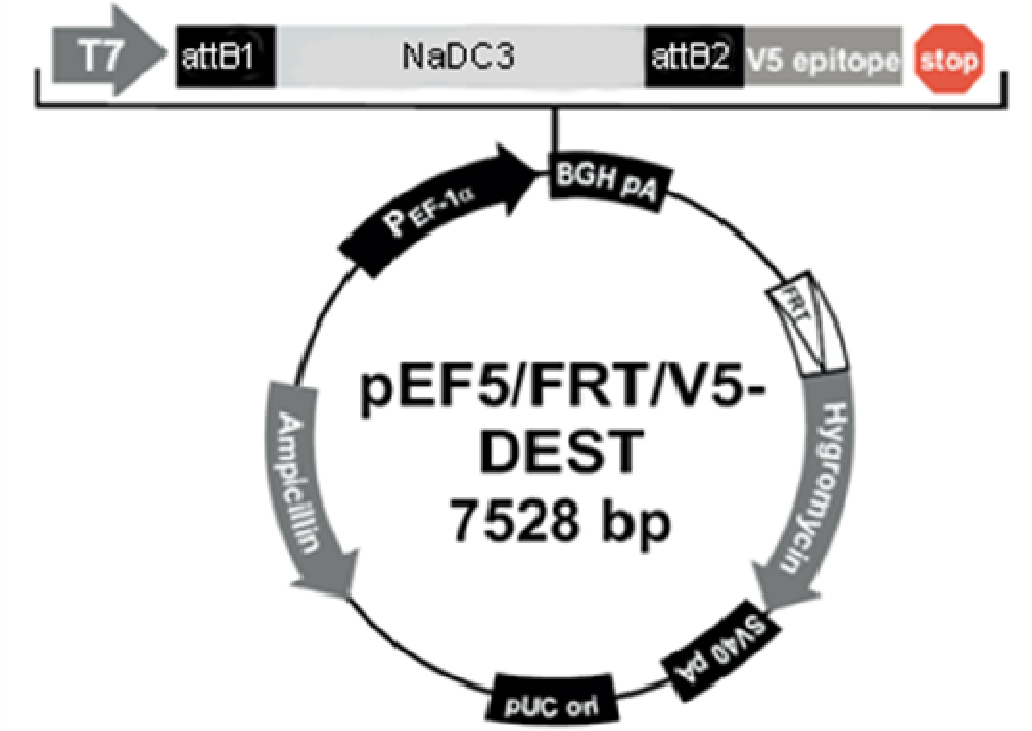

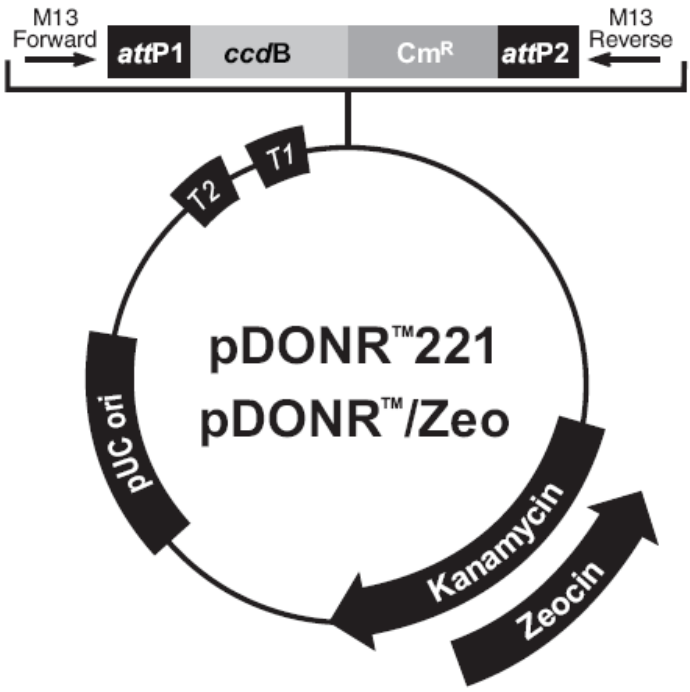

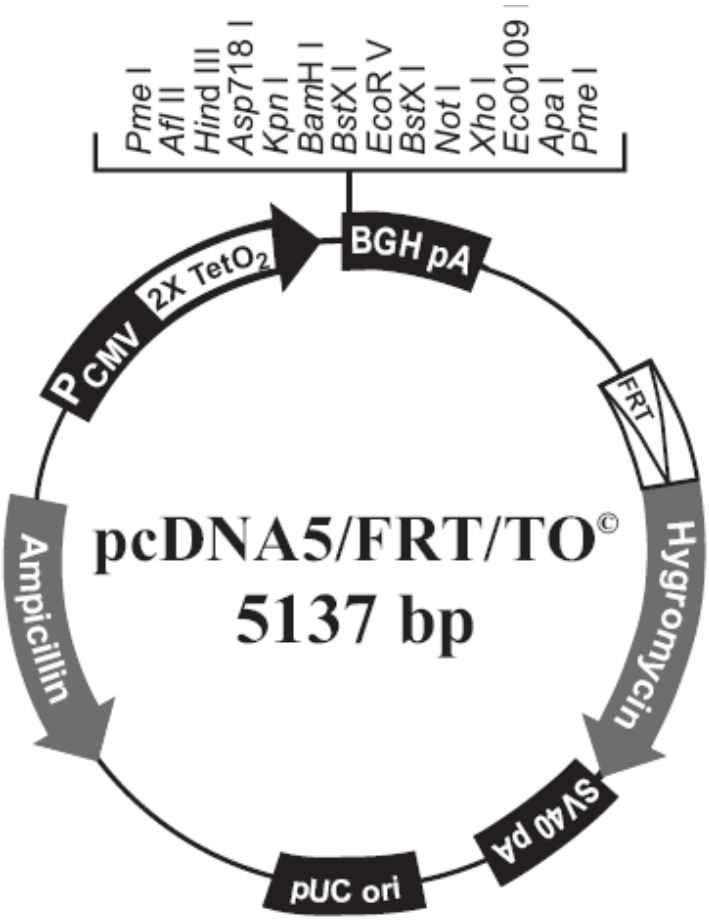
Pme I
Afl II
Hind III
Asp718 I
Kpn I
BamH I
BstX I
EcoR V
BstX I
Not I
Xho I
Eco0109 I
Apa I
Pme I
BGH pA
2X TetO2
P CMV
FRT
Hygromycin
SV40 pA
pUC ori
Ampicillin
pcDNA5/FRT/TO©
5137 bp

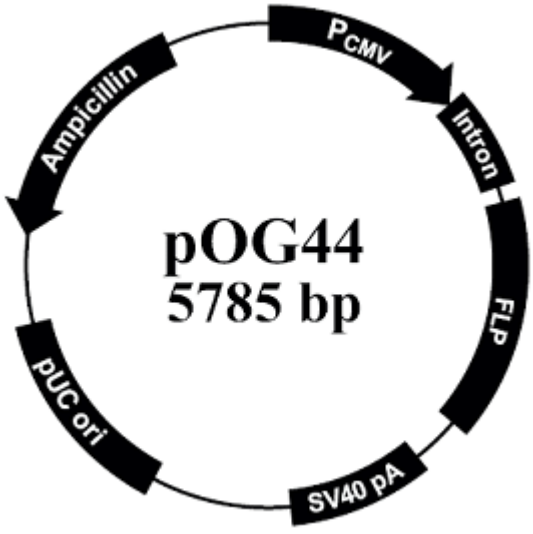
PCMV
Intron
FLP
SV40 pA
pUC ori
Ampicillin
pOG44
5785 bp

7. References

1. Acimovic Y, Coe IR. Molecular evolution of the equilibrative nucleoside transporter family: identification of novel family members in prokaryotes and eukaryotes. *Molecular Biology and Evolution* 2002;19:2199-210.

2. Ahmadi T, Maniar T, Schuster S, Stadtmauer E. Chronic Lymphocytic Leukemia: new concepts and emerging therapies. *Curr.Treat.Options.Oncol.* 2009.

3. Au-Yeung BB, Deindl S, Hsu LY, Palacios EH, Levin SE, Kuriyan J et al. The structure, regulation, and function of ZAP-70. *Immunological Reviews* 2009;228:41-57.

4. Baldwin SA, Beal PR, Yao SY, King AE, Cass CE, Young JD. The equilibrative nucleoside transporter family, SLC29. *Pflugers Archiv.European Journal of Physiology* 2004;447:735-43.

5. Bartels CL, Tsongalis GJ. MicroRNAs: novel biomarkers for human cancer. *Clinical Chemistry* 2009;55:623-31.

6. Bergeron MJ, Simonin A, Burzle M, Hediger MA. Inherited epithelial transporter disorders-an overview. *J.Inherit.Metab Dis.* 2008.

7. Bergmann MA, Goebeler ME, Herold M, Emmerich B, Wilhelm M, Ruelfs C et al. Efficacy of bendamustine in patients with relapsed or refractory chronic lymphocytic leukemia: results of a phase I/II study of the German CLL Study Group. *Haematologica* 2005;90:1357-64.

8. Biermann J, Lang D, Gorboulev V, Koepsell H, Sindic A, Schroter R et al. Characterization of regulatory mechanisms and states of human organic cation transporter 2. *Am.J.Physiol Cell Physiol* 2006;290:C1521-C1531.

9. Boelens J, Lust S, Vanhoecke B, Offner F. Chronic lymphocytic leukaemia. *Anticancer Research* 2009;29:605-15.

10. Boland MP, Fitzgerald KA, O'Neill LA. Topoisomerase II is required for mitoxantrone to signal nuclear factor kappa B activation in HL60 cells. *Journal of Biological Chemistry* 2000;275:25231-8.

11. Boonstra R, Timmer-Bosscha H, Echten-Arends J, van der Kolk DM, van den BA, de Jong B et al. Mitoxantrone resistance in a small cell lung cancer cell line is associated with ABCA2 upregulation. *British Journal of Cancer* 2004;90:2411-7.

12. Borowski E, Bontemps-Gracz MM, Piwkowska A. Strategies for overcoming ABC-transporters-mediated multidrug resistance (MDR) of tumor cells. *Acta Biochimica Polonica* 2005;52:609-27.

13. Briz O, Macias RI, Perez MJ, Serrano MA, Marin JJ. Excretion of fetal biliverdin by the rat placenta-maternal liver tandem. *Am.J.Physiol Regul.Integr.Comp Physiol* 2006;290:R749-R756.

14. Burckhardt BC, Drinkuth B, Menzel C, Konig A, Steffgen J, Wright SH et al. The renal Na(+)-dependent dicarboxylate transporter, NaDC-3, translocates dimethyl- and disulfhydryl-compounds and contributes to renal heavy metal detoxification. *Journal of the American Society of Nephrology* 2002;13:2628-38.

15. Burckhardt BC, Lorenz J, Burckhardt G, Steffgen J. Interactions of benzylpenicillin and non-steroidal anti-inflammatory drugs with the sodium-dependent dicarboxylate transporter NaDC-3. *Cell Physiol Biochem.* 2004;14:415-24.

16. Burckhardt G. Polyspecific organic cation transport: insights into the substrate binding site. *Molecular Pharmacology* 2005;67:1391-2.

17. Burckhardt G, Wolff NA. Structure of renal organic anion and cation transporters. *Am.J.Physiol Renal Physiol* 2000;278:F853-F866.

18. Burns CP, Haugstad BN, Mossman CJ, North JA, Ingraham LM. Membrane lipid alteration: effect on cellular uptake of mitoxantrone. *Lipids* 1988;23:393-7.

19. Caligaris-Cappio F, Ghia P. Novel insights in chronic lymphocytic leukemia: are we getting closer to understanding the pathogenesis of the disease? *Journal of Clinical Oncology* 2008;26:4497-503.

20. Chatton JY, Idle JR, Vagbo CB, Magistretti PJ. Insights into the mechanisms of ifosfamide encephalopathy: drug metabolites have agonistic effects on alpha-amino-3-hydroxy-5-methyl-4-isoxazolepropionic acid (AMPA)/kainate receptors and induce cellular acidification in mouse cortical neurons. *Journal of Pharmacology and Experimental Therapeutics* 2001;299:1161-8.

21. Chekhun VF, Zhylchuk VE, Lukyanova NY, Vorontsova AL, Kudryavets YI. Expression of drug resistance proteins in triple-receptor-negative tumors as the basis of individualized therapy of the breast cancer patients. *Exp.Oncol.* 2009;31:123-4.

22. Chen J, McMillan NA. Molecular basis of pathogenesis, prognosis and therapy in chronic lymphocytic leukaemia. *Cancer Biol.Ther.* 2008;7:174-9.

23. Cheson BD, Rummel MJ. Bendamustine: rebirth of an old drug. *Journal of Clinical Oncology* 2009;27:1492-501.

24. Chiang SY, Azizkhan JC, Beerman TA. A comparison of DNA-binding drugs as inhibitors of. *Biochemistry* 1998;37:3109-15.

25. Chiorazzi N, Rai KR, Ferrarini M. Chronic lymphocytic leukemia. *New England Journal of Medicine* 2005;352:804-15.

26. Ciarimboli G, Ludwig T, Lang D, Pavenstadt H, Koepsell H, Piechota HJ et al. Cisplatin nephrotoxicity is critically mediated via the human organic cation transporter 2. *American Journal of Pathology* 2005;167:1477-84.

27. Ciurea SO, Andersson BS. Busulfan in hematopoietic stem cell transplantation. *Biology of Blood and Marrow Transplantation* 2009;15:523-36.

28. Clarke ML, Mackey JR, Baldwin SA, Young JD, Cass CE. The role of membrane transporters in cellular resistance to anticancer nucleoside drugs. *Cancer Treatment and Research* 2002;112:27-47.

29. Cotter FE, Auer RL. Genetic alteration associated with chronic lymphocytic leukemia. *Cytogenet.Genome Res.* 2007;118:310-9.

30. Crazzolara R, Bendall L. Emerging treatments in acute lymphoblastic leukemia. *Curr.Cancer Drug Targets.* 2009;9:19-31.

31. Dighiero G, Hamblin TJ. Chronic lymphocytic leukaemia. *Lancet* 2008;371:1017-29.

32. Dubielecka PM, Trusz A, Diakowski W, Grzybek M, Chorzalska A, Jazwiec B et al. Mitoxantrone changes spectrin-aminophospholipid interactions. *Molecular Membrane Biology* 2006;23:235-43.

33. Dustin P. Microtubules. *Scientific American* 1980;243:66-76.

34. Fox CP, McMillan AK, Bishton MJ, Haynes AP, Russell NH. IVE (ifosfamide, epirubicin and etoposide) is a more effective stem cell mobilisation regimen than ICE (ifosphamide, carboplatin and etoposide) in the context of salvage therapy for lymphoma. *British Journal of Haematology* 2008;141:244-8.

35. Ganapathy V, Smith SB, Prasad PD. SLC19: the folate/thiamine transporter family. *Pflugers Archiv.European Journal of Physiology* 2004;447:641-6.

36. George RL, Huang W, Naggar HA, Smith SB, Ganapathy V. Transport of N-acetylaspartate via murine sodium/dicarboxylate cotransporter NaDC3 and expression of this transporter and aspartoacylase II in ocular tissues in mouse. *Biochimica et Biophysica Acta* 2004;1690:63-9.

37. Geyer J, Wilke T, Petzinger E. The solute carrier family SLC10: more than a family of bile acid transporters regarding function and phylogenetic relationships. *Naunyn Schmiedebergs Arch.Pharmacol.* 2006;372:413-31.

38. Giovannetti E, Mey V, Loni L, Nannizzi S, Barsanti G, Savarino G et al. Cytotoxic activity of gemcitabine and correlation with expression profile of drug-related genes in human lymphoid cells. *Pharmacological Research* 2007;55:343-9.

39. Gora-Tybor J, Robak T. Targeted drugs in chronic myeloid leukemia. *Current Medicinal Chemistry* 2008;15:3036-51.

40. Graham KA, Leithoff J, Coe IR, Mowles D, Mackey JR, Young JD et al. Differential transport of cytosine-containing nucleosides by recombinant human concentrative nucleoside transporter protein hCNT1. *Nucleosides Nucleotides Nucleic Acids* 2000;19:415-34.

41. Gray JH, Owen RP, Giacomini KM. The concentrative nucleoside transporter family, SLC28. *Pflugers Archiv.European Journal of Physiology* 2004;447:728-34.

42. Griffith DA, Jarvis SM. Nucleoside and nucleobase transport systems of mammalian cells. *Biochimica et Biophysica Acta* 1996;1286:153-81.

43. Gulley J, Dahut WL. Clodronate in the prevention and treatment of skeletal metastasis. *Expert.Rev.Anticancer Ther.* 2005;5:221-30.

44. Hagenbuch B, Meier PJ. Organic anion transporting polypeptides of the OATP/ SLC21 family: phylogenetic classification as OATP/ SLCO superfamily, new nomenclature and molecular/functional properties. *Pflugers Arch.* 2004;447:653-65.

45. Halestrap AP, Meredith D. The SLC16 gene family-from monocarboxylate transporters (MCTs) to aromatic amino acid transporters and beyond. *Pflugers Archiv.European Journal of Physiology* 2004;447:619-28.

46. Halestrap AP, Price NT. The proton-linked monocarboxylate transporter (MCT) family: structure, function and regulation. *Biochemical Journal* 1999;343 Pt 2:281-99.

47. Hamblin AD, Hamblin TJ. The immunodeficiency of chronic lymphocytic leukaemia. *British Medical Bulletin* 2008;87:49-62.

48. Hebbar M, Ychou M, Ducreux M. Current place of high-dose irinotecan chemotherapy in patients with metastatic colorectal cancer. *Journal of Cancer Research and Clinical Oncology* 2009;135:749-52.

49. Hediger MA, Romero MF, Peng JB, Rolfs A, Takanaga H, Bruford EA. The ABCs of solute carriers: physiological, pathological and therapeutic implications of human membrane transport proteins. *Pflugers Archiv.European Journal of Physiology* 2004;447:465-8.

50. Hirano T, Yasuda S, Osaka Y, Kobayashi M, Itagaki S, Iseki K. Mechanism of the inhibitory effect of zwitterionic drugs (levofloxacin and grepafloxacin) on carnitine transporter (OCTN2) in Caco-2 cells. *Biochimica et Biophysica Acta* 2006;1758:1743-50.

51. Hoffman R, Prchal JT, Samuelson S, Ciurea SO, Rondelli D. Philadelphia chromosome-negative myeloproliferative disorders: biology and treatment. *Biology of Blood and Marrow Transplantation* 2007;13:64-72.

52. Horn L, Sandler AB. Emerging data with antiangiogenic therapies in early and advanced non-small-cell lung cancer. *Clin.Lung Cancer* 2009;10 Suppl 1:S7-16.

53. Hosoya K, Kondo T, Tomi M, Takanaga H, Ohtsuki S, Terasaki T. MCT1-mediated transport of L-lactic acid at the inner blood-retinal barrier: a possible route for delivery of monocarboxylic acid drugs to the retina. *Pharmaceutical Research* 2001;18:1669-76.

54. Huang Y. Pharmacogenetics/genomics of membrane transporters in cancer chemotherapy. *Cancer and Metastasis Reviews* 2007;26:183-201.

55. Hulot JS, Villard E, Maguy A, Morel V, Mir L, Tostivint I et al. A mutation in the drug transporter gene ABCC2 associated with impaired methotrexate elimination. *Pharmacogenet.Genomics* 2005;15:277-85.

56. Iyer L, King CD, Whitington PF, Green MD, Roy SK, Tephly TR et al. Genetic predisposition to the metabolism of irinotecan (CPT-11). Role of uridine diphosphate glucuronosyltransferase isoform 1A1 in the glucuronidation of its active metabolite (SN-38) in human liver microsomes. *J.Clin.Invest* 1998;101:847-54.

57. Jamroziak K, Balcerczak E, Smolewski P, Robey RW, Cebula B, Panczyk M et al. MDR1 (ABCB1) gene polymorphism C3435T is associated with P-glycoprotein activity in B-cell chronic lymphocytic leukemia. *Pharmacol.Rep.* 2006;58:720-8.

58. Jeffrey WH, Paul JH. Effect of 5-Fluoro-2'-Deoxyuridine on [H]Thymidine Incorporation by Bacterioplankton in the Waters of Southwest Florida. *Applied and Environmental Microbiology* 1988;54:331-6.

59. Kanai Y, Endou H. Heterodimeric amino acid transporters: molecular biology and pathological and pharmacological relevance. *Curr.Drug Metab* 2001;2:339-54.

60. Kim DH, Park JY, Sohn SK, Lee NY, Baek JH, Jeon SB et al. Multidrug resistance-1 gene polymorphisms associated with treatment outcomes in de novo acute myeloid leukemia. *International Journal of Cancer* 2006;118:2195-201.

61. Kobayashi Y, Ohshiro N, Sakai R, Ohbayashi M, Kohyama N, Yamamoto T. Transport mechanism and substrate specificity of human organic anion transporter 2 (hOat2 [SLC22A7]). *Journal of Pharmacy and Pharmacology* 2005;57:573-8.

62. Koepsell H, Endou H. The SLC22 drug transporter family. *Pflugers Archiv.European Journal of Physiology* 2004;447:666-76.

63. Koepsell H, Lips K, Volk C. Polyspecific organic cation transporters: structure, function, physiological roles, and biopharmaceutical implications. *Pharmaceutical Research* 2007;24:1227-51.

64. Konig J, Seithel A, Gradhand U, Fromm MF. Pharmacogenomics of human OATP transporters. *Naunyn Schmiedebergs Arch.Pharmacol.* 2006;372:432-43.

65. Kruse JP, Gu W. Modes of p53 regulation. *Cell* 2009;137:609-22.

66. Kuhne A, Tzvetkov MV, Hagos Y, Lage H, Burckhardt G, Brockmoller J. Influx and efflux transport as determinants of melphalan cytotoxicity: Resistance to melphalan in MDR1 overexpressing tumor cell lines. *Biochemical Pharmacology* 2009;78:45-53.

67. Kullak-Ublick GA, Glasa J, Boker C, Oswald M, Grutzner U, Hagenbuch B et al. Chlorambucil-taurocholate is transported by bile acid carriers expressed in human hepatocellular carcinomas. *Gastroenterology* 1997;113:1295-305.

68. Kullak-Ublick GA, Stieger B, Meier PJ. Enterohepatic bile salt transporters in normal physiology and liver disease. *Gastroenterology* 2004;126:322-42.

69. Lebeau B, Chouaid C, Baud M, Masanes MJ, Febvre M. Oral second- and third-line lomustine-etoposide-cyclophosphamide chemotherapy for small cell lung cancer. *Lung Cancer* 2009.

70. Lee SG, Choi JR, Kim JS, Park TS, Lee KA, Song J. Therapy-related acute lymphoblastic leukemia with t(9;22)(q34;q11.2):a case study and review of the literature. *Cancer Genetics and Cytogenetics* 2009;191:51-4.

71. Leslie EM, Deeley RG, Cole SP. Toxicological relevance of the multidrug resistance protein 1, MRP1 (ABCC1) and related transporters. *Toxicology* 2001;167:3-23.

72. Leslie EM, Ito K, Upadhyaya P, Hecht SS, Deeley RG, Cole SP. Transport of the beta -O-glucuronide conjugate of the tobacco-specific carcinogen 4-(methylnitrosamino)-1-(3-pyridyl)-1-butanol (NNAL) by the multidrug resistance protein 1 (MRP1). Requirement for glutathione or a non-sulfur-containing analog. *Journal of Biological Chemistry* 2001;276:27846-54.

73. Leslie EM, Mao Q, Oleschuk CJ, Deeley RG, Cole SP. Modulation of multidrug resistance protein 1 (MRP1/ABCC1) transport and atpase activities by interaction with dietary flavonoids. *Molecular Pharmacology* 2001;59:1171-80.

74. Li L, Meier PJ, Ballatori N. Oatp2 mediates bidirectional organic solute transport: a role for intracellular glutathione. *Molecular Pharmacology* 2000;58:335-40.

75. Loadman PM, Calabrese CR. Separation methods for anthraquinone related anti-cancer drugs. *J.Chromatogr.B Biomed.Sci.Appl.* 2001;764:193-206.

76. Lubbert M, Muller-Tidow C, Hofmann WK, Koeffler HP. Advances in the treatment of acute myeloid leukemia: from chromosomal aberrations to biologically targeted therapy. *J.Cell Biochem.* 2008;104:2059-70.

77. Mackey JR, Galmarini CM, Graham KA, Joy AA, Delmer A, Dabbagh L et al. Quantitative analysis of nucleoside transporter and metabolism gene expression in chronic lymphocytic leukemia (CLL): identification of fludarabine-sensitive and -insensitive populations. *Blood* 2005;105:767-74.

78. Mechetner E, Kyshtoobayeva A, Zonis S, Kim H, Stroup R, Garcia R et al. Levels of multidrug resistance (MDR1) P-glycoprotein expression by human breast cancer correlate with in vitro resistance to taxol and doxorubicin. *Clinical Cancer Research* 1998;4:389-98.

79. Meier PJ, Stieger B. Bile salt transporters. *Annu.Rev.Physiol* 2002;64:635-61.

80. Mertens D, Philippen A, Ruppel M, Allegra D, Bhattacharya N, Tschuch C et al. Chronic lymphocytic leukemia and 13q14: miRs and more. *Leukemia and Lymphoma* 2009;50:502-5.

81. Mertl M, Daniel H, Kottra G. Substrate-induced changes in the density of peptide transporter PEPT1 expressed in Xenopus oocytes. *Am.J.Physiol Cell Physiol* 2008;295:C1332-C1343.

82. Molina-Arcas M, Bellosillo B, Casado FJ, Montserrat E, Gil J, Colomer D et al. Fludarabine uptake mechanisms in B-cell chronic lymphocytic leukemia. *Blood* 2003;101:2328-34.

83. Molina-Arcas M, Marce S, Villamor N, Huber-Ruano I, Casado FJ, Bellosillo B et al. Equilibrative nucleoside transporter-2 (hENT2) protein expression correlates with ex vivo sensitivity to fludarabine in chronic lymphocytic leukemia (CLL) cells. *Leukemia* 2005;19:64-8.

84. Noguchi K, Katayama K, Mitsuhashi J, Sugimoto Y. Functions of the breast cancer resistance protein (BCRP/ABCG2) in chemotherapy. *Adv.Drug Deliv.Rev.* 2009;61:26-33.

85. Nozawa T, Minami H, Sugiura S, Tsuji A, Tamai I. Role of organic anion transporter OATP1B1 (OATP-C) in hepatic uptake of irinotecan and its active metabolite, 7-ethyl-10-hydroxycamptothecin: in vitro evidence and effect of single nucleotide polymorphisms. *Drug Metab Dispos.* 2005;33:434-9.

86. Ohashi R, Tamai I, Inano A, Katsura M, Sai Y, Nezu J et al. Studies on functional sites of organic cation/carnitine transporter OCTN2 (SLC22A5) using a Ser467Cys mutant protein. *Journal of Pharmacology and Experimental Therapeutics* 2002;302:1286-94.

87. Okabe M, Unno M, Harigae H, Kaku M, Okitsu Y, Sasaki T et al. Characterization of the organic cation transporter SLC22A16: a doxorubicin importer. *Biochemical and Biophysical Research Communications* 2005;333:754-62.

88. Pajor AM. Molecular properties of the SLC13 family of dicarboxylate and sulfate transporters. *Pflugers Archiv.European Journal of Physiology* 2006;451:597-605.

89. Palumbo A, Rajkumar SV. Treatment of newly diagnosed myeloma. *Leukemia* 2009;23:449-56.

90. Pan G, Elmquist WF. Mitoxantrone permeability in MDCKII cells is influenced by active influx transport. *Mol.Pharm.* 2007;4:475-83.

91. Pastor-Anglada M, Molina-Arcas M, Casado FJ, Bellosillo B, Colomer D, Gil J. Nucleoside transporters in chronic lymphocytic leukaemia. *Leukemia* 2004;18:385-93.

92. Patel RV, Clark LN, Lebwohl M, Weinberg JM. Treatments for psoriasis and the risk of malignancy. *Journal of the American Academy of Dermatology* 2009;60:1001-17.

93. Pierre K, Pellerin L. Monocarboxylate transporters in the central nervous system: distribution, regulation and function. *Journal of Neurochemistry* 2005;94:1-14.

94. Ponisch W, Mitrou PS, Merkle K, Herold M, Assmann M, Wilhelm G et al. Treatment of bendamustine and prednisone in patients with newly diagnosed multiple myeloma results in superior complete response rate, prolonged time to treatment failure and improved quality of life compared to treatment with melphalan and prednisone--a randomized phase III study of the East German Study Group of Hematology and Oncology (OSHO). *Journal of Cancer Research and Clinical Oncology* 2006;132:205-12.

95. Rabow AA, Shoemaker RH, Sausville EA, Covell DG. Mining the National Cancer Institute's tumor-screening database: identification of compounds with similar cellular activities. *Journal of Medicinal Chemistry* 2002;45:818-40.

96. Rees DC, Johnson E, Lewinson O. ABC transporters: the power to change. *Nat.Rev.Mol.Cell Biol.* 2009;10:218-27.

97. Reszka AA, Rodan GA. Mechanism of action of bisphosphonates. *Curr.Osteoporos.Rep.* 2003;1:45-52.

98. Ritzel MW, Ng AM, Yao SY, Graham K, Loewen SK, Smith KM et al. Recent molecular advances in studies of the concentrative Na+-dependent nucleoside transporter (CNT) family: identification and characterization of novel human and mouse proteins (hCNT3 and mCNT3) broadly selective for purine and pyrimidine nucleosides (system cib). *Molecular Membrane Biology* 2001;18:65-72.

99. Ritzel MW, Ng AM, Yao SY, Graham K, Loewen SK, Smith KM et al. Molecular identification and characterization of novel human and mouse concentrative Na+-nucleoside cotransporter proteins (hCNT3 and mCNT3) broadly selective for purine and pyrimidine nucleosides (system cib). *Journal of Biological Chemistry* 2001;276:2914-27.

100. Rizwan AN, Burckhardt G. Organic anion transporters of the SLC22 family: biopharmaceutical, physiological, and pathological roles. *Pharmaceutical Research* 2007;24:450-70.

101. Robak T, Korycka A, Lech-Maranda E, Robak P. Current status of older and new purine nucleoside analogues in the treatment of lymphoproliferative diseases. *Molecules.* 2009;14:1183-226.

102. Rowinsky EK, Donehower RC. Paclitaxel (taxol). *New England Journal of Medicine* 1995;332:1004-14.

103. Saltz LB, Cox JV, Blanke C, Rosen LS, Fehrenbacher L, Moore MJ et al. Irinotecan plus fluorouracil and leucovorin for metastatic colorectal cancer. Irinotecan Study Group. *New England Journal of Medicine* 2000;343:905-14.

104. Schiff PB, Fant J, Horwitz SB. Promotion of microtubule assembly in vitro by taxol. *Nature* 1979;277:665-7.

105. Shang T, Uihlein AV, Van Asten J, Kalyanaraman B, Hillard CJ. 1-Methyl-4-phenylpyridinium accumulates in cerebellar granule neurons via organic cation transporter 3. *Journal of Neurochemistry* 2003;85:358-67.

106. Shen F, Chu S, Bence AK, Bailey B, Xue X, Erickson PA et al. Quantitation of doxorubicin uptake, efflux, and modulation of multidrug resistance (MDR) in MDR human cancer cells. *Journal of Pharmacology and Experimental Therapeutics* 2008;324:95-102.

107. Shnitsar V, Eckardt R, Gupta S, Grottker J, Muller GA, Koepsell H et al. Expression of human organic cation transporter 3 in kidney carcinoma cell lines increases

chemosensitivity to melphalan, irinotecan, and vincristine. *Cancer Research* 2009;69:1494-501.

108. Smith NF, Acharya MR, Desai N, Figg WD, Sparreboom A. Identification of OATP1B3 as a high-affinity hepatocellular transporter of paclitaxel. *Cancer Biol.Ther.* 2005;4:815-8.

109. Steele AJ, Prentice AG, Hoffbrand AV, Yogashangary BC, Hart SM, Nacheva EP et al. p53-mediated apoptosis of CLL cells: evidence for a transcription-independent mechanism. *Blood* 2008;112:3827-34.

110. Suzuki Y, Niitsu N, Hayama M, Katayama T, Ishii R, Osaka M et al. Lymphoproliferative disorders after immunosuppressive therapy for aplastic anemia: a case report and literature review. *Acta Haematologica* 2009;121:21-6.

111. Takeba Y, Kumai T, Matsumoto N, Nakaya S, Tsuzuki Y, Yanagida Y et al. Irinotecan activates p53 with its active metabolite, resulting in human hepatocellular carcinoma apoptosis. *J.Pharmacol.Sci.* 2007;104:232-42.

112. Takeba Y, Sekine S, Kumai T, Matsumoto N, Nakaya S, Tsuzuki Y et al. Irinotecan-induced apoptosis is inhibited by increased P-glycoprotein expression and decreased p53 in human hepatocellular carcinoma cells. *Biological and Pharmaceutical Bulletin* 2007;30:1400-6.

113. Thomas J, Wang L, Clark RE, Pirmohamed M. Active transport of imatinib into and out of cells: implications for drug resistance. *Blood* 2004;104:3739-45.

114. Thomas X, Archimbaud E. Mitoxantrone in the treatment of acute myelogenous leukemia: a review. *Hematology and Cell Therapy* 1997;39:63-74.

115. Tsuji A. Transporter-mediated Drug Interactions. *Drug Metab Pharmacokinet.* 2002;17:253-74.

116. Tucci M, Quatraro C, Dammacco F, Silvestris F. Role of active drug transporters in refractory multiple myeloma. *Curr.Top.Med.Chem.* 2009;9:218-24.

117. Turk D, Szakacs G. Relevance of multidrug resistance in the age of targeted therapy. *Curr.Opin.Drug Discov.Devel.* 2009;12:246-52.

118. Uwai Y, Taniguchi R, Motohashi H, Saito H, Okuda M, Inui K. Methotrexate-loxoprofen interaction: involvement of human organic anion transporters hOAT1 and hOAT3. *Drug Metab Pharmacokinet.* 2004;19:369-74.

119. Vigneswaran N, Beckers S, Waigel S, Mensah J, Wu J, Mo J et al. Increased EMMPRIN (CD 147) expression during oral carcinogenesis. *Experimental and Molecular Pathology* 2006;80:147-59.

120. Vousden KH, Lane DP. p53 in health and disease. *Nat.Rev.Mol.Cell Biol.* 2007;8:275-83.

121. Wang H, Fei YJ, Kekuda R, Yang-Feng TL, Devoe LD, Leibach FH et al. Structure, function, and genomic organization of human Na(+)-dependent high-affinity dicarboxylate transporter. *Am.J.Physiol Cell Physiol* 2000;278:C1019-C1030.

122. Yamaguchi H, Chen J, Bhalla K, Wang HG. Regulation of Bax activation and apoptotic response to microtubule-damaging agents by p53 transcription-dependent and -independent pathways. *Journal of Biological Chemistry* 2004;279:39431-7.

123. Yamaguchi H, Kobayashi M, Okada M, Takeuchi T, Unno M, Abe T et al. Rapid screening of antineoplastic candidates for the human organic anion transporter OATP1B3 substrates using fluorescent probes. *Cancer Letters* 2008;260:163-9.

124. Yanagida O, Kanai Y, Chairoungdua A, Kim DK, Segawa H, Nii T et al. Human L-type amino acid transporter 1 (LAT1): characterization of function and expression in tumor cell lines. *Biochimica et Biophysica Acta* 2001;1514:291-302.

125. Yao SY, Ng AM, Sundaram M, Cass CE, Baldwin SA, Young JD. Transport of antiviral 3'-deoxy-nucleoside drugs by recombinant human and rat equilibrative, nitrobenzylthioinosine (NBMPR)-insensitive (ENT2) nucleoside transporter proteins produced in Xenopus oocytes. *Molecular Membrane Biology* 2001;18:161-7.

126. Yao YY, Zhu Q, Zou LF, Dou HJ, Chen YM, Tang Y et al. [Clinical study on fludarabin combined with cytarabine regimen in the treatment of patients with refractory and relapsed acute myeloid leukemia.]. *Zhongguo Shi Yan.Xue.Ye.Xue.Za Zhi.* 2009;17:774-6.

127. Zenz T, Mohr J, Edelmann J, Sarno A, Hoth P, Heuberger M et al. Treatment resistance in chronic lymphocytic leukemia: the role of the p53 pathway. *Leukemia and Lymphoma* 2009;50:510-3.

128. [Anon]. Harrison's principles of internal medicine, 17th edition. *Library Journal* 2008;133:96.

Declaration

I hereby declare that the work described in this thesis was performed by me unless otherwise specified. This thesis was written by me and submitted to the Georg-August-Universität, Göttingen**,** Germany to obtain the Doctoral degree from the Faculty of Mathematics and Natural Sciences.

September 14, 2009 SHIVANGI GUPTA

Acknowledgements

I express my sincere gratitude to my supervisor **PD Dr. Yohannes Hagos**, for his support, encouragement and unfailing patience throughout my thesis. It is not often that one finds an advisor who always takes the time to listen to problems and help through the roadblocks that unavoidably crop up in the course of research. His guidance was essential for the completion of this work.

I gratefully acknowledge the contribution of **Prof. Dr. Gerhard Burckhardt** who has helped shape the direction of my research through numerous spirited discussions. I thank **Prof. Dr. Thomas Pieler** and **Prof. Dr. Uwe Gross** for agreeing to review my work.

I also acknowledge the cooperation extended to me by all members of the lab. I specifically thank **Prof. Dr. B.C. Burckhardt** and **PD Dr. Wolfgang Krick** for the discussions and help in problem solving. I thank **Mr. Soeren Petzke** and **Ms. Gesche Dallmeyer** for their help in the lab.

I would also like to thank **Prof. Dr. Gerald Wulf** for his collaboration in this project.

I thank all my friends here, especially **Nina Schnedler**, for a wonderful time and support these three years.

My family receives my deepest gratitude and affection for their good cheer and encouragement that enabled me to get through periods of academic doubt and anxiety.

Curriculum Vitae

Name:	Shivangi Gupta
Date of Birth:	14.07.1983
Nationality:	Indian
1986-2001:	**Schooling** (Nursery-Class XII), *RSJMS* and *Modern School, Barakhamba Road, New Delhi*, India
2001- 2004:	**B.Sc(Hons) Biotechnology**, *Ch. Charan Singh University, Meerut*, India
2004- 2006:	**M.Sc. Biochemistry and Molecular Biology**, *University of Bremen*, Germany **Master Thesis**: *Identification of new splice variants and differential expression of HRP-2*. (Centre for Biomolecular Interactions Bremen, Universität Bremen)
2006- 2009:	**Dr.rer.nat (Ph.D Biology)**, *Dept. of Vegetative Physiology, University of Göttingen*, Germany **Ph.D thesis**: *Expression of SLC transporters in Chronic Lymphocytic Leukaemia cells and their interaction with cytostatics*

Scientific publications:

1. Shnitsar Volodymyr, Eckardt Ronny, **Gupta Shivangi**, Grottker Julia, Müller Gerhard A, Koepsell Hermann, Burckhardt Gerhard, Hagos Yohannes *Expression of human organic cation transporter 3 in kidney carcinoma cell lines increases chemosensitivity to melphalan, irinotecan, and vincristine.* Cancer Research 2009

2. Thakar Ketan, Niedenthal Rainer, Okaz Elwy, Franken Sebastian, Jakobs Astrid, **Gupta Shivangi**, Kelm Sørge, Dietz Frank *SUMOylation of the hepatoma-derived growth factor negatively influences its binding to chromatin.* The FEBS journal 2008

Conferences attended:

Mar 25–28, 2007	Deutsche Physiologische Gesellschaft Congress 2007, Hannover, Germany
Aug 11–17, 2007	BioMedical Transporters 2007: Membrane Transporters in Disease and Drug Development, Bern, Switzerland
Sept 12–15, 2007	Aggressive Lymphoma Workshop 2007, Göttingen, Germany
Mar 2–5, 2008	Deutsche Physiologische Gesellschaft Congress 2008, Cologne, Germany *Poster: Interaction of cytostatics with organic cation transporters 1& 2*
Jun 12–14, 2008	CESAR Congress, Göttingen, Germany
Nov 12–22, 2008	Goettinger Transport Tag 2008, Göttingen, Germany *Talk: Interaction of cytostatics with organic cation transporters 1 and 2*
Mar 22–25, 2009	Deutsche Physiologische Gesellschaft Congress 2009, Giessen, Germany *Poster: Organic cation transporter mediated cytotoxicity of irinotecan and paclitaxel*